

Streamlining Decarbonized Construction through Automated Design and Drafting: Ribbed  
Precast Concrete Panels

by

Yu Wei

A thesis submitted in partial fulfillment of the requirements for the degree of

Master of Science

in

Construction Engineering and Management

Department of Civil and Environmental Engineering  
University of Alberta

© Yu Wei, 2023

## **Abstract**

The use of precast concrete panels in panelized construction has gained popularity due to their numerous advantages. However, conventional precast designs encounter challenges, such as high costs, limited flexibility, and restrictions in remodelling. To address these issues, this research introduces the 3i RPCPS (Intelligent, Innovative, and Integrated Ribbed Precast Concrete Panel System). The 3i RPCPS incorporates two-way ribs to provide structural support and achieves a notable reduction in concrete usage (by 60% to 70%). Nevertheless, this innovation necessitates a complex fabrication system involving moulds and formwork, underscoring the importance of precision in shop drawing. This research emphasizes the essential role of BIM in generating detailed shop drawings and fabrication information for precast concrete components. However, this manufacturing-centric BIM model exposes limitations associated with relying solely on traditional methods in the design and drafting processes. It particularly highlights challenges related to repetitive drafting tasks and potential rework due to human errors. Additionally, the conventional drafting approach complicates revisions when design requirements change, resulting in time-consuming and intricate modifications. Aligned with the principles of lean construction, which aims to eliminate waste and improve efficiency, this thesis identifies time-consuming drafting as a bottleneck in the overall project delivery process and is considered a non-value-added activity from the perspective of projects' owners. Consequently, this raises the urgent need for automation in the design and drafting of 3i RPCPS. To address these challenges, the developed methodology introduces a computer model named ConcreteX, developed as an add-on to Revit using the C# programming language. ConcreteX integrates BIM technology and Revit's parametric modelling capabilities, incorporating manufacturing requirements within a 3D model. This integration allows for the generation of shop and fabrication drawings. To demonstrate the

efficiency achieved through automation, a study was conducted to compare the time consumption of model generation between manual and automated processes. A simulation model was developed to further analyze the benefits of ConcreteX within the broader context of the project delivery process. The results illustrate significant time savings in the design and drafting processes, validating the effectiveness of the developed methodology.

Overall, this thesis introduces the innovative ribbed precast concrete panel system known as “3i RPCPS”; meanwhile, it highlights the need and benefits for automation in design and drafting processes in residential building construction. The elegant design of 3i RPCPS not only effectively addresses the challenges of high costs, limited flexibility, and remodelling constraints, thereby compensating for the complexities of the forming system, but also establishes a solid foundation for automating the drafting process. ConcreteX showcases the potential of BIM technology and parametric modelling in streamlining the generation of a manufacturing-centric BIM model, ultimately enhancing efficiency and reducing waste. It emphasizes automation across three levels of drawing: permit drawings, shop drawings, and installation guidelines.

## **Acknowledgements**

I am lucky to encounter many wonderful people during my journey in pursuing my master's degree.

I would like to express my sincere gratitude to all of them.

First and foremost, I am deeply grateful to my supervisor, Mohamed Al-Hussein, for his patient guidance, unwavering support, and constant encouragement.

I would also like to extend my thanks to my colleagues, Mo Adel, Jeffrey Kervin, and Luis Lin for their valuable contributions and collaborative efforts in this research. Additionally, I am thankful to the team at 3i Inc. in Edmonton, AB, Canada, particularly Morgan and Mahmud from the design team, for their support and willingness to share their expertise, which greatly enriched my work.

Special thanks to my dear friends, Mohamed ElMenshawy, Xue Chen, and Nan Zhang for their assistance and moral support throughout this journey.

Lastly, I extend my deepest gratitude to my family, especially my husband, for his love, support, and company. I am also thankful to my grandparents for providing me with early education and enlightenment in the field of civil engineering, as well as to my parents for their unconditional love and encouragement.

# Table of Contents

Abstract.....	<i>ii</i>
Acknowledgements.....	<i>iv</i>
List of Tables .....	<i>viii</i>
List of Figures.....	<i>ix</i>
Chapter 1. Introduction.....	<i>1</i>
1.1 Background and motivation.....	<i>1</i>
1.2 Research objectives.....	<i>4</i>
1.3 Thesis organization .....	<i>5</i>
Chapter 2. Literature Review.....	<i>7</i>
2.1 Panelized construction .....	<i>7</i>
2.1.1 Precast concrete panels .....	<i>9</i>
2.2 BIM implementation in panelized construction .....	<i>10</i>
2.2.1 Development and benefits.....	<i>10</i>
2.2.2 Limitation and challenges .....	<i>12</i>
2.3 BIM-Based automation in design.....	<i>13</i>
Chapter 3. Methodology .....	<i>15</i>
3.1 Overview .....	<i>15</i>
3.2 3i Ribbed Precast Concrete Panel System (3i RPCPS) overview.....	<i>17</i>
3.2.1 Reinforced concrete ribbed panel .....	<i>17</i>
3.2.2 Formwork system .....	<i>20</i>
3.2.3 Connections and lifting.....	<i>21</i>
3.3 Automated parametric design for solid panel.....	<i>22</i>

3.3.1 Logic for Vertical Rib placement.....	25
3.3.2 Logic for reinforcement placement.....	30
3.3.3 Logic for Styrofoam placement.....	35
3.3.4 Logic for connection and lifting placement.....	42
3.4 Design of structure layout around opening.....	<b>45</b>
3.5 Automated parametric design of precast wall panels with openings.....	<b>47</b>
3.5.1 Structure layout around window openings.....	47
3.5.2 Structure layout around door openings.....	60
3.6 Development of user interface (UI).....	<b>71</b>
Chapter 4. Application Implementation.....	<b>76</b>
4.1 Overview.....	<b>76</b>
4.2 Inputs for prototype system.....	<b>79</b>
4.2.1 BIM model preparation.....	79
4.2.2 Information extraction from a BIM model.....	80
4.2.3 User-defined inputs.....	82
4.3 Functionality implementation and time study.....	<b>83</b>
4.3.1 Automatic panel label generation.....	83
4.3.2 Automatic generation of wall connection.....	86
4.3.3 Automatic structural generation.....	92
Chapter 5. Case Study.....	<b>107</b>
5.1 Study 1—Evaluating time savings in design and drafting with ConcreteX.....	<b>108</b>
5.2 Study 2—Analyzing the impact of ConcreteX on project delivery.....	<b>110</b>
5.2.1 Simulation model.....	110

5.2.2 Validation.....	112
5.2.3 Simulation results and discussion .....	114
Chapter 6. Conclusion.....	<b>122</b>
6.1 Summary.....	122
6.2 Contributions .....	124
6.3 Limitations and future work.....	125
References.....	<b>127</b>
Appendix A: Structural Layouts for Ribbed Panel.....	<b>132</b>
Appendix B: Simulation Reports.....	<b>136</b>

## List of Tables

Table 3-1. Coordinates of rebar embedded in Top and Bottom Ribs .....	32
Table 3-2. Tab feature for Windows Form .....	72
Table 4-1. Input parameters extracted from BIM model .....	81
Table 4-2. Input parameters as defined by user .....	82
Table 4-3. Wall Name Mapper dictionary .....	84
Table 4-4. Drafting time for manual and ConcreteX performance for generating panel name ....	85
Table 4-5. Drafting time for manual and ConcreteX performance for generating 45-degree connection method .....	92
Table 4-6. Drafting time for manual and ConcreteX performance for generating structural layout of solid wall.....	102
Table 5-1. Drafting time for manual and ConcreteX performance for generating desired model with fabrication detail .....	110
Table 5-2. Duration distribution for each activity .....	112
Table 5-3. Design and drafting time collected from both simulation Models A and M.....	113
Table 5-4. Comparison of drafting time for basement project—real-world versus simulation..	113
Table 5-5. Simulation results—utilization rates and waiting file (Model M).....	115
Table 5-6. Simulation results—utilization rates and waiting file (Model A) .....	117
Table 5-7. Project delivery time comparison—manual drafting versus automated drafting with ConcreteX .....	119
Table 5-8. Comparison of delivered projects count in one month—manual drafting versus automated drafting with ConcreteX.....	121

## List of Figures

Figure 3-1. Overview of framework .....	15
Figure 3-2. Structure layout for basic concrete wall panel .....	18
Figure 3-3. Energy-Saving concrete wall panel.....	18
Figure 3-4. Styrofoam in 3i RPCPS.....	20
Figure 3-5. Locations and usage of Styrofoam.....	21
Figure 3-6. Location and usage of steel connectors.....	22
Figure 3-7. Front and top view of ribbed precast concrete wall panel .....	23
Figure 3-8. Different scenarios for placing Vertical Ribs.....	25
Figure 3-9. Objective structural layout .....	27
Figure 3-10. Positions of Vertical Ribs.....	28
Figure 3-11. Coordinates for start-point of Vertical Rib .....	29
Figure 3-12. Concrete cover in top and section view of concrete panel.....	30
Figure 3-13. Top and section view for rebar embedded in Top and Bottom Ribs .....	31
Figure 3-14. Coordinates of rebar embedded in Edge and Vertical Rib.....	33
Figure 3-15. Coordinates of wire mesh.....	35
Figure 3-16. Parameters and coordinates of L-shape Styrofoam.....	36
Figure 3-17. Parameters and coordinates of U-shape and L-shape-45-degree Corner Styrofoam.....	38
Figure 3-18. Parameters and coordinates of Flat-shape Styrofoam.....	40
Figure 3-19. Coordinates of Wedge Anchor.....	44
Figure 3-20. The contrast between two designs.....	46
Figure 3-21. Parameters for the structural layout around window opening .....	48
Figure 3-22. Determining window opening parameters for Header and Sill Rib start-points.....	49

Figure 3-23. Determining window opening parameters for Header and Sill Rib end-points .....	51
Figure 3-24. Header and Sill Rib parameters in the <i>y</i> -direction .....	52
Figure 3-25. Header and Sill Rib Coordinates around window opening.....	53
Figure 3-26. Left Side Rib parameters around window opening.....	54
Figure 3-27. Right Side Rib parameters around window opening.....	55
Figure 3-28. Side Rib parameters around window opening in the <i>y</i> -direction .....	56
Figure 3-29. Side Rib coordinates around window opening.....	57
Figure 3-30. Cripple Rib parameters above/below window opening in the <i>x</i> -direction.....	58
Figure 3-31. Cripple Rib coordinates above/below window opening .....	59
Figure 3-32. Parameters for the structural layout around door opening .....	61
Figure 3-33. Determining door opening parameters for Header Rib start-points.....	62
Figure 3-34. Determining door opening parameters for Header Rib end-points.....	63
Figure 3-35. Coordinates of Header Rib above door opening .....	64
Figure 3-36. Parameters for door left Side Rib.....	65
Figure 3-37. Parameters for door right Side Rib.....	66
Figure 3-38. Parameter for door Side Rib in the <i>y</i> -direction .....	67
Figure 3-39. Door Side Rib coordinates .....	68
Figure 3-40. Cripple Rib parameters above/below window opening in the <i>x</i> -direction.....	69
Figure 3-41. Cripple Rib coordinates above door opening.....	71
Figure 3-42. User interface of 3i RPCPS design .....	72
Figure 4-1. Classes in system design of automation design and drafting using UML .....	78
Figure 4-2. 3D Revit model prepared for prototype system .....	79
Figure 4-3. Wall panel label created for prototype system.....	85

Figure 4-4. Dynamic wall pair selection with combo box update .....	86
Figure 4-5. Classification of wall connections based on interior angles .....	88
Figure 4-6. Suggested connection methods for wall connection .....	90
Figure 4-7. Input parameters for rib thickness and Styrofoam .....	93
Figure 4-8. Void family for structural generation.....	94
Figure 4-9. Void placement distance for structural integrity .....	95
Figure 4-10. Variation in connection lengths across different connection methods.....	96
Figure 4-11. Storage of connection length and edge width information in wall ends .....	97
Figure 4-12. Parameters used in Void placement .....	99
Figure 4-13. Flow chart of Void arrangement determination .....	101
Figure 4-14. Automated generation principle for structural layout around openings.....	104
Figure 5-1. 3D Revit model and floor plan for the case study basement.....	108
Figure 5-2. Output from ConcreteX: model with manufacturing details.....	109
Figure 5-3. Main layout of current project delivery process simulation model.....	111
Figure 5-4. Impact of drafter count on project waiting time.....	116

# **Chapter 1. Introduction**

## **1.1 Background and motivation**

Recently, the Canadian housing market has witnessed a substantial increase in demand attributed to favourable economic conditions and continuous immigration. This surge is exemplified by the record-breaking construction of 65,462 homes in 2022 (Statistics Canada, 2023). The heightened construction activity has placed significant strain on trade contractors and the availability of skilled labour. As a result, the industry is currently facing challenges such as extended lead times and prolonged construction cycles, resulting in project delays and overall inefficiencies. To tackle these challenges, panelized construction has emerged as a promising solution. By manufacturing building components in a controlled factory environment, panelized construction reduces lead times and minimizes the impact of adverse weather conditions on construction schedules. This approach enhances productivity and efficiency throughout the construction process, resulting in accelerated project timelines and improved overall performance.

In North America, concrete is widely used as the primary material for basement construction. As the demand for housing increases, panelized construction utilizing precast concrete panels has emerged as a viable solution. While precast concrete designs have seen some successful adoption, they continue to face challenges in the home-building industry in North America. They are often perceived as costly, lacking flexibility, and restrictive when it comes to remodelling or necessary modifications. However, recognizing these limitations, we introduce the 3i RPCPS (Intelligent, Innovative and Integrated Ribbed Precast Concrete Panel System) as our research focus, aiming to address these drawbacks and provide a more adaptable and cost-effective solution.

The 3i RPCPS features two-way ribs (vertical and horizontal ribs) designed to withstand structural loads such as deflection, bending, and shear, with specific attention to the spacing between the vertical ribs. The main innovation of the panel lies in its ability to reduce concrete usage by 60% to 70% due to the presence of ribs. However, this feature also necessitates the implementation of a new and complex fabrication system, involving moulds and formwork. Additionally, it highlights the need for a more accurate drafting system.

To enhance efficiency and streamline project delivery, Building Information Modelling (BIM) has become a valuable tool in the construction industry. BIM facilitates off-site manufacturing by enabling efficient collaboration, information exchange, and coordination among project stakeholders. With BIM, the 3i RPCPS studied in this thesis can be seamlessly integrated into the construction workflow. BIM allows for the creation of detailed 3D models that encompass ribbed precast concrete panels, enabling accurate visualization and coordination of various building components.

To successfully implement BIM in prefabricated construction industry, it is crucial to design BIM models with adequate fabrication details. Manufacturing-centric BIM requires a high level of detail (LOD), which significantly increases the modelling time when transitioning from one LOD level to another. In the case of the PCF system studied in this research, the repetitive modelling of panel structures consumes a considerable amount of time. The placement of detailed components, such as formwork, is closely tied to the panel's structural layout. When wall dimensions change, it necessitates the redesign of not only the panel structure but also all related components, making model revisions time-consuming and challenging. Moreover, manual design processes often suffer from limitations such as potential errors, and inconsistencies in design outputs.

From the perspective of overall project delivery in panelized construction, the process can be categorized into design and drafting, manufacturing, and installation stages. The design and drafting stages play a crucial role in creating accurate and detailed plans for the manufacturing and installation processes. However, compared to the typically efficient and time-effective manufacturing and installation stages, the detailed BIM-based design and drafting process is identified as a bottleneck. According to the principles of lean construction, this bottleneck leads to various types of waste. One such waste is the idle time experienced by workers in the manufacturing stage, as they must wait for the design and drafting phase to be completed before they can proceed with their tasks. This idle time can result in decreased efficiency and increased costs. Furthermore, the design and drafting bottleneck can cause prolonged project wait times for modelling, leading to delays in the overall project delivery. These delays extend the lead times and can have negative impacts on project schedules, customer satisfaction, and financial aspects.

The clear need to automate BIM-based construction designs has become evident. Automation plays a crucial role by reducing manual effort and facilitating seamless information transfer between project stages. With automation, design iteration and drafting tasks can be expedited, leading to improved efficiency and accuracy. By minimizing manual errors and reducing rework, the project delivery stages become more synchronized and aligned. Additionally, automation helps mitigate potential delays caused by manual processes or information gaps. This ensures optimal utilization of resources, including time and labour, resulting in a smoother workflow and increased productivity. Overall, automation is essential for streamlining construction processes and optimizing project outcomes.

## 1.2 Research objectives

The primary objective of this research is to develop an automated BIM-based design and drafting tool specifically tailored for ribbed precast concrete panels. The tool aims to automate the design and drafting process, resulting in enhanced drafting accuracy, increased drafting efficiency, and improved productivity in the production of ribbed precast concrete panels. This, in turn, contributes to better project delivery outcomes.

To achieve these goals, the research focuses on the following specific objectives:

1. Gain in-depth familiarity with the construction and design procedures within the panelized ribbed precast concrete panel industry. This involves observing and studying the practices of design and manufacturing teams involved in the industry.
2. Develop an automated BIM-based 3i RPCPS design and drafting system to enhance project delivery efficiency with the following objectives:
  - Automate the generation of detailed BIM models with precise fabrication information for the manufacturing process, effectively reducing design and drafting time.
  - Generate an accurate Bill of Materials (BOM) to facilitate precise procurement and expedite material preparation for manufacturing.
3. Develop a production simulation system that integrates discrete-event simulation in order to accurately replicate the current project delivery process, allowing for the assessment of the impact of automation design on the overall project delivery process.

### **1.3 Thesis organization**

This thesis is organized into six unique chapters. Chapter 1 introduces the research topic, Chapter 2 presents a comprehensive literature review, Chapter 3 outlines the research methodology employed, Chapter 4 focuses on the implementation of the developed approach, Chapter 5 presents a detailed case study, and Chapter 6 concludes the thesis with key findings and recommendations.

Chapter 2 is divided into three main sections, each addressing a specific aspect of the research topic. The first section provides an in-depth exploration of panelized construction with a focus on ribbed precast concrete panels. The second section delves into the limitations encountered when integrating BIM in panelized construction. Lastly, the third section examines the concept of BIM-based automated tools and their potential application in the context of panelized construction.

Chapter 3 presents the developed framework for the automation design and drafting tool, comprising two main components: the knowledge-based design and the rule-based mathematical algorithms design. The knowledge-based model design incorporates industry expertise and best practices, while the rule-based mathematical algorithms provide the necessary computational power to generate precise and efficient panel layouts. This chapter is dedicated to introducing the rule-based design of mathematical algorithms. The methodology is structured into four stages, as follows: (1) automated parametric design of ribbed precast concrete panels without openings, (2) designing the structure layout to accommodate openings, (3) automated parametric design of the structure layout surrounding openings, and (4) developing a user interface that connects the user with the design logic, considering their preferences.

Chapter 4 consists of two main sections. The first section introduces the input requirements for the automation tool, outlining the data and parameters needed to effectively use the automation design

and drafting tool developed in the previous chapters. This section ensures that users have a clear understanding of the necessary inputs for the tool to function optimally. The second section focuses on the implementation of the knowledge-based design and rule-based mathematical algorithms developed in Chapter 3. This is achieved by using object-oriented programming (OOP) methodology and the Revit API. The section highlights the development process of the automation design and drafting tool, named ConcreteX, and demonstrates how the tool leverages OOP and the Revit API to facilitate efficient and accurate design automation.

Chapter 5 focuses on evaluating the effectiveness and efficiency of the developed prototype system through two comprehensive studies. The first study examines the time-saving benefits and efficiency gains of using ConcreteX compared to manual drafting. It specifically focuses on the design and drafting process and provides insights into the extent to which ConcreteX reduces drafting time. The second study involves the development of a simulation model that encompasses the project delivery process. This model replicates the various stages of project delivery. By incorporating the simulation model, the benefits of implementing ConcreteX can be analyzed, including improvements in production rate and overall reduction in lead time.

Chapter 6 summarizes the research outcomes and their contributions to the construction industry, along with recommendations for future research.

## **Chapter 2. Literature Review**

### **2.1 Panelized construction**

The main motivation of the shift in the construction sector to prefabricated buildings is the desire to build structures that are more efficient in several aspects, namely: energy use, cost, and quality (Arturo Garza-Reyes et al., 2012). The Construction Industry Council conducted a study that characterized off-site production as a technique that significantly improved both the product and the process by facilitating manufacturing and assembly in a factory setting. One of the main methods used in prefabricated buildings is panelized construction (Miles and Whitehouse, 2013).

Panelized construction is a manufacturing technique, which fabricates various components such as: wall and floor panels in a closed environment. This type of process produces pre-built panels, and may include pre-installed windows, doors, and skylights. To minimize delays in permits, approvals and inspections, these panels are designed to comply with the building code and regulations (Zhang et al., 2022). Once fabricated, these components are then transported to the construction site and fixed on the foundation of the project (The Canadian Timber Company, 2007).

As highlighted by Lopez and Froese (2016), panelized construction has some advantages over modular construction. First, the ease of transportation due to flat, rectangular panels that are easily and efficiently stacked, and do not require large amounts of volume. Furthermore, panelized components are less likely to be damaged during transit as they can be safely secured on the truck, limiting movements, accidents, or losses. In contrast, assembled modules that are complete with walls and roofs pose a challenge to secure and are at a higher risk of damage during transport. Lopez and Froese (2016) also note that the equipment required for on-site assembly of panels does not require much space, making it more convenient to transport. In addition, the insulation

technology used for joining panels offers superior thermal resistance (R-value) and airtightness, reducing heat loss during colder months (Lopez and Froese, 2016).

Panelized construction is characterized by more features related to standardization in the housing sector and can lower construction expenses through the adoption of mass production techniques in a manner similar to the manufacturing processes (NAHB, 2002b). This approach also minimizes weather related factors that can affect the construction timeline, enhances the consistency of wall construction, and improves the quality by fabricating them in a controlled setting. It also mitigates storage and traffic issues through just-in-time delivery, reduces the need for on-site material storage, and speeds up the timeline for interior finishes, since they can start once the structure is set up, due to the high quality of the prefabricated interior walls (Lindow and Jasinski, 2003). Furthermore, panelized construction reduces labour costs, since it does not require highly skilled labour on site, and enhances quality control in building management (Mousa, 2007). These benefits are the key to boosting the performance of panelized homes and minimizing future maintenance complications.

Despite these benefits, there is still hesitation among most of the consumers when it comes to buying prefabricated homes. For instance, in the US, barely 0.2 percent of spending on new housing goes towards homes that are built using panelized systems, taking into consideration that this sector represents 4 percent of the country's economic activity (NAHB, 2002a). This reason, together with insufficient training for code officials, the risk of damage during transport, and the associated transportation costs, as well as the high price of equipment and upfront investments, contributes to the delay of the construction industry in adopting panelized and modular methods (NAHB 2002a).

### **2.1.1 Precast concrete panels**

In recent years, the housing sector has experienced a remarkable surge in demand, fueled by a robust economy and sustained immigration. As a testament to this trend, the construction of homes reached a record-breaking 65,462 units in 2022 (Statistics Canada, 2023). This boom has burdened specialized contractors and reduced the availability of skilled manpower in construction.

Accordingly, this situation has led to prolonged lead times and extended project completion time becoming more common in the industry. Dennis (2002) claims that the popular profit equation in many sectors, including construction, relies on subtracting costs from fixed prices. To boost profits in such a business climate, managers are forced to decrease costs. However, traditional construction management strategies that majorly focus on managing activities and controlling costs may not contribute effectively to reducing project cycle durations, costs, or increasing profits (Nahmens, 2011). This issue paves the way for exploring the opportunities of precast concrete in residential construction.

The utilization of precast concrete in residential construction provides an effective solution to the aforementioned issues. As summarized by Yu (2008), Zielinska and Zielinski (1982) introduced a ribbed panel system for precast concrete houses, while Hurd (1986) introduced an insulated precast concrete foundation (PCF) system that is still used by some manufacturers today. During the 1990s, several precast concrete housing projects drew interest and demonstrated the practicality and cost efficiency of precast concrete in residential construction (Hurd, 1994; Einea et al., 1994; Von Der Ahe et al., 1999).

Despite these successful efforts, precast concrete designs are still viewed within the home-building industry as expensive, inflexible, and restrictive when it comes to remodelling or any required

modifications (Holmes et al., 2005). To tackle these issues, researchers at the University of Alberta, in collaboration with their industrial partners, have developed a precast concrete foundation (PCF) system. This system is designed to meet functional needs, reduce overall costs, and ensure flexibility. It features a modularized rib structure, external insulation, and simplified bolted connections as its unique elements.

These developments in precast concrete technology can significantly change the industry's perceptions and encourage wider adoption of precast concrete designs in residential construction. By tackling cost-related issues, enhancing flexibility, and facilitating remodelling needs, the PCF system studied in this research presents a promising solution for more efficient and cost-effective residential construction using precast concrete.

## **2.2 BIM implementation in panelized construction**

### **2.2.1 Development and benefits**

One notable aspect of BIM is its ability to enhance visual communication between designers and models, enabling the identification of construction clashes through the intelligent attributes assigned to model components. Most BIM software includes robust features that allow for monitoring changes within the design stage, providing instant updates whether they originate from the same discipline or not. This functionality proves invaluable in preventing design errors, wasted effort, and misunderstandings during the early stages of conception. BIM streamlines the modification process within a project, eliminating the labourious and cumbersome procedures typically associated with conventional 2D Computer-aided design (CAD) drawings (McFarland, 2007).

BIM is portrayed as a solution for the issues that are typically tied to conventional practices in the construction sector. In the UK, a joint definition by the Royal Institute of British Architects (RIBA), Construction Project Information Committee (CPIC), and buildingSmart describes BIM as a digital model of the physical and functional traits of a facility, forming a shared resource of knowledge and providing a dependable basis for decision-making throughout its lifespan, from the earliest conceptual stage to demolition. It is the recognition of BIM as a process, with BIM software systems viewed as tools that enhance these processes. This technological advancement in BIM is used to foster collaboration among the stakeholders by facilitating the exchange of information. The practicality of BIM systems lies in its capability to allow engineers to build the project in a virtual environment before actual construction commences (Vernikos, 2012). By modelling the project virtually before the commencement of the construction on site, BIM provides a degree of precision, overcoming the limitations found in traditional design methods (C. Zhang et al., 2016). This allows for informed decision-making within a virtual environment based on the outcomes of different iterations. BIM is seen as an incentive for other initiatives in the construction industry, such as lean construction, sustainability, and off-site manufacturing.

BIM can significantly improve the off-site manufacturing in a variety of ways. It provides increased accuracy in determining material needs, thereby reducing excess ordering and minimizing waste at construction sites. BIM also helps fabricators and contractors by offering a 3D model that outlines the location of components. BIM can store building data to assist the project's life cycle throughout the maintenance and eventual deconstruction and material recycling at its end of its lifecycle. The proper application of BIM technologies can precisely depict the geometry, behaviour, and properties of individual building components, thereby facilitating their integration into standardized building parts or volumes in a digital format (Nawari, 2012). The

vast amount of information that is linked to BIM models paves the way for collaboration and information exchange between designers, suppliers, manufacturers, and end users. Ezcan et al. (2013) claims that the primary benefits of BIM lie in bridging gaps in off-site manufacturing and its ability to improve designs, enhance collaboration, and serve as a hub for accurate and comprehensive data, thereby avoiding exaggerated lead time, high costs, and modification issues. In summary, Eastman and Sacks (2008) describe BIM as a way to improve off-site manufacturing by allowing "construction data to be machine-readable and components to be manufactured without human intervention."

### **2.2.2 Limitation and challenges**

Despite the technological advancements of BIM and its effectiveness in information exchange with various stakeholders, it is still not capable of supporting the panelized construction in an efficient way (Liu et al., 2017).

In industry practice, the architect who leads the project design tends to focus more on design elements specific to architecture and uses the implicit knowledge through the project design. As such, considerable information is often overlooked and not well documented. Other disciplines encounter the same issue as well. This improper documentation or information exchange results in abortive work, waste, and increased cost.

On the other hand, the growing industrialization of building construction raises the bar for building designers, imposing new challenges on BIM and design requirements in general (Alwisy et al., 2012). To promote the adoption of BIM within the Canadian building industry, especially within the modular or prefabricated construction sector, BIM models must be detailed enough to support the manufacturing process. However, in current practice, developing detailed models requires

substantial manual efforts that professionals are drifting away from, limiting the use of BIM models in the panelized industry. The level of detail (LoD) in building objects within a BIM model varies from LoD 100 to LoD 500 (ASBO, 2013). As LoD increases, more building information and design details are required to be included in the BIM models to represent the size, shape, location, quantity, orientation, and non-geometric information of the building as well (Ramaji and Memari, 2016). The advancement from one LoD level to another can increase the modelling time by two to eleven times (Leite et al., 2011). In most cases, objects built in a BIM model are roughly designed by architects and engineers (i.e., to LoD 300 or less). These models cannot meet the needs of contractors and fabricators, as they require more details for generation of shop drawings and fabrications drawings for manufacturing.

The term “manufacturing-centric BIM” in this study requires a BIM model with an LoD of 350 or higher, that can represent detailed subcomponents of building components, such as ribs, steel connectors, insulation, reinforcement, wood nailer, etc. (Webster, 2014). However, the inclusion of all these details requires a lengthy design process that is labourious and time-consuming. The primary obstacle for professionals who are trying to implement efficient BIM in the construction sector is to find a solution that is cost-effective, as designers must dedicate a substantial amount of time to model the building design at the appropriate level of detail, such as manufacturing-centric BIM (Ding et al., 2014). Additionally, they must ensure that shop drawings are precise enough to fulfill manufacturing requirements. This causes a demand for construction intelligence applications in the design and drafting domains.

### **2.3 BIM-Based automation in design**

Liu et al. (2018) formulated a rule-based strategy for light frame wall paneling, involving designing the boarding layout and planning the material sheet cutting automatically for light-frame

wall panels through BIM integration. The design rules for the layout are implicitly incorporated in the knowledge of tradespeople. Automated design is deduced by exploring all design possibilities to reach the best solution. This method is faster and less susceptible to mistakes compared to traditional manual methods.

Another development FrameX is an application designed to automate the design and drafting of structural elements in light-frame wood construction. The first step in the application is to execute wood design using the platform construction method and generate shop drawings and quantity take-offs automatically in accordance with the BIM model. This process reduces design and drafting time, improves the productivity of the designer, and minimizes errors (Manrique Mogollon, 2009; Alwisy et al., 2012; Liu et al., 2017).

Tian (2019) suggested a knowledge-driven procedure to automate cabinet layout drafting. The cutting stock algorithm, optimized for this purpose, minimizes waste by automatically generating designs to cut cabinet panels from standard-sized wood sheets. More research conducted by Zhang (2022) developed a rule-oriented strategy that integrates the BIM model with the automated design system. This strategy includes a rule-based pipe route planning method and an optimal cutting stock algorithm. This automation streamlines design and production efficiency in the context of panelized construction for a drainage system design.

The aforementioned research discussed the application of an add-on in Revit to automate the design process and is an efficient way to shorten the design process, reduce mistakes, and cut down the overall time for project delivery.

# Chapter 3. Methodology

## 3.1 Overview

This section presents the methodology implemented in this research, which is illustrated in Figure 3-1 as a framework consisting of inputs, criteria, main process, and output. The software Revit is used as the platform for this framework, allowing for the automation of design and drafting for 3i RPCPS.

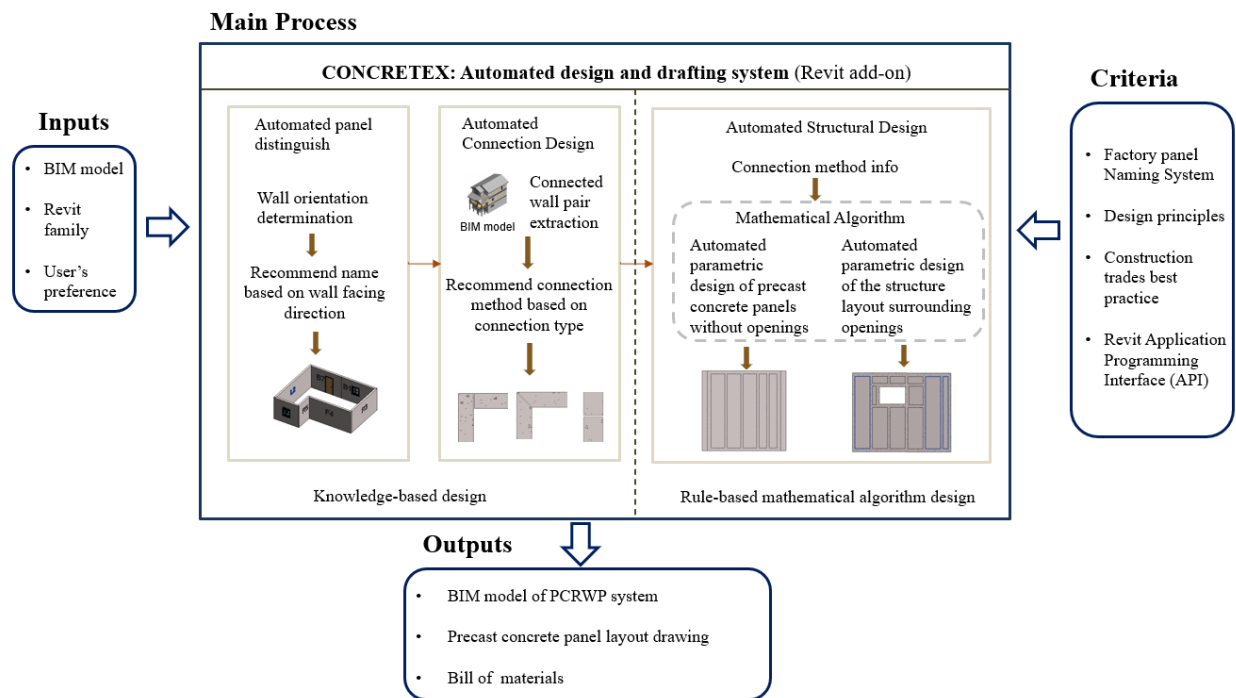


Figure 3-1. Overview of framework.

The system identifies inputs, and corresponding data is collected and stored for later use in different stages, including: (1) The 3D BIM model serves as a primary input for the methodology, providing crucial information about the building's walls and openings, which is then used to automate the design and drafting of the ribbed precast concrete wall panels. This information includes the dimensions and locations of openings, such as doors and windows, which are essential

for designing the structure layout surrounding openings. (2) Revit families offer a standardized and intelligent method for representing building components through parametric 3D models. (3) User preferences can be incorporated into the design process through the user interface, which allows the user to input their design requirements and receive a customized design for the 3i RPCPS.

To set up constraints of the 3i RPCPS generation process, the following four criteria are used: (1) Factory Panel Naming System: uses a standardized naming system for factory panels to ensure consistency and clarity in the design process. (2) Design Principles: adheres to established design principles, including efficiency, sustainability, safety, and regulatory compliance to guide the generation process of 3i RPCPSs. (3) Construction Trades Best Practices: integrates best practices from the construction trades industry to optimize designs for construction, installation, operation, and maintenance of 3i RPCPSs. (4) Revit Application Programming Interface (API): leverages the Revit API to enhance automation capabilities, streamline design workflows, and customize design rules specific to 3i RPCPSs.

Figure 3-1 illustrates the framework for generating an automation design and drafting tool, comprising of two essential components: (1) Knowledge-based design: this component serves as the bedrock of the automation design and drafting tool. Leveraging a repository of domain-specific knowledge from designers, the knowledge-based design empowers the automation tool to generate comprehensive designs that faithfully mirror the results of manual drafting. (2) Rule-based mathematical algorithm design: these algorithms serve as the backbone of the automation tool and are responsible for generating structural layouts for panels.

By clearly defining all inputs and criteria, and establishing a mathematical algorithm, the framework enables the automation of design and drafting processes for a 3i RPCPS. The resulting outputs of this system include a comprehensive 3D model of the 3i RPCPS with accompanying details, production drawings, and a bill of materials (BOM). The successful implementation of this automation system has the potential to significantly streamline the design and drafting process for 3i RPCPSs, providing the construction industry with an efficient and cost-effective solution.

This methodology chapter introduces the rule-based design of the mathematical algorithm.

## **3.2 3i Ribbed Precast Concrete Panel System (3i RPCPS) overview**

The aim of this section is to enhance comprehension of the 3i RPCPS by breaking it down into three distinct components. The first component focuses on the main concrete body, including its structural layout and reinforcement. The second component centers on the Styrofoam XPS (referred as Styrofoam in the remaining of the work) formwork system, while the final segment examines the steel connectors associated with this ribbed precast concrete panel system.

### **3.2.1 Ribbed reinforced concrete panel**

The primary element of the 3i RPCPS is a reinforced concrete panel that features two-way ribs. These ribs are reinforced to provide the panel with increased durability and safety by resisting compression and shear forces. The concrete wall panel structure is available in two variations: The Basic panel and the Energy-Saving panel, which are depicted in Figure 3-2 and Figure 3-3, respectively.

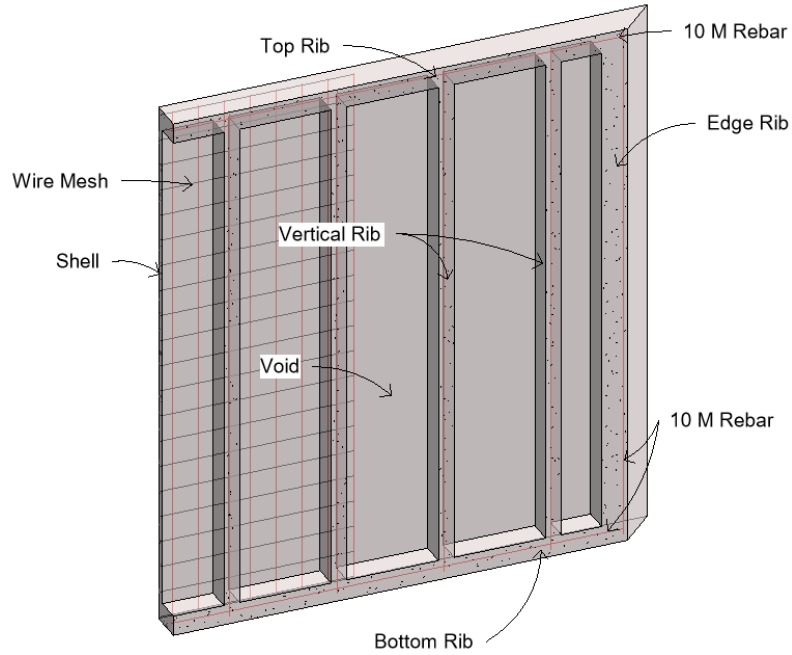


Figure 3-2. Structure layout for basic concrete wall panel.

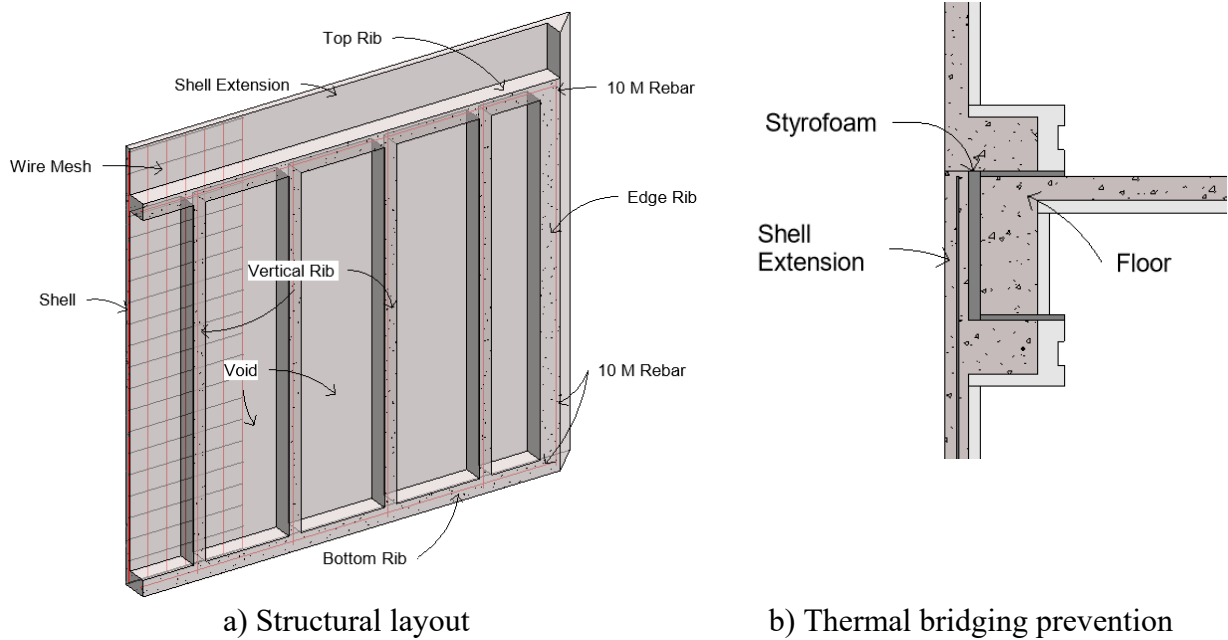


Figure 3-3. Energy-Saving concrete wall panel.

The Energy-Saving panel is designed to work seamlessly with the Energy-Saving precast concrete floor or ceiling to create an integrated precast building system that eliminates thermal bridges. The selection of either the Basic or Energy-Saving panel structure is dependent on the client's ceiling preferences and requirements. To meet the reinforcement criteria for residential buildings according to the national building code (NBC), rebar is incorporated into all ribs, while wire mesh is embedded in the entire Shell area of the wall panel.

The basic definitions of structural components in the research are illustrated in Figure 3-2 and Figure 3-3. The detailed descriptions of the terms are as follows:

- 1) Top and Bottom Rib: ribs are horizontal, reinforced with default 10 M rebar, and located at the top and bottom of the panel. These ribs provide a larger contact surface, making it easier and more stable to bolt the panel to other panels, floors, or ceilings.
- 2) Edge Rib: ribs are located at the two ends of a concrete panel, running vertically from the bottom to the top, and featuring a 45-degree wedge shape.
- 3) Vertical Rib: all ribs that run vertically from the bottom to the top of a concrete panel, located between the two Edge Ribs.
- 4) Void: a cavity located between the Vertical Ribs in a concrete panel. It is designed to save some amount of concrete material and provide space for insulation and electrical wires to pass through inside the panel.
- 5) Shell: a thin layer of concrete that is designed without any ribs.
- 6) Shell Extensions: A Shell Extension is located on the top of an Energy-Saving concrete wall panel type, which is covered with Styrofoam on the interior and used as an exterior cover for the floor to prevent thermal bridging, as shown in Figure 3-3b.

### 3.2.2 Formwork system

The Styrofoam has adequate stiffness to serve as the formwork during precast, and it can increase the R value of concrete panels to reduce conductive flow of heat. Therefore, the Styrofoam formwork can stay on the concrete panel as insulation of the concrete panel system, thus saving time to remove formwork. Different shapes of Styrofoam listed in Figure 3-4 are used to shape different structural components on concrete wall panels. The detailed descriptions of the terms are as follows:

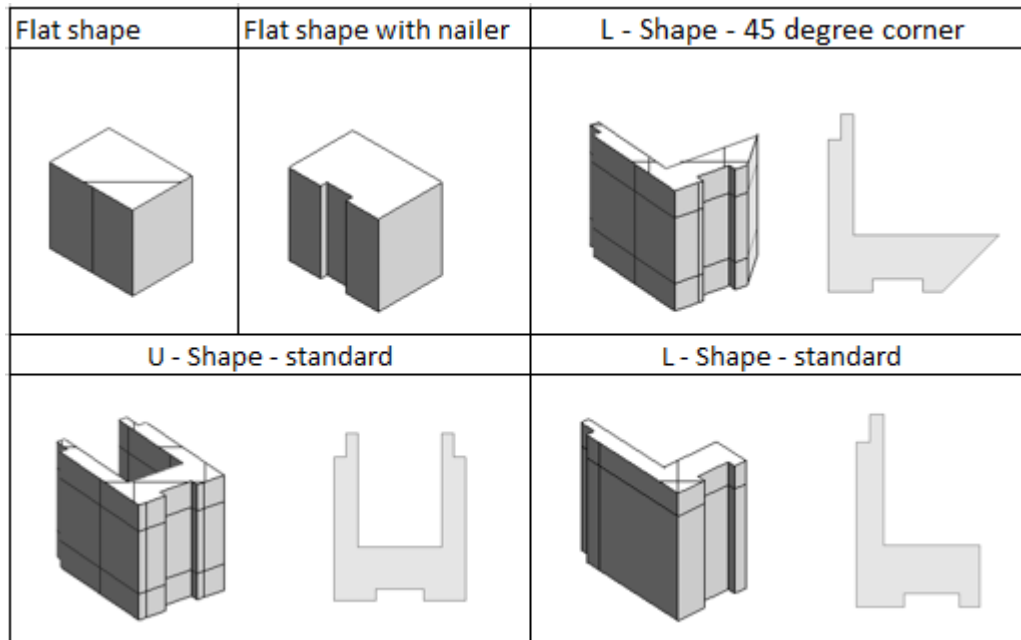


Figure 3-4. Styrofoam in 3i RPCPS.

- 1) Flat-shape: used to shape the surface of the concrete Shell, and can be used between the openings and the Vertical Ribs to secure the openings.
- 2) Flat-shape with Nailer: has the same usage as the Flat-shape, but includes a space designed to place a wood nailer, so that drywall and other finishing can be installed directly on the panels during the onsite installation stage.

- 3) L-shape-45-degree Corner: used to shape the Edge Rib with 45-degree wedge.
- 4) L-shape-standard: used to shape the Top and Bottom Ribs.
- 5) U-shape-standard: used to shape all Vertical Ribs.

Figure 3-5 provides a better understanding of the Styrofoam formwork system by showing the location and usage of the different types of Styrofoam. All the aforementioned Styrofoam is designed with a lip, which can work with the Flat-shape Styrofoam to provide a better seal and prevent leaking during the pouring of concrete. This is illustrated in detail in Figure 3-5.

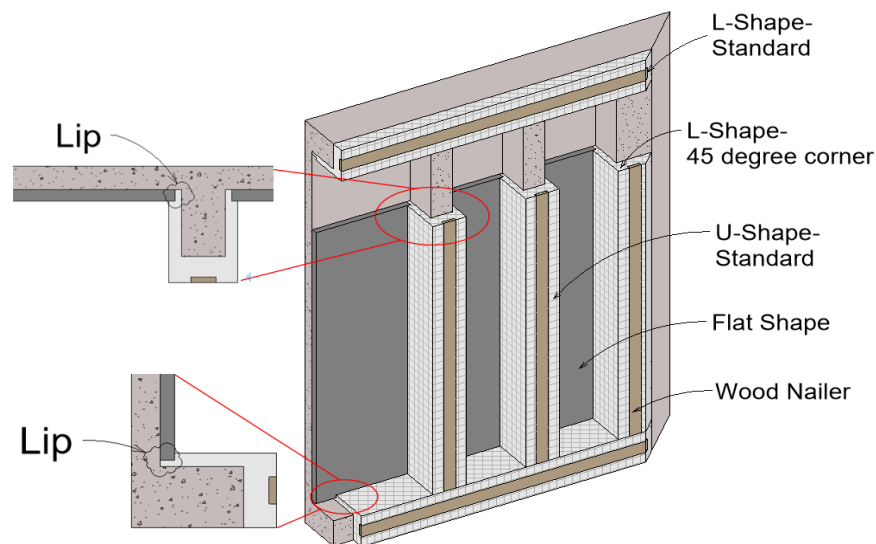


Figure 3-5. Locations and usage of Styrofoam.

### 3.2.3 Connections and lifting

Connecting wall panels together and transporting them to the site requires various steel connectors and parts for tilting and lifting. Figure 3-6 provides basic definitions of the different shapes of steel connectors used in the research. The following are detailed descriptions of the terms:

- 1) L-shape Steel Connector: used on the corner of the concrete wall in the vertical direction to connect two walls together from inside.

- 2) L-shape Flat Steel Connector: used on the corner of the concrete wall to connect two walls together from top and bottom.
- 3) Connecting Insert: an embedded nut in concrete panels to help fasten the steel connector and wall panel together by screwing the bolt into it.
- 4) Wedge Anchor: used for bolting reinforced concrete panels to footings.
- 5) Lifting Anchor: used to tilt up the concrete reinforced ribbed panel 90 degrees from a flat position to a standing position and can also be used to lift panels for transfer and on-site installation.

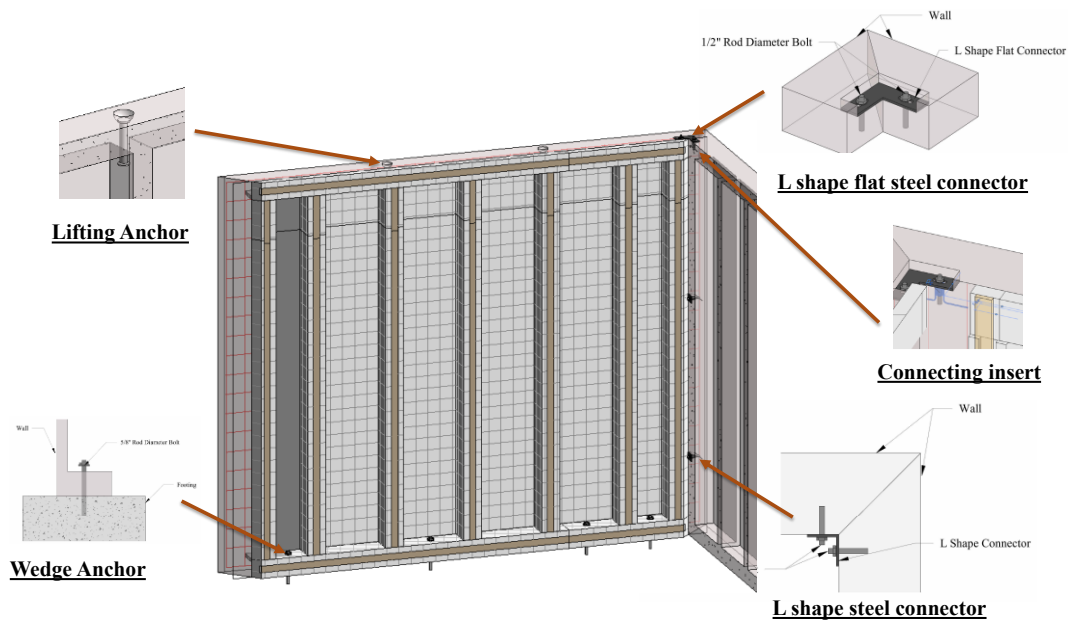


Figure 3-6. Location and usage of steel connectors.

### 3.3 Automated parametric design for solid panel

To automate the generation of a 3i RPCPS, the calculation logic must determine the position of each component within the system. The position is defined as the distance between the component's start-point and the origin in the  $x$ -,  $y$ -, and  $z$ -directions, which represent the

component's start-point coordinates in 3D space. This section introduces the calculation logic for each component, such as ribs, various types of Styrofoam, and steel connectors. Detailed position calculations for various components in the ribbed precast concrete wall panel system are presented in the calculation section below. The parameters used in these calculations are defined for the wall dimensions and other numerical values. The basic definitions of parameters in the research are illustrated in Figure 3-7. Detailed descriptions of the parameters are provided accompanying each given equation.

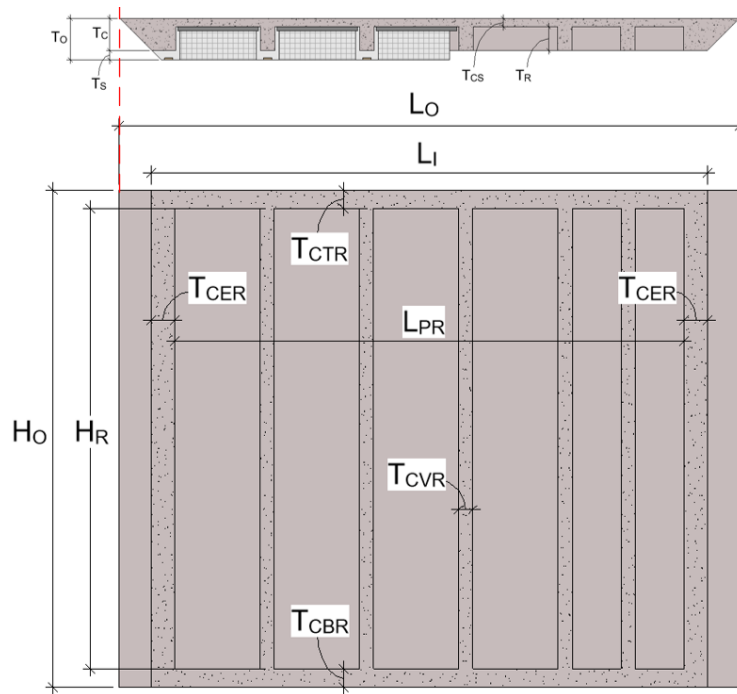


Figure 3-7. Front and top view of ribbed precast concrete wall panel.

The relations between parameters can be expressed as follows:

$$T_R = T_C - T_{CS}$$

$$T_O = T_C + T_S$$

$$H_O = H_R + T_{CBR} + T_{CTR}$$

$$L_I = T_{CER} * 2 + L_{PR}$$

$$L_O = T_C * 2 + L_I = T_C * 2 + T_{CER} * 2 + L_{PR}$$

where:

$T_O$  is the thickness of the ribbed precast concrete wall panel,

$T_c$  is the thickness of concrete composite of the ribbed precast concrete wall panel,

$T_S$  is the thickness of Styrofoam which covered on the Rib structure,

$T_{CS}$  is the thickness of the concrete Shell,

$T_R$  is the depth of the concrete rib, and the depth of the Void,

$T_{CTR}$  is the thickness of the Top Rib,

$T_{CBR}$  is the thickness of the Bottom Rib,

$T_{CER}$  is the thickness of the Edge Rib,

$H_O$  is the height of the ribbed precast concrete wall panel,

$H_R$  is the height of concrete rib, and the height of Void,

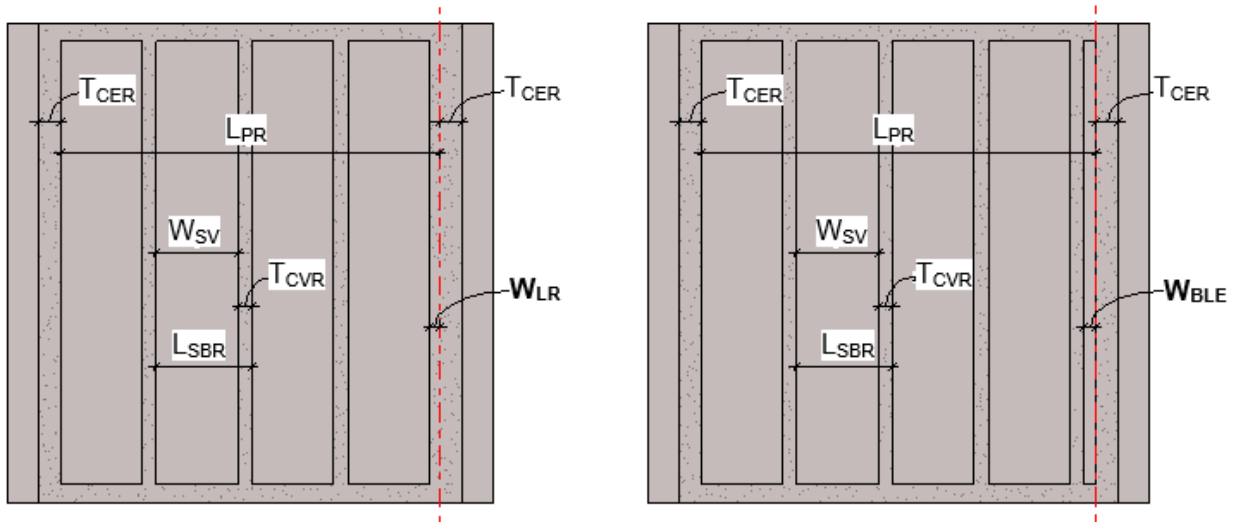
$L_O$  is the length of the ribbed precast concrete wall panel, which is the length of the exterior wall,

$L_I$  is the length of the inner wall, without counting the length of the 45-degree wedge,

$L_{PR}$  is the distance between the Edge Ribs on two ends. The space defined by  $L_{PR}$  is used for placing Vertical Ribs.

### 3.3.1 Logic for Vertical Rib placement

This section introduces the calculation logic used to determine the positions of Vertical Ribs in the 3i RPCPS. Two scenarios for placing Vertical Ribs based on the length for placing Vertical Ribs ( $L_{PR}$ ) are illustrated in Figure 3-8a and Figure 3-8b: (1)  $L_{PR}$  is insufficient to place the last rib, and (2) All ribs can fit into  $L_{PR}$ . In Scenario 1, the width of the last rib ( $W_{LR}$ ) must be defined as a parameter. In Scenario 2, the distance between the last rib and the Edge Rib at the most right ( $W_{BLE}$ ) must be defined as a parameter. Figure 3-8 provides a visual representation of the basic definitions of parameters used in this research. Detailed descriptions of the relevant parameters are provided accompanying each given equation.



a) Scenario 1: Last rib cannot fit in panel

b) Scenario 2: Last rib can fit in panel

Figure 3-8. Different scenarios for placing Vertical Ribs.

Based on the parameters created for the calculation of rib placement, these two scenarios can be represented by the following equations:

$$\text{Scenario 1: } \begin{cases} \text{MOD}(L_{PR}/L_{SBR}) > W_{SV} \\ \text{MOD}(L_{PR}/L_{SBR}) = 0 \end{cases} \quad (3-1)$$

$$\text{Scenario 2: } 0 < \text{MOD}(L_{PR}/L_{SBR}) \leq W_{SV} \quad (3-2)$$

The equation for  $W_{LR}$  is as follows:

$$W_{LR} = \begin{cases} \text{MOD}(L_{PR}/L_{SBR}) - W_{SV} & (\text{MOD}(L_{PR}/L_{SBR}) > W_{SV}) \\ T_{CVR} & (\text{MOD}(L_{PR}/L_{SBR}) = 0) \\ 0 & (0 < \text{MOD}(L_{PR}/L_{SBR}) \leq W_{SV}) \end{cases} \quad (3-3)$$

The equation for  $W_{BLE}$  is as follows:

$$W_{BLE} = \begin{cases} 0 & (\text{MOD}(L_{PR}/L_{SBR}) > W_{SV} \text{ or } = 0) \\ \text{MOD}(L_{PR}/L_{SBR}) & (0 < \text{MOD}(L_{PR}/L_{SBR}) \leq W_{SV}) \end{cases} \quad (3-4)$$

where:

$W_{LR}$  is the width of the last rib if  $L_{PR}$  is not long enough to place the last rib,

$W_{BLE}$  is the distance between the last rib and the rightmost Edge Rib if  $L_{PR}$  can fit all ribs,

$L_{PR}$  is the distance between the Edge Ribs on two ends. The space defined by  $L_{PR}$  is used for placing Vertical Ribs.

$W_{SV}$  is the standard width of the Void, and the standard width between Vertical Ribs,

$T_{CVR}$  is the thickness of the Vertical Rib,

$L_{SBR}$  is the standard distance between ribs from center to center, where  $W_{SV} + T_{CVR} = L_{SBR}$ ,

With the  $W_{LR}$  and  $W_{BLE}$  parameters now defined, the calculation objective is to adjust the rib layout in two cases: (1) when Scenario 1 occurs, and (2) when the distance between the last rib and the rightmost Edge Rib ( $W_{BLE}$ ) is less than 4 inches in Scenario 2. In these cases, the rib layout needs to be adjusted as shown in Figure 3-9, where the last Vertical Rib must be positioned in the middle between the rib on its left and the rightmost Edge Rib. Consequently, the distance between

the last rib and the rib on its left equals the distance between the last rib and the rightmost Edge Rib, which can be defined as parameter  $W_{BRA}$ . Another parameter that needs to be defined is the number of ribs after adjustment ( $N_{RIB}$ ). The basic definitions of these parameters are presented in Figure 3-9, with detailed descriptions provided accompanying each given equation.

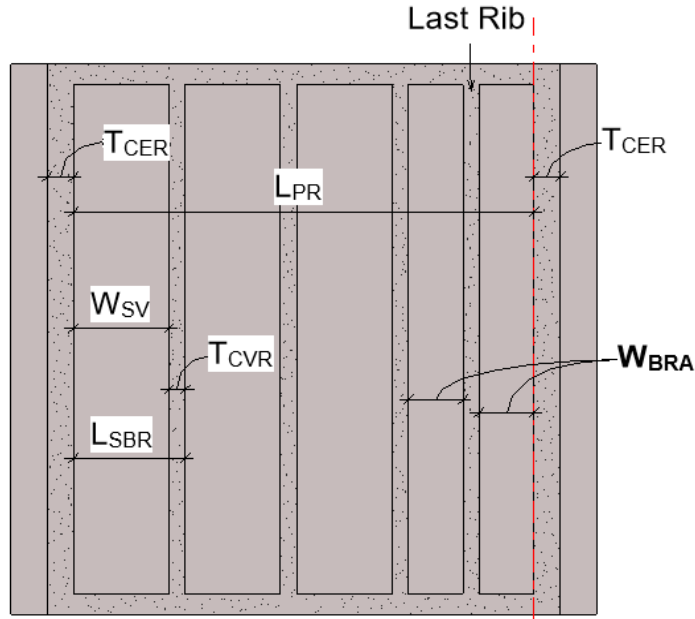


Figure 3-9. Objective structural layout.

The equation for  $N_{RIB}$  is as follows:

$$N_{RIB} = \begin{cases} Roundup(L_{PR}/L_{SBR}, 0) & (MOD(L_{PR}/L_{SBR}) > W_{SV} \text{ or } = 0) \\ Roundup(L_{PR}/L_{SBR}, 0) - 1 & (0 < MOD(L_{PR}/L_{SBR}) \leq W_{SV}) \end{cases} \quad (3-5)$$

where:

$N_{RIB}$  is the number of Vertical Ribs in the adjusted layout of ribs.

The equation for  $W_{BRA}$  is as follows:

$$W_{BRA} = \begin{cases} 0 & (W_{BLE} \geq 4) \\ (W_{SV} + W_{BLE}) / 2 & (0 < W_{BLE} < 4) \\ (W_{SV} - (T_{CVR} - W_{LR})) / 2 & (W_{LR} > 0) \end{cases} \quad (3-6)$$

where:

$W_{BRA}$  is the distance between the last rib and the rib on its left after the rib layout adjustment. It is also the adjusted distance between the last rib and the rightmost Edge Rib.

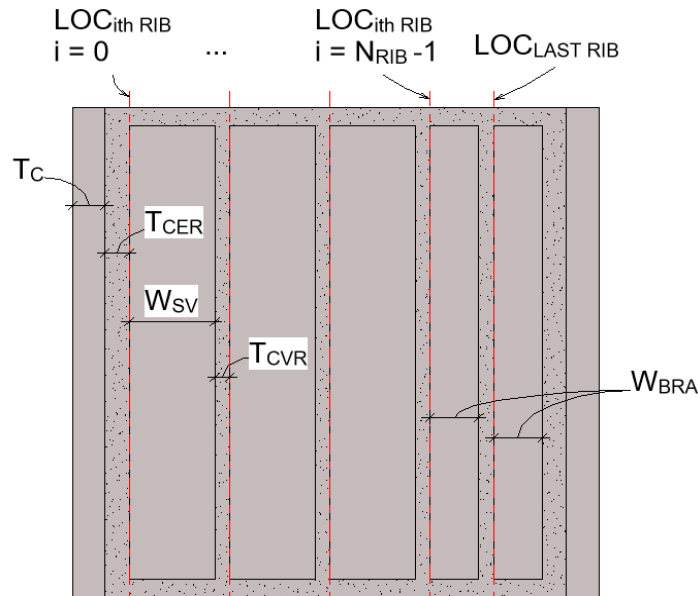


Figure 3-10. Positions of Vertical Ribs.

The locations of ribs and reinforcements can be determined based on the four critical parameters defined earlier:  $W_{LR}$ ,  $W_{BLE}$ ,  $N_{RIB}$ , and  $W_{BRA}$ . The parameters representing the locations of ribs are depicted in Figure 3-10, and their detailed descriptions are presented accompanying each given equation.

The equation for determining the location of the  $i^{th}$  rib for  $i$  in the range  $[0, N_{RIB} - 1]$  after adjustment is as follows:

$$LOC_{i^{th}RIB} = T_C + T_{CER} + (W_{SV} + T_{CVR}) * i \quad (3-7)$$

where:

$LOC_{ith\ RIB}$ : Location of  $i^{th}$  Rib for  $i$  in the range  $[0, N_{RIB} - 1]$ , which is the distance from the original start-point of the wall to the start of the rib in the  $x$ -direction.

The equation for the location of the last rib (after adjustment) is as follows:

$$LOC_{LAST\ RIB} = \quad (3-8)$$

$$\begin{cases} T_C + T_{CER} + (W_{SV} + T_{CVR}) * N_{RIB} & (W_{BLE} \geq 4) \\ T_C + T_{CER} + (W_{SV} + T_{CVR}) * (N_{RIB} - 1) + W_{BRA} + T_{CVR} & (0 < W_{BLE} < 4 \text{ or } W_{LR} > 0) \end{cases}$$

where:

$LOC_{LAST\ RIB}$  is the location of the last rib, which is the distance from the origin to the start of the rib in the  $x$ -direction.

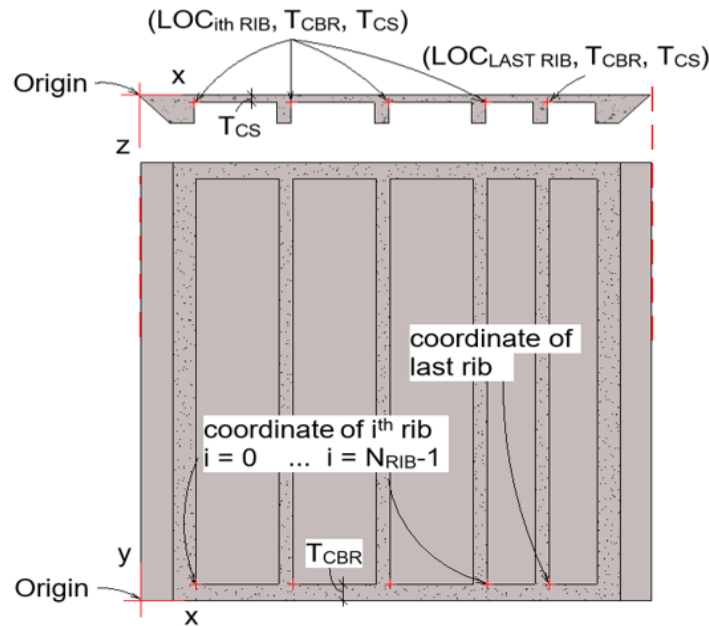


Figure 3-11. Coordinates for start-point of Vertical Rib.

The calculation for the location of the Vertical Rib in the  $x$ -direction enables the start-point coordinates for the rib to be derived. These coordinates are shown in Figure 3-11.

The origin depicted in Figure 3-11 is the origin of the Cartesian coordinate plane for each concrete wall panel, located at the bottom left corner on the exterior wall of every wall panel. It serves as a starting point for the concrete wall panel. Thus, the coordinates for the  $i^{\text{th}}$  rib in 3D space are  $(LOC_{ith\ RIB}, T_{CBR}, T_{CS})$ , and the coordinates of the last rib in 3D space are  $(LOC_{LAST\ RIB}, T_{CBR}, T_{CS})$ .

### 3.3.2 Logic for reinforcement placement

This section presents the calculation logic for determining the respective positions of the wire mesh and various rebar members separately. In this calculation, parameters such as the length and height of the rebar are defined as presented in the following subsections. One important input parameter for this calculation is the concrete cover, which is the minimum distance between the surface of embedded reinforcement and the outer surface of the concrete. The concrete cover determines the start- and end-points of the rebar and wire mesh in the ribbed precast concrete wall panel system. Therefore, three parameters related to the concrete cover are defined, namely,  $C_{CE}$ ,  $C_{CI}$  and  $C_{CO}$ , which are the concrete covers for the exterior, interior, and other face of the wall panel, respectively, as shown in Figure 3-12.



Figure 3-12. Concrete cover in top and section view of concrete panel.

### 3.3.2.1 Rebar in the Top and Bottom Ribs

The parameters used in the calculation of rebar embedded in the Top and Bottom Rib are presented in Figure 3-13. Detailed descriptions of the relevant parameters are provided accompanying each given equation.

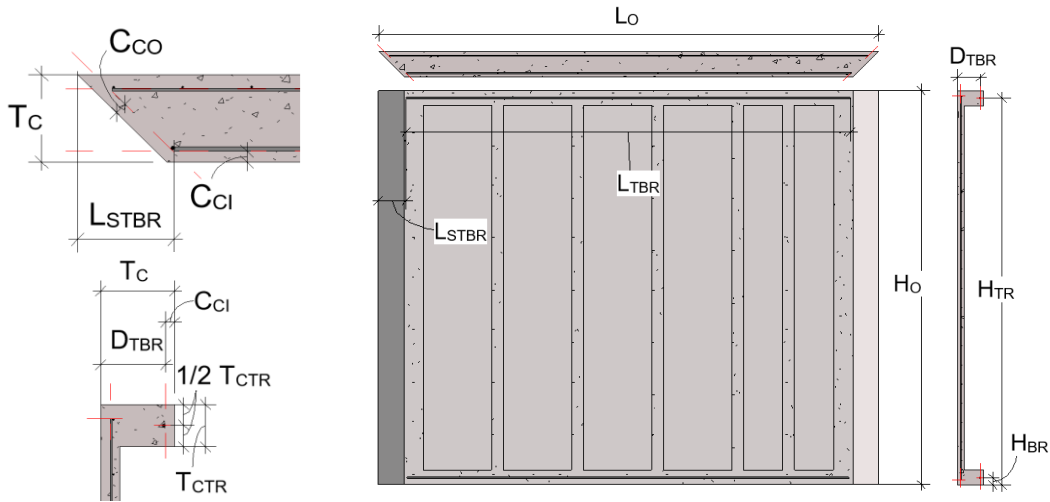


Figure 3-13. Top and section view for rebar embedded in the Top and Bottom Ribs.

The respective equations for  $L_{STBR}$  and  $L_{TBR}$  are as follows:

$$L_{STBR} = T_C - C_{CI} + \sqrt{2} * C_{CO} \quad (3-9)$$

$$L_{TBR} = L_O - 2 * (T_C - C_{CI} + \sqrt{2} * C_{CO}) \quad (3-10)$$

where:

$L_{STBR}$  is the distance between origin to start-point of the Top and Bottom Ribs in the  $x$ -direction,

$L_{TBR}$  is the length of the top and bottom rebar.

The equation for  $D_{TBR}$  is as follows:

$$D_{TBR} = T_C - C_{CI} \quad (3-11)$$

where:

$D_{TRB}$  is the distance between the origin to any point on the Top and Bottom Ribs in the  $z$ -direction.

The respective equations for  $H_{BR}$  and  $H_{TR}$  are as follows:

$$H_{BR} = \frac{1}{2} * T_{CBR} \quad (3-12)$$

$$H_{TR} = H_O - \frac{1}{2} * T_{CTR} \quad (3-13)$$

where:

$H_{BR}$  is the distance between the origin to any point on the Bottom Rib in the  $y$ -direction,

$H_{TR}$  is the distance between the origin to any point on the Top Rib in the  $y$ -direction.

The coordinates of the top and bottom rebar are shown in Table 3-1 below:

Table 3-1. Coordinates of rebar embedded in Top and Bottom Ribs

	Coordinates of start-point	Coordinates of end-point
Top rebar	$(L_{STBR}, H_{TR}, D_{TBR})$	$(L_{STBR} + L_{TBR}, H_{TR}, D_{TBR})$
Bottom rebar	$(L_{STBR}, H_{BR}, D_{TBR})$	$(L_{STBR} + L_{TBR}, H_{BR}, D_{TBR})$

### 3.3.2.2 Rebar in vertical direction

In the previous section, the positioning of horizontal rebar was discussed, and in this section, the focus shifts to determining the positioning of vertical rebar. The parameters involved in calculating the placement of rebar embedded in the Edge and Vertical Ribs are illustrated in Figure 3-14, and detailed descriptions of the relevant parameters are provided accompanying each given equation.

As the location of the Vertical Rib in the  $x$ -direction has already been determined, the location of

the rebar embedded in the Vertical Rib in the  $x$ -direction can be represented using the same parameters as  $LOC_{ith\ RIB}$  and  $LOC_{LAST\ RIB}$  calculated using Equations 3-7 and 3-8.

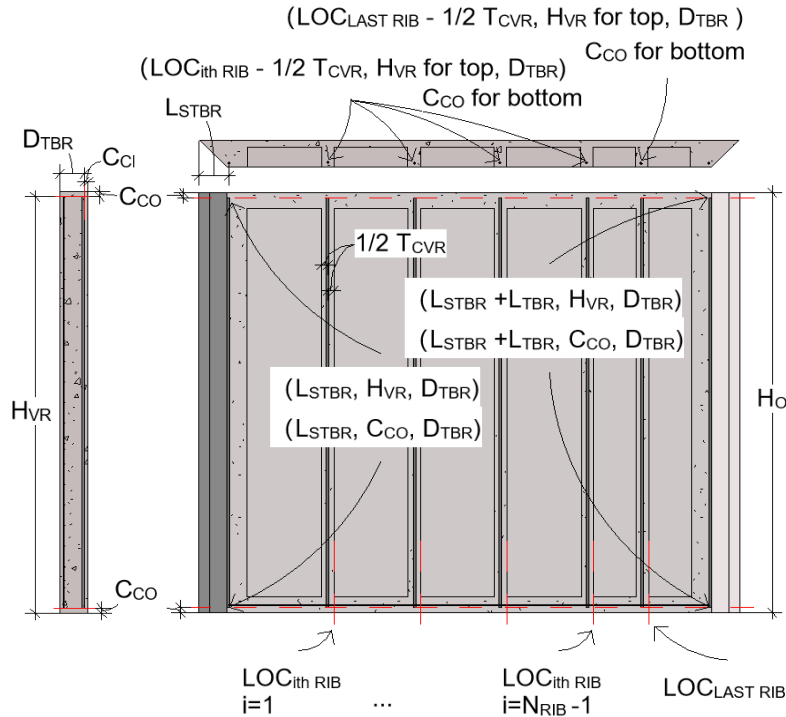


Figure 3-14. Coordinates of rebar embedded in Edge and Vertical Rib.

Figure 3-14 shows the relationship between the position of the Vertical Rib and that of the embedded rebar. The detailed image of the 45-degree wedge in Figure 3-13 illustrates that the rebar embedded in the Edge Rib is at the same location as the start-point of the horizontal rebar embedded in the Top and Bottom Ribs in the  $x$ -direction. Therefore, parameter  $L_{STBR}$ , defined in Equation 3-9, can be used to represent any point on the edge rebar in the  $x$ -direction. Parameter  $D_{TRB}$ , defined in Equation 3-11, can be used to represent any point on the rebar embedded in the Vertical and Edge Ribs in the  $z$ -direction, as the thickness of the concrete cover for the interior face  $C_{CI}$  remains constant along the  $y$ -direction of the wall panel. The coordinates for the ribs embedded in the edge and Vertical Ribs are shown in Figure 3-14.

The equation for  $H_{VR}$  is as follows:

$$H_{VR} = H_O - C_{CO} \quad (3-14)$$

where:

$H_{VR}$  is the distance between origin to top point of rebar in the  $y$ -direction,

$C_{CO}$  is the concrete cover for other face, used as the distance between the origin to the bottom point of the rebar in the  $y$ -direction.

### 3.3.2.3 Wire mesh

In the calculation logic for determining the location of wire mesh, the parameters  $C_{CO}$  and  $H_{VR}$  can be used to denote the start- and end-points of the wire mesh in the  $y$ -direction. This is because the concrete cover on the other face remains constant along the  $x$ -axis of the wall panel. The height of the wire mesh in the  $y$ -direction is equal to the height of the rebar ( $H_{VR}$ ) determined in Equation 3-14. The parameter  $C_{CE}$  can be employed to designate any point on the wire mesh along the  $z$ -axis, as the concrete cover for the exterior face is uniform across the  $xy$ -plane of the wall panel. The parameters that are involved in the location representation in the  $x$ -direction of the wire mesh are illustrated in Figure 3-15, and their detailed explanations are provided accompanying each given equation. Once all the parameters have been defined, they can be used to represent the coordinates of the four corner points on the wire mesh, as depicted in Figure 3-15.

The respective equations for  $L_{SWM}$  and  $L_{WM}$  are as follows:

$$L_{SWM} = C_{CE} + \sqrt{2} * C_{CO} \quad (3-15)$$

$$L_{WM} = L_O - 2 * (C_{CE} + \sqrt{2} * C_{CO}) \quad (3-16)$$

where:

$L_{SWM}$  is the distance between the origin and the start-point of the wire mesh in the  $x$ -direction, and

$L_{WM}$  is the length of the wire mesh in the  $x$ -direction.

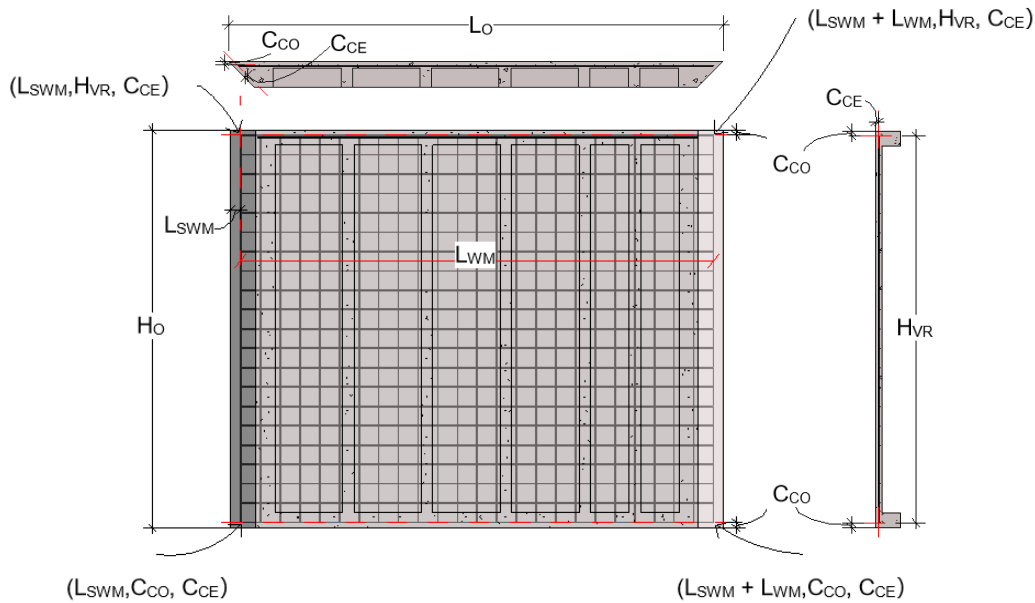


Figure 3-15. Coordinates of wire mesh.

### 3.3.3 Logic for Styrofoam placement

This section introduces the calculation logic for determining the positions of various types of Styrofoam separately. As a result of the constraint of the size of raw material, the maximum length ( $L_{max}$ ) for any type of Styrofoam is limited to 97 inches. If the length of concrete that requires coverage exceeds  $L_{max}$ , it is necessary to determine the start-point of the new, continued Styrofoam piece.

#### 3.3.3.1 L-shape Styrofoam

The L-shape Styrofoam is used as formwork to shape the Top and Bottom Ribs. This section presents the parameters involved in the calculation of the L-shape Styrofoam placement, and their

details are depicted in Figure 3-16. The descriptions of the parameters are presented in detail accompanying each given equation.

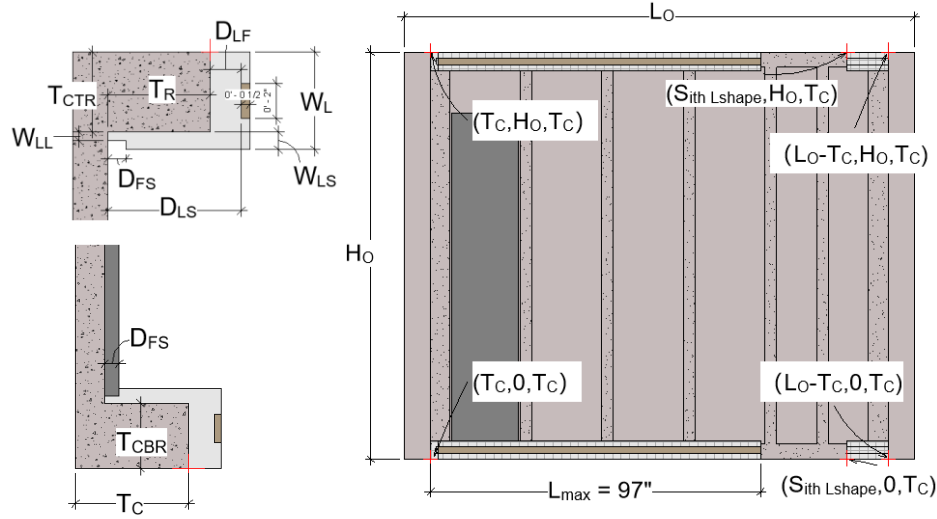


Figure 3-16. Parameters and coordinates of L-shape Styrofoam.

The relations among parameters of the L-shape Styrofoam are shown in the following equations:

$$W_{LL} = \frac{1}{2} * W_{LS} \quad (3-17)$$

$$D_{LS} = D_{LF} + T_R \quad (3-18)$$

$$W_L = T_{CTR} + W_{LS} = T_{CBR} + W_{LS} \quad (3-19)$$

The start-point of  $i^{\text{th}}$  L-shape for  $i$  in the range  $[1, \text{Rounddown}(L_I / L_{max}) + 1]$  in the  $x$ -direction is calculated as follows:

$$S_{ith Lshape} = T_C + (i - 1) * L_{max} \quad (3-20)$$

where:

$W_L$  is the width of the L-shape Styrofoam,

$W_{LS}$  is the width of the side of the L-shape Styrofoam,

$W_{LL}$  is the width of the lip of the L-shape Styrofoam,

$D_{LS}$  is the depth of the L-shape Styrofoam,

$D_{LF}$  is the depth of the face on L-shape Styrofoam,

$D_{FS}$  is the depth of the Flat-shape Styrofoam,

$T_R$  is the depth of the concrete rib, and the depth of the Void,

$T_{CTR}$  is the thickness of the Top Rib,

$T_{CBR}$  is the thickness of the Bottom Rib,

$L_O$  is the length of the ribbed precast concrete wall panel, which is equal to the length of the exterior wall.

Based on the parameters defined above, the coordinates representing the start- and end-points of the L-shape Styrofoam are shown in Figure 3-16.

### **3.3.3.2 U-shape and L-shape-45-degree Corner Styrofoam**

The preceding section addressed the positioning of horizontal Styrofoam, while this section shifts the focus to determining the position of the vertical Styrofoam employed to shape the ribs. The U-shape Styrofoam serves as formwork to shape Vertical Ribs, and the L-shape-45-degree Corner Styrofoam is used to shape Edge Ribs. This section introduces the parameters involved in the calculation of these two types of Styrofoam and depicts their details in Figure 3-17. The descriptions of the parameters are presented in detail under each given equation.

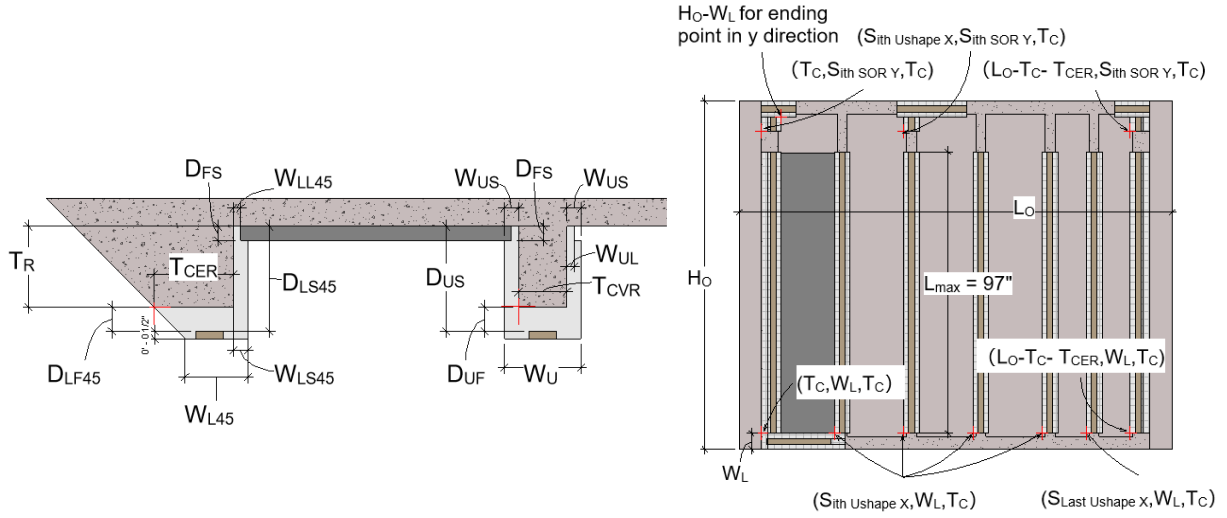


Figure 3-17. Parameters and coordinates of U-shape and L-shape-45-degree Corner Styrofoam.

The relations among parameters are as follows:

$$W_{LL45} = \frac{1}{2} * W_{LS45} \quad (3-21)$$

$$D_{LS45} = D_{LF45} + T_R \quad (3-22)$$

$$W_{L45} = T_{CER} + W_{LS45} - D_{LF45} - 0.5'' \quad (3-23)$$

$$W_{UL} = \frac{1}{2} * W_{US} \quad (3-24)$$

$$D_{US} = D_{UF} + T_R \quad (3-25)$$

$$W_U = T_{CVR} + 2 * W_{US} \quad (3-26)$$

where:

$W_{L45}$  is the width of the L-shape-45-degree Corner Styrofoam,

$W_{LS45}$  is the width of the side on L-shape-45-degree Corner Styrofoam,

$W_{LL45}$  is the width of the lip on L-shape Styrofoam,

$D_{LS45}$  is the depth of the L-shape-45-degree Corner Styrofoam,

$D_{LF45}$  is the depth of the face of the L-shape-45-degree Corner Styrofoam,

$W_U$  is the width of the U-shape Styrofoam,

$W_{US}$  is the width of the side of the U-shape Styrofoam,

$W_{UL}$  is the width of the lip of the U-shape Styrofoam,

$D_{US}$  is the depth of the U-shape Styrofoam,

$D_{UF}$  is the depth of the face on the U-shape Styrofoam,

$D_{FS}$  is the depth of Flat-shape Styrofoam,

$T_R$  is the Depth of the concrete rib, and the depth of the Void,

$T_{CER}$  is the thickness of the Edge Rib,

$T_{CVR}$  is the thickness of the Vertical Rib.

The start-point of  $i^{\text{th}}$  U-shape Styrofoam for  $i$  in the range  $[1, N_{RIB}]$  in the  $x$ -direction is expressed as follows:

$$S_{ith\ Ushape\ x} = \begin{cases} LOC_{ith\ RIB} - T_{CVR} & (i \in [1, N_{RIB} - 1]) \\ LOC_{LAST\ RIB} - T_{CVR} & (i = N_{RIB} \text{ means last rib}) \end{cases} \quad (3-27)$$

where:

$LOC_{ith\ RIB}$  is the location of the  $i^{\text{th}}$  Rib for  $i$  in the range  $[1, N_{RIB} - 1]$ , which is the distance from the original start-point of the wall to the start of the rib in the  $x$ -direction,

LOC<sub>LAST RIB</sub> is the location of the last rib, which is the distance from the origin to the start of the rib in the  $x$ -direction.

The start-point of the  $i^{\text{th}}$  Styrofoam on the rib for  $i$  in the range  $[1, \text{Rounddown}((H_o - 2 * W_L) / L_{max}) + 1]$  in the  $y$ -direction is expressed as follows:

$$S_{ith\ SOR\ Y} = W_L + (i - 1) * L_{max} \quad (3-28)$$

Based the parameters defined above, the coordinates representing the start- and end-points of the U-shape and L-shape-45-degree Corner Styrofoam are shown in Figure 3-17.

### 3.3.3.3 Flat-shape Styrofoam

The Flat-shape Styrofoam is used to shape the surface of the concrete Shell, and also serves as a means of securing openings between the Vertical Ribs. This section introduces the parameters involved in the calculation of the placement of the Flat-shape Styrofoam and depicts their details in Figure 3-18. The descriptions of the parameters are presented in detail accompanying each given equation.

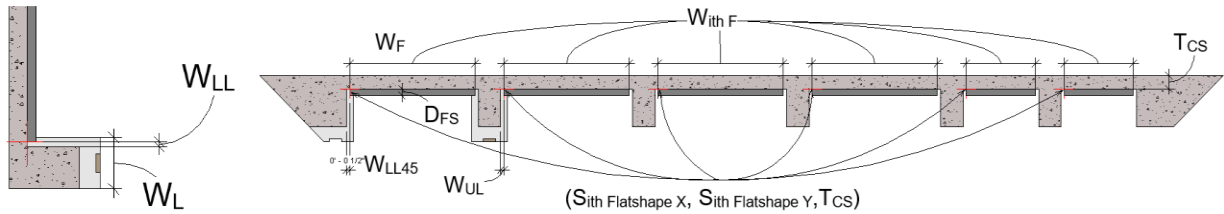


Figure 3-18. Parameters and coordinates of Flat-shape Styrofoam.

The start-point of the  $i^{\text{th}}$  Flat-shape for  $i$  in the range  $[0, N_{RIB}]$  in the  $x$ -direction is expressed as follows:

$$S_{ith Flatshape X} = \begin{cases} LOC_{ith RIB} + W_{LL45} & (i = 0) \\ LOC_{ith RIB} + W_{UL} & (i \in [1, N_{RIB} - 1]) \\ LOC_{LAST RIB} + W_{UL} & (i = N_{RIB}) \end{cases} \quad (3-29)$$

The width of the  $i^{th}$  Flat-shape for  $i$  in the range  $[1, N_{RIB} + 1]$  is expressed as follows:

$$W_{ith FS} = \begin{cases} W_{SV} - W_{LL45} - W_{UL} & (i = 1) \\ W_{SV} - 2 * W_{UL} & (i \in [2, N_{RIB} - 1]) \\ i = N_{RIB} \begin{cases} W_{SV} - 2 * W_{UL} & (W_{BLE} \geq 4) \\ W_{BRA} - 2 * W_{UL} & (0 < W_{BLE} < 4 \text{ or } W_{LR} > 0) \end{cases} \\ i = N_{RIB} + 1 \begin{cases} W_{BLE} - W_{LL45} - W_{UL} & (W_{BLE} \geq 4) \\ W_{BRA} - W_{LL45} - W_{UL} & (0 < W_{BLE} < 4 \text{ or } W_{LR} > 0) \end{cases} \end{cases} \quad (3-30)$$

The start-point of the  $i^{th}$  Flat-shape Styrofoam on the concrete Shell for  $i$  in the range  $[1, Rounddown((H_o - 2 * (W_L - W_{LL})) / L_{max}) + 1]$  in the  $y$ -direction is calculated as follows:

$$S_{ith Flatshape Y} = W_L - W_{LL} + (i - 1) * L_{max} \quad (3-31)$$

where:

$W_F$  is the width of Flat-shape Styrofoam,

$D_{FS}$  is the depth of Flat-shape Styrofoam,

$W_{LL45}$  is the width of the lip on L-shape Styrofoam,

$W_{UL}$  is the width of the lip on U-shape Styrofoam,

$W_L$  is the width of the L-shape Styrofoam,

$W_{LL}$  is the width of the lip on L-shape Styrofoam,

$W_{SV}$  is the standard width of the Void, and the standard width between Vertical Ribs,

$W_{BLE}$  is the distance between the last rib and the rightmost Edge Rib if  $L_{PR}$  can fit all ribs,

$W_{BRA}$  is the distance between the last rib and the rib on its left after the rib layout adjustment. It is also the adjusted distance between the last rib and the rightmost Edge Rib.

The coordinates representing the start-point of the Flat-shape Styrofoam based on the parameters defined above are shown in Figure 3-18.

### 3.3.4 Logic for connection and lifting placement

In this section, the respective calculations for determining the positions of different types of steel connectors are introduced separately.

#### 3.3.4.1 Tilting and lifting

A Lifting Anchor is used to tilt up the concrete reinforced ribbed panel 90 degrees, from lying horizontally to vertically. It can also be used to lift panels up for transfer and on-site installation. The calculations related to the Lifting Anchor in this study include only the number of Lifting Anchors. The position of the Lifting Anchor needs to be determined manually based on the location of the gravity center. The number of Lifting Anchors is determined by considering both the weight of the concrete panel and the capacity of the Lifting Anchor. To prevent the failure of concrete cracking during lifting, a safety factor (SF) is applied. In this research, an even number of Lifting Anchors were designed.

The equation for  $V_{CP}$  is as follows:

$$V_{CP} = ((L_O - T_C) * H_O * T_C - (L_{PR} - T_{CVR} * N_{RIB}) * H_R * T_R) / 61020 \quad (3-32)$$

where:

$V_{CP}$  is the concrete volume used for the concrete wall panel; unit is  $m^3$ . 61020 helps convert the unit from  $inch^3$  to  $m^3$ ,

$T_{CVR}$  is the thickness of the Vertical Rib.

$L_O$  is the length of the ribbed precast concrete wall panel, which is the length of the exterior wall,

$L_{PR}$  is the distance between the Edge Ribs on two ends. The space defined by  $L_{PR}$  is used for placing Vertical Ribs.

The equation for  $W_{CP}$  is as follows:

$$W_{CP} = V_{CP} * \rho_C \quad (3-33)$$

where:

$W_{CP}$  is the weight of concrete used in the concrete panel; unit is ton,

$\rho_C$  is the concrete density; unit is  $ton/m^3$ .

The equation for  $N_{LA}$  is as follows: (3-34)

$$N_{LA} = \begin{cases} Roundup(W_{CP}/CAP_{LA}/SF)/2 & (MOD(Roundup(W_{CP}/CAP_{LA}/SF)/2) = 0 \\ Roundup(W_{CP}/CAP_{LA}/SF)/2 + 1 & (MOD(Roundup(W_{CP}/CAP_{LA}/SF)/2) > 0 \end{cases}$$

where:

$N_{LA}$  is the number of Lifting Anchors needed for the concrete panel.

$CAP_{LA}$  is the capacity of each Lifting Anchor; unit is  $ton/Lifting\ Anchor$ .

### 3.3.4.2 Wedge Anchor

Wedge Anchor is used to bolt reinforced concrete panel to footings. It should be placed at the center at the bottom of every other Void. If the number of Vertical Ribs ( $N_{RIB}$ ) is an odd number, there should also be a Wedge Anchor put in the last Void. Therefore, the number and locations of Wedge Anchors can be determined based on the number and locations of ribs ( $N_{RIB}$ ,  $LOC_{ith\ RIB}$ ,  $LOC_{LAST\ RIB}$ ) as calculated using Equations 3-5, 3-7, and 3-8. The parameters involved in the

calculation of a Wedge Anchor are illustrated in Figure 3-19. Detailed descriptions of the parameters are presented accompanying each given equation.

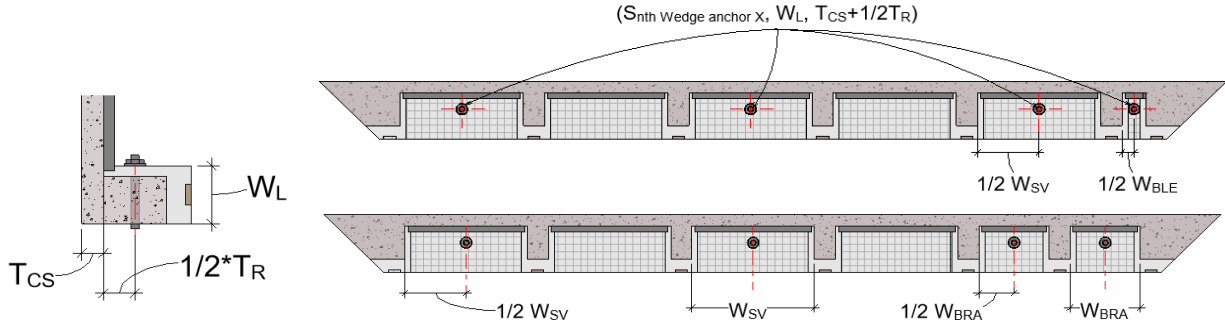


Figure 3-19. Coordinates of Wedge Anchor.

The equation for calculating the number of Wedge Anchors ( $N_{WEDGE\ ANCHOR}$ ) needed for a concrete panel is as follows:

$$N_{WEDGE\ ANCHOR} = \begin{cases} \frac{N_{RIB}}{2} + 1 & (MOD(N_{RIB}/2) = 0) \\ \frac{(N_{RIB}+1)}{2} + 1 & (MOD(N_{RIB}/2) \neq 0) \end{cases} \quad (N_{RIB} > 0) \quad (3-35)$$

The start-point of the  $n^{th}$  Wedge Anchor for  $n$  in the range  $[1, N_{WEDGE\ ANCHOR}]$  in the  $x$ -direction is calculated as follows:

When the number of ribs ( $N_{RIB}$ ) is even, which can be represented by the following equation:

$$MOD(N_{RIB}/2) = 0$$

$$S_{n^{th}\ Wedge\ anchor\ X} \quad (3-36)$$

$$= \begin{cases} LOC_{ith\ RIB} + \frac{1}{2} * W_{SV} & (n \in [1, N_{WEDGE\ ANCHOR} - 1]) \\ n = N_{WEDGE\ ANCHOR} \begin{cases} LOC_{LAST\ RIB} + \frac{1}{2} * W_{BLE} & (W_{BLE} \geq 4) \\ LOC_{LAST\ RIB} + \frac{1}{2} * W_{BRA} & (0 < W_{BLE} < 4\ or\ W_{LR} > 0) \end{cases} \end{cases}$$

For  $i$  in  $LOC_{ith\ RIB}$ :  $i = (n - 1) * 2$

When the number of ribs ( $N_{RIB}$ ) is odd, which can be represented by the equation:

$$MOD(N_{RIB}/2) \neq 0$$

$$S_{n^{th}\ Wedge\ anchor\ X} \tag{3-37}$$

$$= \begin{cases} LOC_{ith\ RIB} + \frac{1}{2} * W_{SV} & (n \in [1, N_{WEDGE\ ANCHOR} - 2]) \\ n = N_{WEDGE\ ANCHOR} - 1 \begin{cases} LOC_{ith\ RIB} + \frac{1}{2} * W_{SV} & (W_{BLE} \geq 4) \\ LOC_{ith\ RIB} + \frac{1}{2} * W_{BRA} & (0 < W_{BLE} < 4\ or\ W_{LR} > 0) \end{cases} \\ n = N_{WEDGE\ ANCHOR} \begin{cases} LOC_{LAST\ RIB} + \frac{1}{2} * W_{BLE} & (W_{BLE} \geq 4) \\ LOC_{LAST\ RIB} + \frac{1}{2} * W_{BRA} & (0 < W_{BLE} < 4\ or\ W_{LR} > 0) \end{cases} \end{cases}$$

For  $i$  in  $LOC_{ith\ RIB}$ :  $i = (n - 1) * 2$

The coordinates representing the positions of the Wedge Anchors based on the parameters defined above are shown in Figure 3-19.

### 3.4 Design of structure layout around opening

The aforementioned section discussed the manufacturing of a typical ribbed panel. However, several panels are required to accommodate various openings that occur in typical residential buildings. These openings may include doors or windows, and may vary in dimension and location within the panel. While openings appear on a panel, additional beams and ribs are needed to strengthen the structure around the openings.

If Vertical Ribs are placed on both sides of the opening and Cripple Ribs are inserted at equal distances between the Vertical Ribs, as shown in Figure 3-20a, the consistent Vertical Rib spacing

is disrupted. Therefore, to keep the beneficial and consistent distance between Vertical Ribs, as shown in Figure 3-20b, horizontal ribs can be placed above and below the opening between the standard Vertical Ribs that are closest to the opening. Side Ribs can then be placed between the top and bottom horizontal ribs next to the opening. To maintain the integrity of the panel, Cripple Ribs are used instead of Vertical Ribs, and are placed above and below the window opening at the same location where the Vertical Rib would have been.

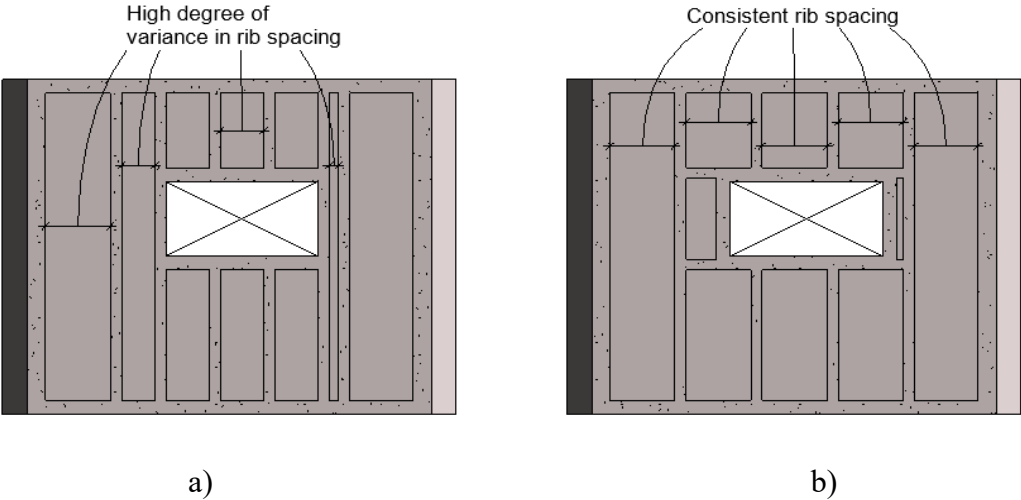


Figure 3-20. The contrast between two designs.

This design helps maintain the consistent distance between the Vertical Ribs while accommodating openings of different dimensions and locations within the panel. By adding additional beams and ribs around the opening, the structure’s strength is reinforced without disrupting the even spacing of the Vertical Ribs. This is an important feature of the concrete panel system, as it allows for greater flexibility in design while maintaining the benefits of a consistent manufacturing process. The details of the layout design are introduced in the next section.

The design of the structure around the opening highlights the benefits of the concrete panel system. This new design considers not only the design stage, but also the manufacturing and installation

stages. Instead of relying on feedback, feedforward is used to provide future-oriented solutions and shorten the time required for the manufacturing and installation processes.

During the manufacturing stage, Styrofoam blocks are used to support the formwork Styrofoam during concrete pouring and curing. To ensure even support, the blocks must have exact dimensions. By maintaining the same distance between the Vertical Ribs on the concrete panel, different sizes of supporting blocks do not need to be produced each time for panels of different sizes. This not only saves time and money but also allows for the unlimited reuse of the same size of supporting block during the manufacturing stage. Additionally, it makes setting up the formwork easier for workers, which saves production time and reduces human error.

Furthermore, during the installation stage onsite, drywall or other finishing materials can be installed directly onto the ribbed precast concrete wall panel. Due to the consistent 2-foot Vertical Rib spacing, which aligns with the standard 4-foot wide and 8-foot long drywall sheets, the need for cutting the plywood sheets is minimized, saving raw material and reducing waste. This also makes the installation process more efficient and reduces the risk of errors, ensuring a smoother and faster installation process.

### **3.5 Automated parametric design of precast wall panels with openings**

#### **3.5.1 Structure layout around window openings**

There are two types of openings in this concrete wall panel system: windows and doors. Given that the structural layout around the openings differs from the structural layout without openings in Section 3.2, this section describes how layout change affects the positioning of the ribs. The basic definitions of structural components' designs to accommodate openings are illustrated in Figure 3-21b. The detailed descriptions of the terms are as follows:

- (1) Header Rib: horizontal rib located above the opening.
- (2) Sill Rib: horizontal rib located below the opening.
- (3) Side Rib: vertical rib located on the left and right sides of the opening.
- (4) Cripple Rib: vertical rib located above the Header or below the Sill Rib.

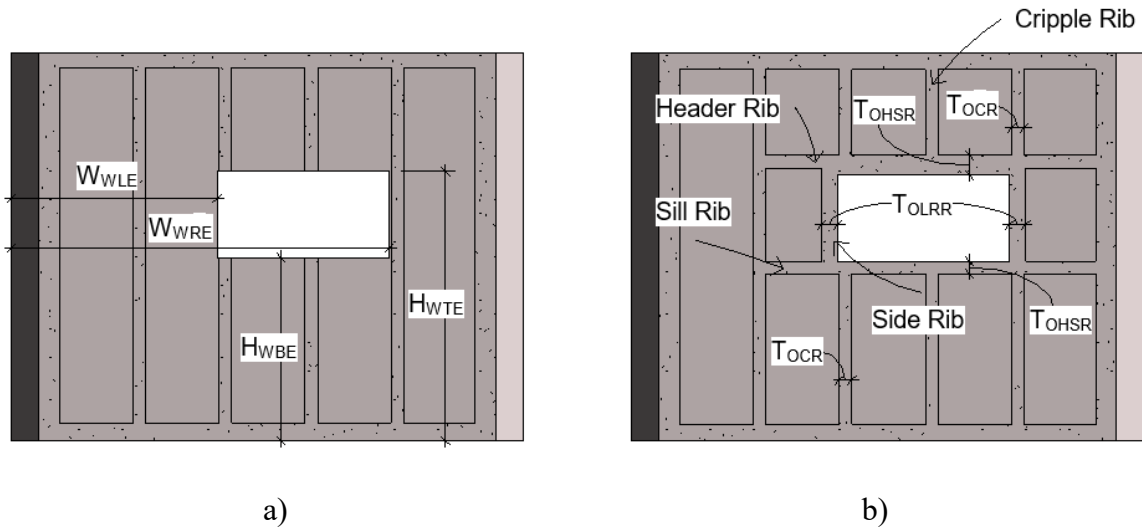
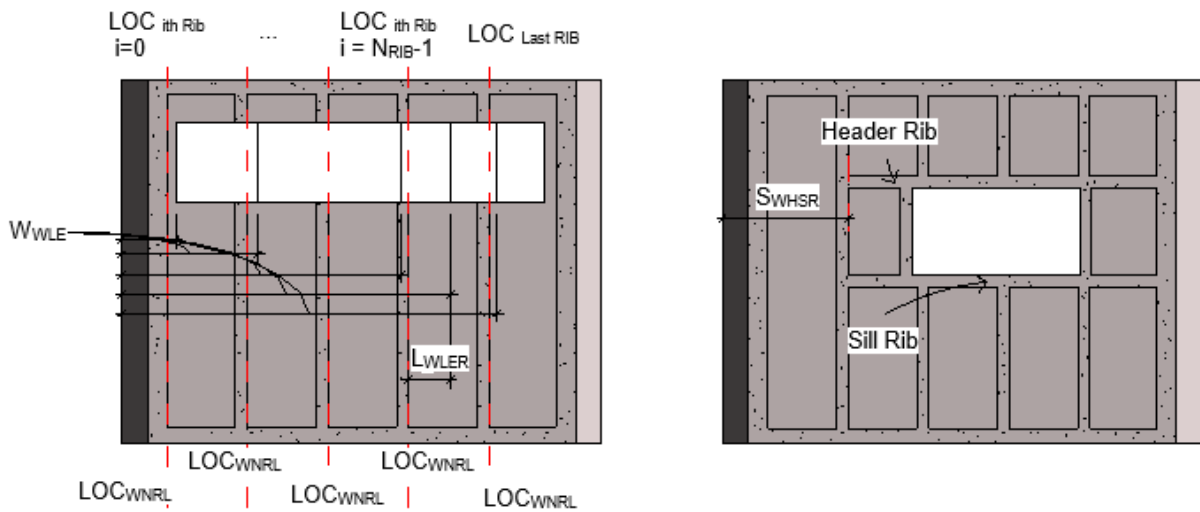


Figure 3-21. Parameters for the structural layout around window opening.

In this section, the calculation logic used to determine the positions of the ribs around a window opening is introduced. Basic parameters related to window opening such as the height of the bottom and top edges ( $H_{WBE}$ ,  $H_{WTE}$ ), and the distance between the origin and the left/right edge of the window ( $W_{WLE}$ ,  $W_{WRE}$ ) in the  $x$ -direction are illustrated in Figure 3-21a. Moreover, the parameters representing the thickness of ribs around an opening are illustrated in Figure 3-21b, where  $T_{OHSR}$  is the thickness of the Header and Sill Ribs around the opening,  $T_{OLRR}$  is the thickness of the left and right ribs around the opening, and  $T_{OCR}$  is the thickness of the Cripple Rib below and above the opening.

### 3.5.1.1 Header and Sill Ribs

The respective start- and end-points of the Header and Sill Ribs are determined separately. Although the location of the window on each concrete wall panel may vary, the principle for generating the rib structure around it remains the same. As noted in Section 3.3, the standard distance between Vertical Ribs is not subject to change. The Header and Sill Rib are positioned between the Vertical Ribs, their locations, in turn, having been determined using Equations 3-7 and 3-8. Therefore, the location of Vertical Ribs ( $LOC_{ith\ RIB}$ ,  $LOC_{LAST\ RIB}$ ) can serve as a reference line. By comparing the  $LOC_{ith\ RIB}$  and the location of the window edge ( $W_{WLE}$ ,  $W_{WRE}$ ), the location of the nearest rib ( $LOC_{WNRL}$ ,  $LOC_{WNRR}$ ) next to the window edge can be identified. Using the distance between the nearest rib and the window edge ( $L_{WLER}$ ,  $L_{WRE}$ ), the start- and end-points of the Header and Sill Ribs can be determined.



a) Window left edge position variability

b) Start-point of Header/Sill Rib

Figure 3-22. Determining window opening parameters for Header and Sill Rib start-points.

Figure 3-22a demonstrates the possible locations of the window opening's left edge along the  $x$ -direction, which can exist anywhere between the Vertical Ribs. By comparing the  $W_{WLE}$  value

with the Vertical Rib locations ( $LOC_{i^{th}RIB}$ ,  $LOC_{LAST RIB}$ ), the nearest Vertical Rib to the left side of the window can be identified. The start-point of the Header Rib ( $S_{WHSR}$ ), as shown in Figure 3-22b, can then be determined by calculating the distance between nearest Vertical Rib and the window's left edge ( $L_{WLER}$ ). Detailed descriptions of the relevant parameters are provided accompanying each given equation.

The following equation represents the location of the nearest Vertical Rib to the left side of the window ( $LOC_{WNRL}$ ) along the  $x$ -direction:

$$LOC_{WNRL} \quad (3-38)$$

$$= \begin{cases} LOC_{i^{th}RIB} & (LOC_{i^{th}RIB} + W_{US} \leq W_{WLE} < LOC_{i+1^{th}RIB} + W_{US} \quad i \in [0, N_{RIB} - 1]) \\ LOC_{N_{RIB}-1^{th}RIB} & (LOC_{i^{th}RIB} + W_{US} \leq W_{WLE} < LOC_{LAST RIB} + W_{US} \quad i = N_{RIB} - 1) \\ LOC_{LAST RIB} & (LOC_{LAST RIB} + W_{US} \leq W_{WLE}) \end{cases}$$

where:

$W_{US}$  is the width of the side of the U-shape Styrofoam.

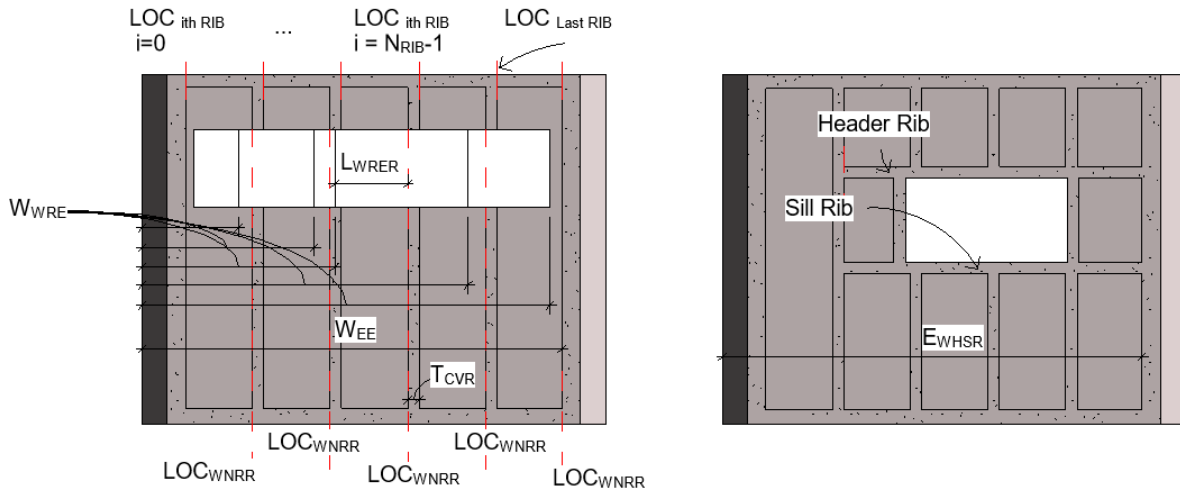
The equation for calculating the distance between the left edge of the window opening and the nearest Vertical Rib ( $L_{WLER}$ ) in the  $x$ -direction is as follows:

$$L_{WLER} = W_{WLE} - LOC_{WNRL} \quad (3-39)$$

The start-point of the Header/Sill Rib around window opening in the  $x$ -direction is calculated as follows (the value of  $i$  from Equation 3-38 is used):

$$S_{WHSR} = \begin{cases} i = 0 & LOC_{0^{th}RIB} \\ 1 \leq i \leq N_{RIB} - 1 & \begin{cases} LOC_{i-1^{th}RIB} & (3 < L_{WLER} < 6.5) \\ LOC_{i^{th}RIB} & (L_{WLER} \leq 3 \text{ or } L_{WLER} \geq 6.5) \end{cases} \\ i = N_{RIB} & \begin{cases} LOC_{N_{RIB}-1^{th}RIB} & (3 < L_{WLER} < 6.5) \\ LOC_{LAST RIB} & (L_{WLER} \leq 3 \text{ or } L_{WLER} \geq 6.5) \end{cases} \end{cases} \quad (3-40)$$

Figure 3-23a demonstrates the potential positions of the window's right edge. The end-point of the window's Header Rib can be determined using the same logic described in the previous paragraph. By comparing the location of the Vertical Ribs with the location of the window's right edge ( $W_{WRE}$ ), the end-point of the Header Rib can be determined. The basic definitions of the parameters involved in this calculation are illustrated in Figure 3-23, and detailed descriptions of the parameters are presented accompanying each given equation.



a) Window right edge position variability

b) End-point of Header/Sill Rib

Figure 3-23. Determining window opening parameters for Header and Sill Rib end-points.

The equation for calculating the location of nearest rib next to the right side of window ( $LOC_{WNRR}$ ) in the  $x$ -direction is as follows:

$$\begin{aligned}
 & LOC_{WNRR} && (3-41) \\
 & = \begin{cases} LOC_{i+1}^{th} RIB - T_{CVR} & (LOC_{i}^{th} RIB - T_{CVR} - W_{US} \leq W_{WRE} < LOC_{i+1}^{th} RIB - T_{CVR} - W_{US} \quad i \in [0, N_{RIB} - 1]) \\ LOC_{LAST RIB} - T_{CVR} & (LOC_{i}^{th} RIB - T_{CVR} - W_{US} \leq W_{WRE} < LOC_{LAST RIB} - T_{CVR} - W_{US} \quad i = N_{RIB} - 1) \\ W_{EE} & (LOC_{LAST RIB} - T_{CVR} - W_{US} \leq W_{WRE}) \end{cases}
 \end{aligned}$$

where:

$W_{EE}$  is the distance between the origin and the rightmost Edge Rib in the  $x$ -direction.

The equation for calculating the distance between the right edge of the window opening and the nearest rib next to it ( $L_{WRER}$ ) in the  $x$ -direction is as follows:

$$L_{WRER} = LOC_{WNRR} - W_{WRE} \quad (3-42)$$

The end-point of the Header/Sill Rib around the window opening in the  $x$ -direction is calculated as follows (the value of  $i$  from the calculation of  $LOC_{WNRR}$  is used):

$$E_{WHSR} = \begin{cases} 0 \leq i < N_{RIB} - 2 & \begin{cases} LOC_{i+2^{th}RIB} - T_{CVR} & (3 < L_{WRER} < 6.5) \\ LOC_{i+1^{th}RIB} - T_{CVR} & (L_{WRER} \leq 3 \text{ or } L_{WRER} \geq 6.5) \end{cases} \\ i = N_{RIB} - 2 & \begin{cases} LOC_{LAST RIB} - T_{CVR} & (3 < L_{WRER} < 6.5) \\ LOC_{i+1^{th}RIB} - T_{CVR} & (L_{WRER} \leq 3 \text{ or } L_{WRER} \geq 6.5) \end{cases} \\ i = N_{RIB} - 1 & \begin{cases} W_{EE} & (3 < L_{WRER} < 6.5) \\ LOC_{LAST RIB} - T_{CVR} & (L_{WRER} \leq 3 \text{ or } L_{WRER} \geq 6.5) \end{cases} \\ i = N_{RIB} & W_{EE} \end{cases} \quad (3-43)$$

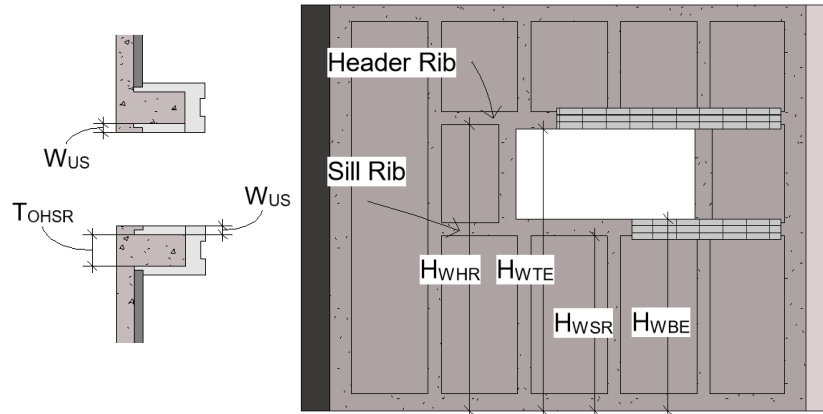


Figure 3-24. Header and Sill Rib parameters in the  $y$ -direction.

The subsequent step involves determining the height of the window Sill Rib ( $H_{WSR}$ ) and the height of the Header Rib ( $H_{WHR}$ ). This process takes into account the width of the U-shape Styrofoam used as formwork for the rib structure surrounding the window opening. Figure 3-24 presents the relevant details for this step.

The equation for calculating the height of the window Sill Rib ( $H_{WSR}$ ) is as follows:

$$H_{WSR} = H_{WBE} - W_{US} - T_{OHSR} \quad (3-44)$$

where:

$H_{WBE}$  is the height of the window's bottom edge,

$T_{OHSR}$  is the thickness of the Header and Sill Ribs around the opening.

The equation for calculating the height of the window Header Rib ( $H_{WHR}$ ) is as follows:

$$H_{WHR} = H_{WTE} + W_{US} \quad (3-45)$$

where:

$H_{WTE}$  is the height of the window's top edge,

$W_{US}$  is the width of the side on U-shape Styrofoam.

Based on the parameters defined above, the coordinates representing the respective positions of the window Header and Sill Rib are shown in Figure 3-25.

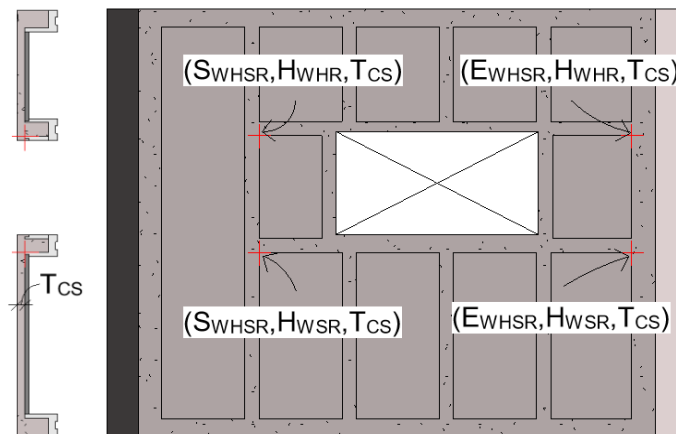


Figure 3-25. Header and Sill Rib Coordinates around window opening.

### 3.5.1.2 Window Side Rib

In order to provide stable support around the window opening, two Side Ribs must be placed adjacent to each side of the window's left and right edges. To locate the Side Rib, the distance between the start- or end-point of the Header Rib and the left or right edge of the window is calculated. Depending on the calculated distance, it can be determined whether the Side Rib needs to be placed or not. The respective locations of the left and right Side Ribs are determined separately.

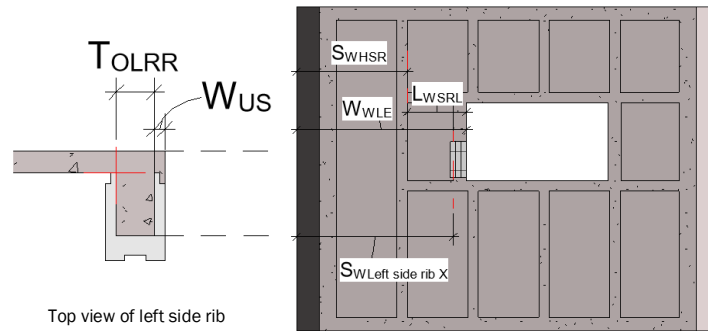


Figure 3-26. Left Side Rib parameters around window opening.

The first step is to calculate the location of the left Side Rib in the  $x$ -direction. The basic parameters involved in this calculation are defined in Figure 3-26, with detailed descriptions of the relevant parameters provided accompanying each given equation.

The equation for determining the distance between the start-point of the Header Rib and the left edge of the window ( $L_{WSRL}$ ) is as follows:

$$L_{WSRL} = W_{WLE} - S_{WHSR} \quad (3-46)$$

where:

$W_{WLE}$  is the distance between the origin and the left edge of the window,

$S_{WHSR}$  is the start-point of the Header/Sill Rib around the window opening in the  $x$ -direction.

The equation for determining the start-point of the window left Side Rib in the  $x$ -direction is as follows:

$$S_{W_{Left\ side\ rib\ X}} = \begin{cases} \text{no left rib will be placed} & (L_{WSRL} \leq 3) \\ W_{WLE} - W_{US} - T_{OLRR} & (L_{WSRL} > 3) \end{cases} \quad (3-47)$$

where:

$T_{OLRR}$  is the thickness of the left and right ribs around the opening,

$W_{US}$  is the width of the side of the U-shape Styrofoam.

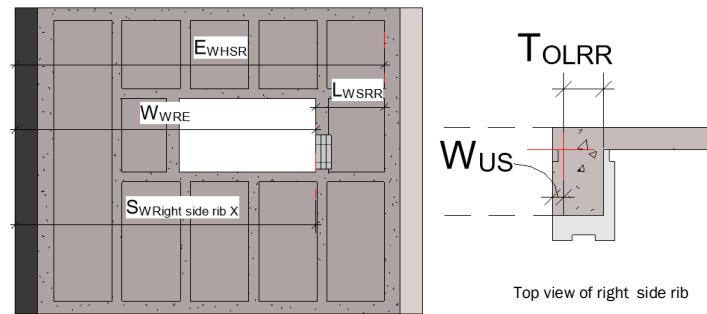


Figure 3-27. Right Side Rib parameters around window opening.

Next, the location of the right Side Rib in the  $x$ -direction is calculated. The basic definitions of the parameters involved in this calculation are illustrated in Figure 3-27, with detailed descriptions provided under the relevant equations.

The equation for calculating the distance between the end-point of the Header Rib and the right edge of the window ( $L_{WSRR}$ ) is as follows:

$$L_{WSRR} = E_{WHSR} - W_{WRE} \quad (3-48)$$

where:

$W_{WRE}$  is the distance between the origin and the right edge of the window,

$E_{WHSR}$  is the end-point of the Header/Sill Rib around the window opening in the  $x$ -direction.

The start-point of the right Side Rib in the  $x$ -direction is calculated as follows:

$$S_{WRight\ side\ rib\ x} = \begin{cases} \text{no right rib will be placed} & (L_{WSRR} \leq 3) \\ W_{WRE} + W_{US} & (L_{WSRR} > 3) \end{cases} \quad (3-49)$$

where:

$W_{US}$  is the width of the side of the U-shape Styrofoam.

The fundamental definitions of the parameters involved in the calculation for determining the start- and end-points of the Side Rib in the  $y$ -direction are demonstrated in Figure 3-28. Detailed explanations of the relevant parameters are provided accompanying each given equation.

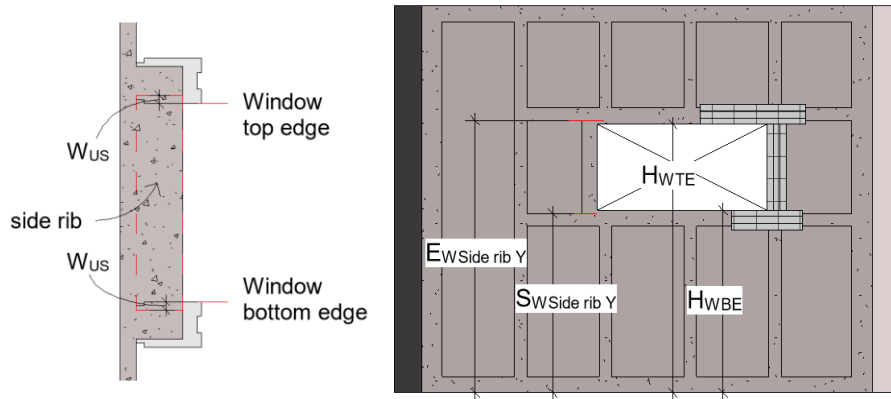


Figure 3-28. Side Rib parameters around window opening in the  $y$ -direction.

The start-point of the Side Rib in the  $y$ -direction is calculated as follows:

$$S_{WSide\ rib\ Y} = H_{WBE} - W_{US} \quad (3-50)$$

where:

$H_{WBE}$  is the height of the window's bottom edge.

The end-point of the Side Rib in the  $y$ -direction is calculated as follows:

$$E_{WSide\ rib\ Y} = H_{WHR} = H_{WTE} + W_{US} \quad (3-51)$$

where:

$H_{WHR}$  is the height of the window Header Rib,

$H_{WTE}$  is the height of the window's top edge.

Based on the parameters defined above, the coordinates representing the position of the window Side Rib are shown in Figure 3-29.

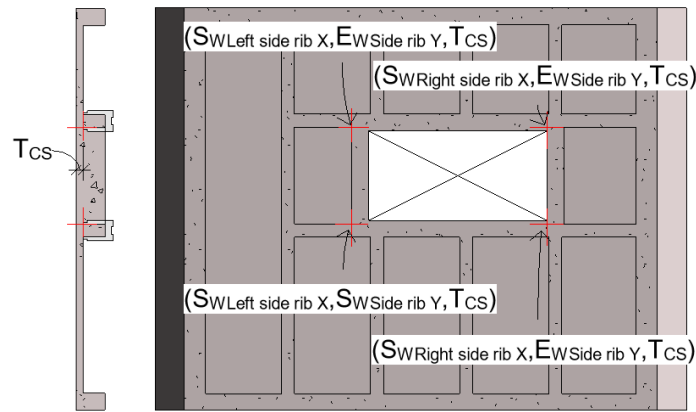


Figure 3-29. Side Rib coordinates around window opening.

### 3.5.1.3 Cripple Rib

In Section 3.2, the concrete panel without an opening was introduced, where the Vertical Ribs are placed at a standard distance from each other. However, in this section, the inclusion of openings breaks the continuity of Vertical Ribs. To maintain the integrity of the panel, Cripple Ribs are used instead of Vertical Ribs, and are placed above or below the window opening at the same location where the Vertical Rib would have been. The  $x$ -coordinate of the Cripple Rib is the same as the  $x$ -coordinate of the Vertical Rib, but the start- and end-points in the  $y$ -direction are adjusted to

accommodate the opening. This ensures that the overall strength and consistency of the panel is maintained even with the inclusion of openings. The basic definitions of parameters involved in this calculation are illustrated in Figure 3-30. Detailed descriptions of the relevant parameters are provided accompanying each given equation.

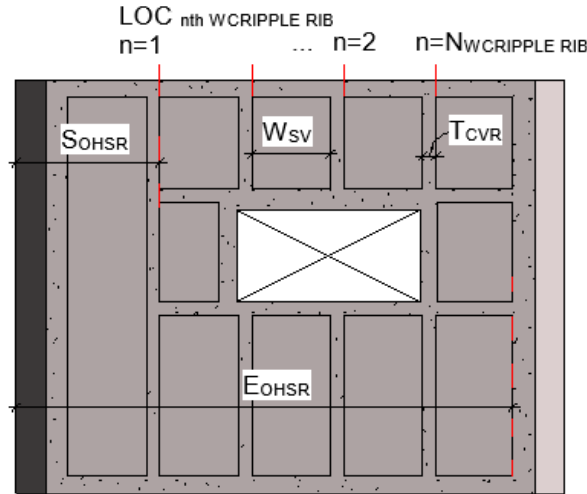


Figure 3-30. Cripple Rib parameters above/below window opening in the  $x$ -direction.

To locate the Cripple Rib, the start- and end-points of the Header and Sill Ribs ( $S_{WHSR}$ ,  $E_{WHSR}$ ) are used. By comparing the value of  $LOC_{ith\ RIB}$  for  $i$  in the range  $[1, N_{RIB} - 1]$  and  $LOC_{LAST\ RIB}$  with the value of  $S_{OHSR}$  and  $E_{OHSR}$ , the location of Cripple Ribs can be determined.

The equation for determining the number of Cripple Ribs around a window is as follows:

$$N_{WCRIPPLE\ RIB} = Rounddown((E_{WHSR} - S_{WHSR}) / (W_{SV} + T_{CVR})) \quad (3-52)$$

The equation for determining the location of the Cripple Ribs around a window is as follows:

$$LOC_{nth\ WCRIPPLE\ RIB} = S_{WHSR} + (W_{SV} + T_{CVR}) * n \quad n \in [1, N_{WCRIPPLE\ RIB}] \quad (3-53)$$

where:

$W_{SV}$  is the standard width of the Void, and the standard width between Vertical Ribs,

$T_{CVR}$  is the thickness of the Vertical Ribs.

After locating the Cripple Ribs in the  $x$ -direction, the respective start- and end-points of the lower and upper Cripple Ribs in the  $y$ -direction are calculated separately. The basic definitions of parameters involved in this calculation are illustrated in Figure 3-31. Detailed descriptions of the relevant parameters are provided accompanying each given equation.

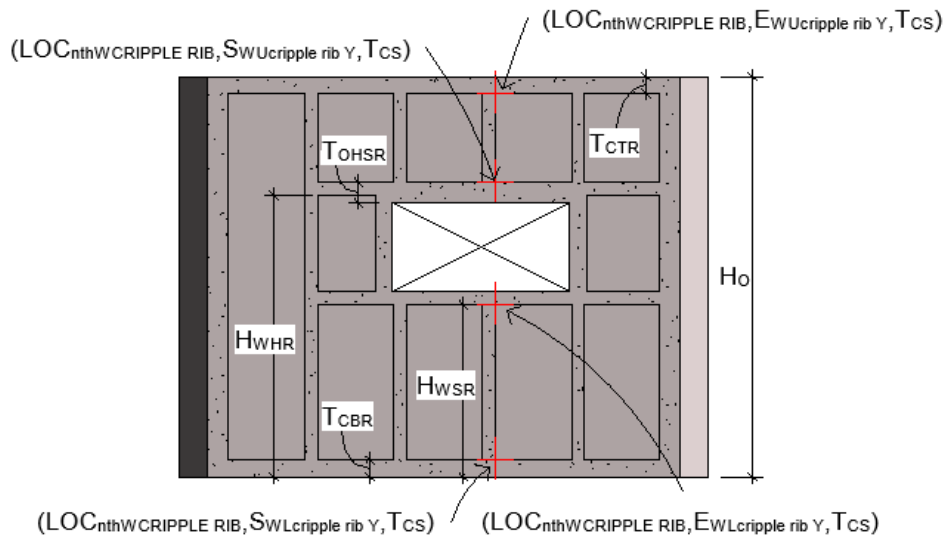


Figure 3-31. Cripple Rib coordinates above/below window opening.

The respective equations for determining the start- and end-points of the lower Cripple Ribs in the  $y$ -direction are as follows:

$$S_{WLcripple\ rib\ Y} = T_{CBR} \quad (3-54)$$

$$E_{WLcripple\ rib\ Y} = H_{WSR} \quad (3-55)$$

where:

$T_{CBR}$  is the thickness of the Bottom Rib,

$H_{WSR}$  is the height of the window Sill Rib.

The respective equations for determining the start- and end-points of the upper Cripple Ribs in the  $y$ -direction are as follows:

$$S_{WUcripple\ rib\ Y} = H_{WHR} + T_{OHSR} \quad (3-56)$$

$$E_{WUcripple\ rib\ Y} = H_O - T_{CTR} \quad (3-57)$$

where:

$H_{WHR}$  is the height of the window Header Rib,

$H_O$  is the height of the ribbed precast concrete wall panel,

$T_{CBR}$  is the thickness of the Top Rib,

$T_{OHSR}$  is the thickness of the Header and Sill Rib around the opening.

Based on the parameters defined above, the coordinates representing the position of the Cripple Ribs are shown in Figure 3-31.

### 3.5.2 Structure layout around door openings

This section provides a comprehensive explanation of the calculation methodology designed to determine the optimal position of the ribs around the door opening. The parameters related to the door opening, such as the height of the top edge ( $H_{DTE}$ ), the distance between the origin, and the left/right edge of the door in the  $x$ -direction ( $W_{DLE}$ ,  $W_{DRE}$ ), are graphically represented in Figure 3-32a. Figure 3-32b visually depicts the parameters that signify the thickness of the rib around the opening, wherein  $T_{OHSR}$  corresponds to the thickness of the Header Rib above the opening,  $T_{OLRR}$

denotes the thickness of the left and right rib around the opening, and  $T_{OCR}$  represents the thickness of the Cripple Rib above the opening.

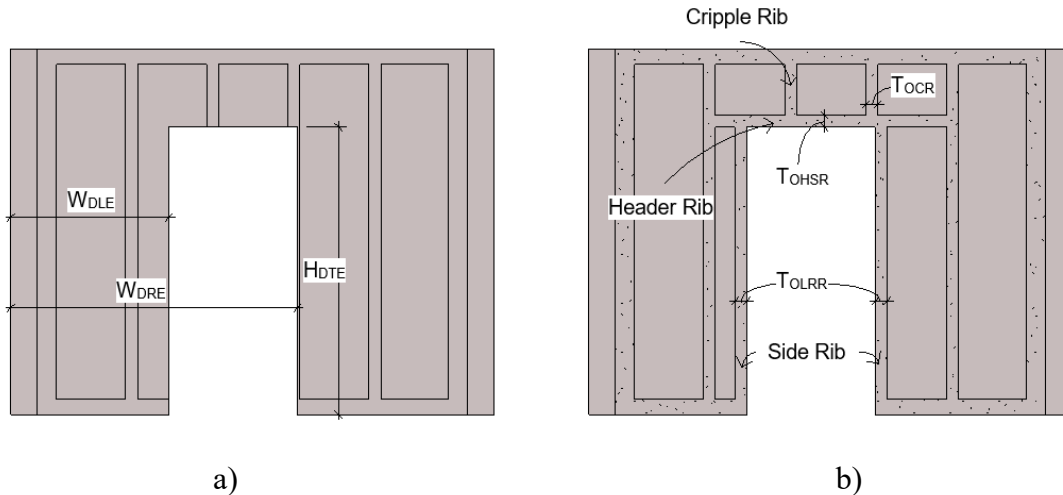


Figure 3-32. Parameters for the structural layout around door opening.

### 3.5.2.1 Header Rib

The logic for calculating the start- and end-points of the Header Ribs is the same as for the window openings. Figure 3-33a demonstrates the possible locations of the door opening's left edge along the  $x$ -direction, which can exist anywhere between the Vertical Ribs. By comparing the  $W_{DLE}$  value with the Vertical Rib locations ( $LOC_{ith\ RIB}$ ,  $LOC_{LAST\ RIB}$ ), the nearest Vertical Rib to the left side of the door can be identified. The start-point of the Header Rib ( $S_{DHR}$ ), as shown in Figure 3-33b, can then be determined by calculating the distance between the nearest Vertical Rib and the door's left edge ( $L_{DLER}$ ). Detailed descriptions of the relevant parameters are provided under each given equation.

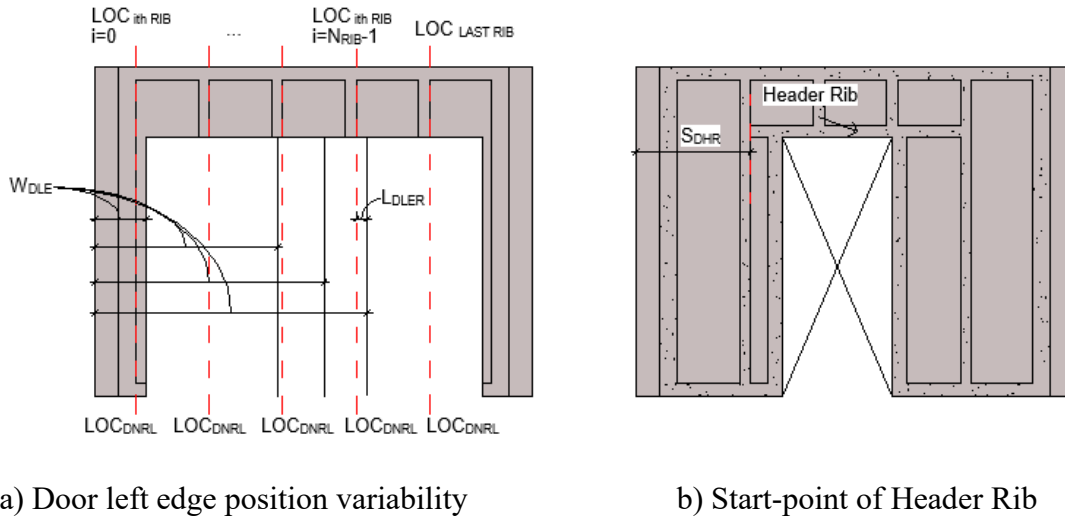
The equation for calculating the location of the nearest rib next to the left edge of the door ( $LOC_{DNRL}$ ) in the  $x$ -direction is as follows:

$$LOC_{DNRL} \quad (3-58)$$

$$= \begin{cases} LOC_{i^{th}RIB} & (LOC_{i^{th}RIB} + W_{US} \leq W_{DLE} < LOC_{i+1^{th}RIB} + W_{US} \quad i \in [0, N_{RIB} - 1]) \\ LOC_{N_{RIB}-1^{th}RIB} & (LOC_{i^{th}RIB} + W_{US} \leq W_{DLE} < LOC_{LAST RIB} + W_{US} \quad i = N_{RIB} - 1) \\ LOC_{LAST RIB} & (LOC_{LAST RIB} + W_{US} \leq W_{DLE}) \end{cases}$$

where:

$W_{US}$  is the width of the side of the U-shape Styrofoam.



a) Door left edge position variability

b) Start-point of Header Rib

Figure 3-33. Determining door opening parameters for Header Rib start-points.

The equation for calculating the distance between the left edge of the door opening and the nearest rib next to it ( $L_{DLER}$ ) in the  $x$ -direction is as follows:

$$L_{DLER} = W_{DLE} - LOC_{DNRL} \quad (3-59)$$

The start-point of the Header/Sill Rib around the door opening in the  $x$ -direction is calculated as follows (the value of  $i$  from the calculation of  $LOC_{DNRL}$  is used):

$$S_{DHR} = \begin{cases} i = 0 & LOC_{0^{th}RIB} \\ 1 \leq i \leq N_{RIB} - 1 & \begin{cases} LOC_{i-1^{th}RIB} \\ LOC_{i^{th}RIB} \end{cases} \\ i = N_{RIB} & \begin{cases} LOC_{N_{RIB}-1^{th}RIB} \\ LOC_{LAST RIB} \end{cases} \end{cases} \quad \begin{matrix} (3 < L_{DLER} < 6.5) \\ (L_{DLER} \leq 3 \text{ or } L_{DLER} \geq 6.5) \\ (3 < L_{DLER} < 6.5) \\ (L_{DLER} \leq 3 \text{ or } L_{DLER} \geq 6.5) \end{matrix} \quad (3-60)$$

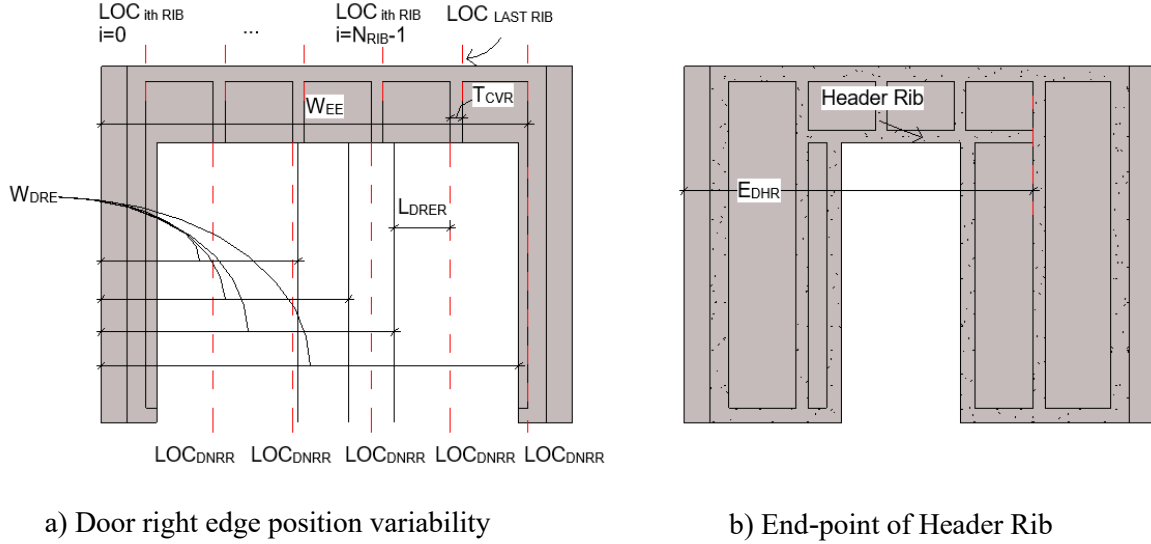


Figure 3-34. Determining door opening parameters for Header Rib end-points.

Figure 3-34a demonstrates the potential positions of the window's right edge, and the end-point of the door's Header Rib can be determined using the same logic described in the previous paragraph. By comparing the location of the Vertical Ribs with the location of the door's right edge ( $W_{DRE}$ ), the end-point of the Header Rib can be determined. The basic definitions of the parameters involved in this calculation are illustrated in Figure 3-34, and detailed descriptions of the parameters are presented accompanying each given equation.

The equation for calculating the location of the nearest rib next to the right edge of the door in the  $x$ -direction is as follows:

$$\begin{aligned}
 &LOC_{DNRR} \tag{3-61} \\
 &= \begin{cases} LOC_{i+1}^{th RIB} - T_{CVR} & (LOC_{i}^{th RIB} - T_{CVR} - W_{US} \leq W_{DRE} < LOC_{i+1}^{th RIB} - T_{CVR} - W_{US} \quad i \in [0, N_{RIB} - 1]) \\ LOC_{LAST RIB} - T_{CVR} & (LOC_{i}^{th RIB} - T_{CVR} - W_{US} \leq W_{DRE} < LOC_{LAST RIB} - T_{CVR} - W_{US} \quad i = N_{RIB} - 1) \\ W_{EE} & (LOC_{LAST RIB} - T_{CVR} - W_{US} \leq W_{DRE}) \end{cases}
 \end{aligned}$$

where:

$W_{EE}$  is the distance between the origin and the rightmost Edge Rib in the  $x$ -direction.

The equation for calculating the distance between the right edge of the door opening and the nearest rib next to it ( $L_{DRER}$ ) in the  $x$ -direction is as follows:

$$L_{DRER} = LOC_{DNRR} - W_{DRE} \quad (3-62)$$

The end-point of the Header/Sill Rib around the door opening in the  $x$ -direction is calculated as follows (the value of  $i$  from Equation 3-61 is used):

$$E_{DHR} = \begin{cases} 0 \leq i < N_{RIB} - 2 & \begin{cases} LOC_{i+2^{th}RIB} - T_{CVR} & (3 < L_{DRER} < 6.5) \\ LOC_{i+1^{th}RIB} - T_{CVR} & (L_{DRER} \leq 3 \text{ or } L_{DRER} \geq 6.5) \end{cases} \\ i = N_{RIB} - 2 & \begin{cases} LOC_{LAST RIB} - T_{CVR} & (3 < L_{DRER} < 6.5) \\ LOC_{i+1^{th}RIB} - T_{CVR} & (L_{DRER} \leq 3 \text{ or } L_{DRER} \geq 6.5) \end{cases} \\ i = N_{RIB} - 1 & \begin{cases} W_{EE} & (3 < L_{DRER} < 6.5) \\ LOC_{LAST RIB} - T_{CVR} & (L_{DRER} \leq 3 \text{ or } L_{DRER} \geq 6.5) \end{cases} \\ i = N_{RIB} & W_{EE} \end{cases} \quad (3-63)$$

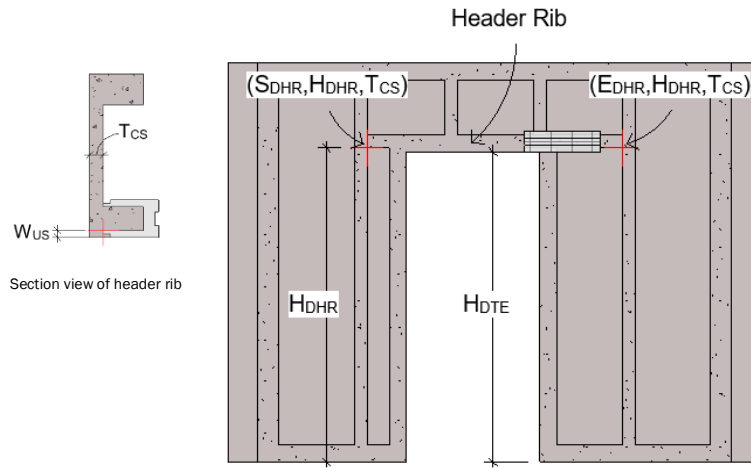


Figure 3-35. Coordinates of Header Rib above door opening.

To proceed with the positioning of the rib structure encircling the window opening, it is essential to undertake the subsequent step, which involves determining the height of the door Header Rib ( $H_{DHR}$ ) using a calculated approach that considers the width of the side of the U-shape Styrofoam. The specifics of this stage are visually demonstrated in Figure 3-35 for clarity.

The equation for calculating the height of the door Header Rib ( $H_{DHR}$ ) is as follows:

$$H_{DHR} = H_{DTE} + W_{US} \quad (3-64)$$

where:

$H_{DTE}$  is the height of the door's top edge,

$W_{US}$  is the width of the side on U-shape Styrofoam.

The coordinates representing the position of the door Header Rib based on the parameters defined above are shown in Figure 3-35.

### 3.5.2.2 Door Side Rib

The calculation logic for determining the optimal placement of the door Side Rib closely follows that of the window Side Rib. First, the location of the left Side Rib in the  $x$ -direction must be calculated. The fundamental parameters used in this calculation are depicted in Figure 3-36, and a comprehensive description of the relevant parameters is provided accompanying each given equation.

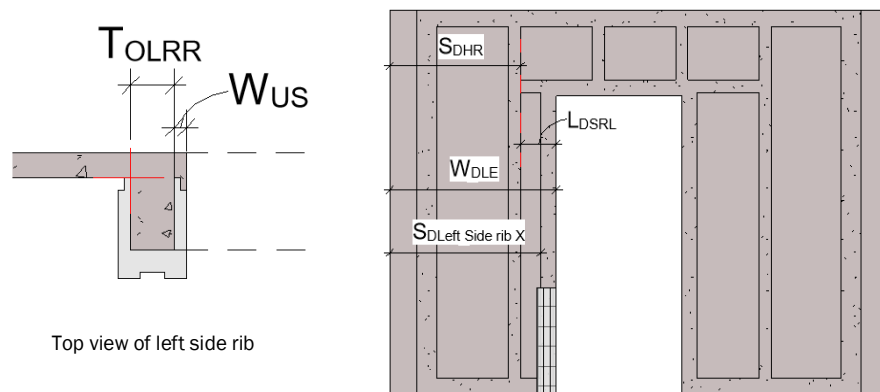


Figure 3-36. Parameters for door left Side Rib.

The equation for calculating the distance between the start-point of the Header Rib and the left edge of door ( $L_{DSRL}$ ) is as follows:

$$L_{DSRL} = W_{DLE} - S_{DHR} \quad (3-65)$$

where:

$W_{DLE}$  is the distance between the origin and the left edge of the door,

$S_{DHR}$  is the start-point of the Header Rib above the window opening in the  $x$ -direction.

The start-point of the left side door rib in the  $x$ -direction is calculated as follows:

$$S_{DLeft\ side\ rib\ x} = \begin{cases} \text{no left rib will be placed} & (L_{DSRL} \leq 3) \\ W_{DLE} - W_{US} - T_{OLRR} & (L_{DSRL} > 3) \end{cases} \quad (3-66)$$

where:

$T_{OLRR}$  is the thickness of the left and right ribs around the opening,

$W_{US}$  is the width of the side on U-shape Styrofoam.

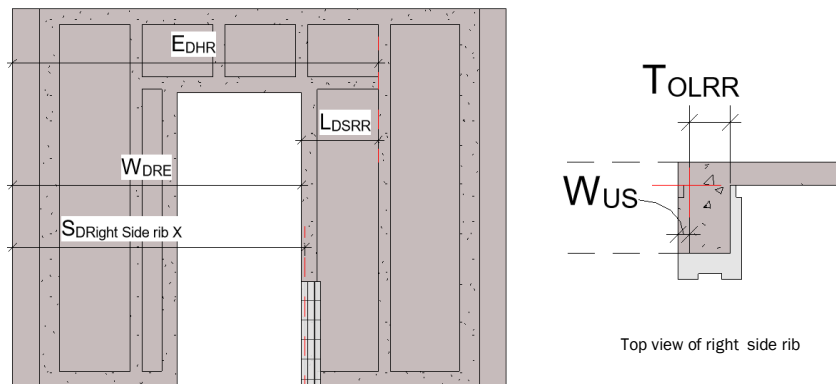


Figure 3-37. Parameters for door right Side Rib.

The ideal position of the right Side Rib in the  $x$ -direction is then calculated. The fundamental parameters employed in this calculation are graphically represented in Figure 3-37, and their detailed explanations are presented in the corresponding equations section.

The equation for calculating the distance between the end-point of the Header Rib and the right edge of the window ( $L_{DSRR}$ ) is as follows:

$$L_{DSRR} = E_{DHR} - W_{DRE} \quad (3-67)$$

where:

$W_{DRE}$  is the distance between the origin and the right edge of the door,

$E_{DHR}$  is the end-point of the Header Rib above the door opening in the  $x$ -direction.

The start-point of the right Side Rib in the  $x$ -direction is calculated as follows:

$$S_{DRight\ side\ rib\ X} = \begin{cases} \text{no right rib will be placed} & (L_{DSRR} \leq 3) \\ W_{DRE} + W_{US} & (L_{DSRR} > 3) \end{cases} \quad (3-68)$$

where:

$W_{US}$  is the width of the side of the U-shape Styrofoam.

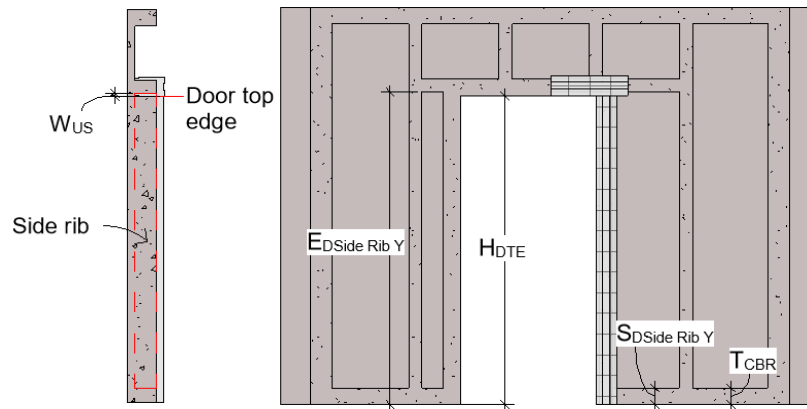


Figure 3-38. Parameter for door Side Rib in the  $y$ -direction.

The fundamental parameters essential to the calculation for establishing the start- and end-points of the Side Rib in the  $y$ -direction are illustrated in Figure 3-38. Detailed descriptions of the relevant parameters are provided accompanying each given equation.

The start-point of the Side Rib in the  $y$ -direction is calculated as follows:

$$S_{D Side rib Y} = T_{CBR} \quad (3-69)$$

The end-point of the Side Rib in the  $y$ -direction is calculated as follows:

$$E_{D Side rib Y} = H_{DHR} = H_{DTE} + W_{US} \quad (3-70)$$

where:

$H_{DHR}$  is the height of the door Header Rib,

$H_{DTE}$  is the height of the door's top edge.

The coordinates representing the position of the door Side Rib based on the parameters defined above are shown in Figure 3-39.

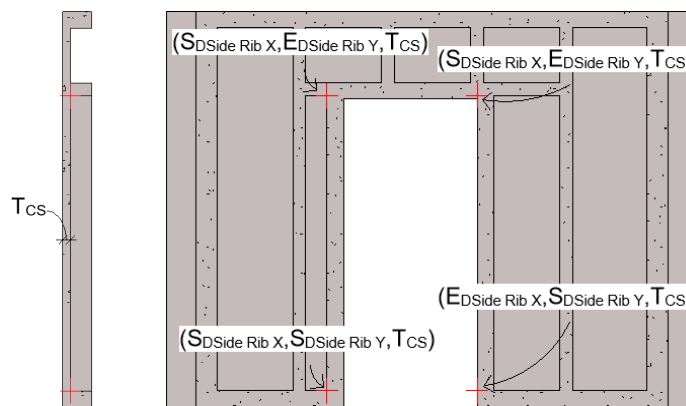


Figure 3-39. Door Side Rib coordinates.

### 3.5.2.3 Cripple Rib

For the concrete panel without any openings, the Vertical Ribs are uniformly placed at a standard distance from each other. However, in this section, the addition of door openings interrupts the continuity of Vertical Ribs. To ensure the structural integrity of the panel, Cripple Ribs are implemented in place of Vertical Ribs, and are positioned above door opening at the same location as the Vertical Ribs would have been. The  $x$ -coordinate of the Cripple Rib follows that of the Vertical Rib, while the start- and end-points in the  $y$ -direction are adjusted to accommodate the opening, thereby maintaining the overall strength and consistency of the panel. The fundamental definitions of the parameters involved in this calculation are illustrated in Figure 3-40, while detailed explanations of the relevant parameters are provided accompanying each given equation.

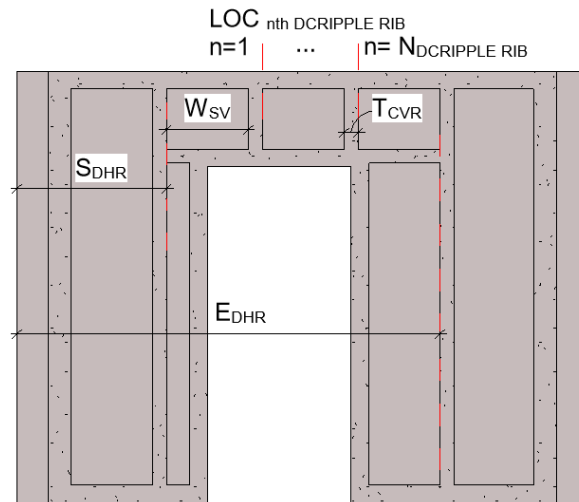


Figure 3-40. Cripple Rib parameters above/below the window opening in the  $x$ -direction.

The equation for calculating the number of Cripple Ribs above a door opening is as follows:

$$N_{DCRIPPLE RIB} = Rounddown((E_{DHR} - S_{DHR}) / (W_{SV} + T_{CVR})) \quad (3-71)$$

The equation for calculating the location of Cripple Ribs above a door is as follows:

$$LOC_{n^{th}DCRIPPLE\ RIB} = S_{DHR} + (W_{SV} + T_{CVR}) * n \quad n \in [1, N_{DCRIPPLE\ RIB}] \quad (3-72)$$

where:

$W_{SV}$  is the standard width of the Void, and the standard width between Vertical Ribs,

$T_{CVR}$  is the thickness of the Vertical Rib.

The fundamental parameters for calculating the start- and end-points of the Cripple Ribs in the  $y$ -direction are illustrated in Figure 3-41 for reference. (Detailed descriptions of the parameters are illustrated accompanying each given equation.)

The respective equations for determining the start- and end-points of a Cripple Rib above a door opening in the  $y$ -direction are as follows:

$$S_{DUcripple\ rib\ Y} = H_{DHR} + T_{OHSR} \quad (3-73)$$

$$E_{DUcripple\ rib\ Y} = E_{WUcripple\ rib\ Y} = H_O - T_{CTR} \quad (3-74)$$

where:

$H_{DHR}$  is the height of the door Header Rib,

$H_O$  is the height of the ribbed precast concrete wall panel,

$T_{CBR}$  is the thickness of the Top Rib,

$T_{OHSR}$  is the thickness of the Header and Sill Rib around the opening.

The coordinates representing the position of Cripple Ribs based on all parameters defined above are shown in Figure 3-41.

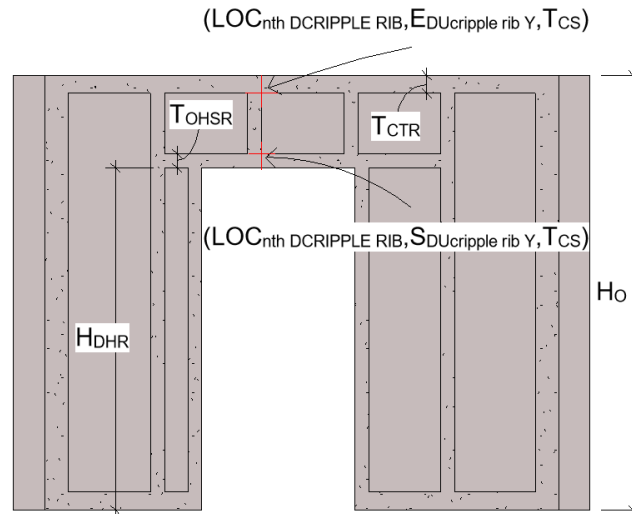


Figure 3-41. Cripple Rib coordinates above door opening

### 3.6 Development of user interface (UI)

In this section, the user interface designed for this prototype system is introduced. The mathematical algorithms described in the preceding sections are incorporated into a prototype system that automates the design of 3i RPCPSs. To provide a connection between the user and the embedded code, a user interface is developed. This user interface serves as an intermediary, allowing the user to interact with the system effectively. Its primary functions include (1) Input: Users are able to enter data and commands, such as numerical values and selections, to define the parameters of the system. (2) Output: The system provides feedback to the user, including error messages and confirmation messages, to inform them of the results of their actions. (3) Customization: The user interface is customizable, allowing users to adapt the appearance and behaviour of the system to their individual preferences and needs.

As depicted in Figure 3-42, this user interface was developed using Windows Form and includes essential details about the wall being designed, such as its name and type, as well as seven tabs that are structured as follows: structure, Styrofoam, panel length, layout around openings, concrete

cover, rebar, and Lifting Anchor. After collecting all the parameters that were defined in the previous chapter, it was determined which ones needed to be set by the user and they were assigned as input parameters in their corresponding tabs. The detailed function of each box under different tabs is illustrated in Table 3-2.

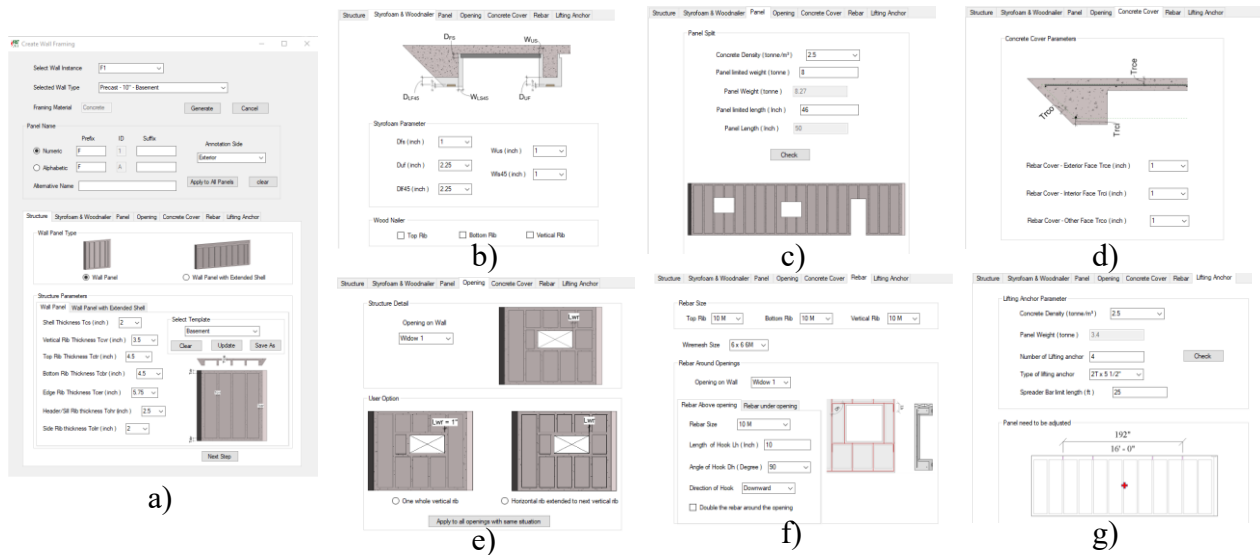


Figure 3-42. User interface of 3i RPCPS design: (a) Main page with tabs, (b) Styrofoam tab, (c) Panel tab, (d) Concrete cover tab, (e) Layout around openings tab, (f) Rebar tab, (g) Lifting Anchor tab

Table 3-2. Tab feature for Windows Form.

Tab Parameter	Feature
Wall instance name and type	Enable the user to explore all wall objects chosen in the system by either name or wall type for framing purposes and display their relevant parameters in a tab that can be customized by the user for each panel.

Structure

The user can choose between two types of wall panels. Once the type of wall has been selected, corresponding tabs are activated to allow the user to customize the thickness values of different kinds of ribs. To increase convenience, a "select template" option is incorporated to save the default values of rib thickness for both the basement and upper levels as templates, which users can choose from instead of typing them in manually. The input parameters are used to determine the layout of ribs for ribbed precast concrete panels.

Styrofoam and wood nailer

Users can determine the face and side thickness of different types of Styrofoam to assist in the calculation of concrete volume and weight, as well as the identification of the location coordinates for placing the Styrofoam.

Panel

Within this tab, each wall object can be divided into a particular number of panels with lengths and weight determined by the user. The maximum panel length and weight is established based on the type of equipment and available transportation method. When the "check" button is clicked, the add-on verifies the lengths and weights of all the selected wall instances to determine if any of them exceed the limits. If any wall instances fail to meet the requirements, a message box appears informing the user which panel exceeds the weight or length limitation, prompting them to return to the model to split the panel. Once the panel has been split, the system can obtain the new coordinates for the start- and end-points of the wall.

Users have two options for displaying the openings on the selected wall panel. The first option maintains the original location of the openings, while the second option shifts the openings to some amount usage of concrete material. If the option to shift the openings is selected, a message box appears indicating the number of inches by which the opening is to be shifted. Based on this information, users can discuss with their clients to determine if the shift distance conflicts with their requirements. After the discussion, users can then make a final decision on which option to choose. This option can specify the locations of ribs around openings.

Openings

Users can define the value of a concrete cover on different faces of the wall panel. This information is used to establish the start and end-point coordinates of the rebar.

Concrete cover

The rebar detail, such as size and details of the hook around openings, can be modified by need.

Rebar

Once the concrete panel has been generated, the location of the Lifting Anchor can be determined separately. The system can identify the center of gravity and place the Lifting Anchor automatically in a symmetrical position to the center of gravity. Users can click on the check button to ensure that the distance between the first and last Lifting Anchor does not exceed the

Lifting Anchor

maximum length, which is determined by the length of the spreader bar used by the crane. If the distance between the first and last Lifting Anchor exceeds the spreader bar limit, a dialog box appears prompting the user to adjust the location of the Lifting Anchor.

---

## Chapter 4. Application Implementation

### 4.1 Overview

To evaluate the feasibility of the developed method, a prototype system, ConcreteX, was developed, utilizing Autodesk Revit as the platform due to its robust capabilities as a parametric modelling tool. This functionality enables users to manipulate individual components within a "family" environment, providing a greater degree of precision and control over the building design. Furthermore, the use of parametric models allows for efficient design modifications, as users can make quick and easy adjustments to related parameters in order to achieve the desired outcome. Additionally, Revit offers an API (Application Programming Interface) that serves as a comprehensive dictionary of code, supporting the graphical interface across various programming languages. This allows developers to easily enhance the functionality of their software without having to write their own code from scratch.

The ConcreteX prototype system is developed using Visual Studio and implemented in the C# programming language. Guided by the Revit API, the system enables automated design and drafting of the 3i RPCPS. The prototype system encompasses several key functions, including:

1. **Automatic Wall Name Generation:** The system generates wall names automatically based on the wall facing direction (for example, the wall facing left is labelled as L), ensuring consistent and organized identification of wall components.
2. **Automatic Wall Connection Generation:** Different connection types are accommodated by the system, which automatically generates wall connections based on predefined parameters. This feature streamlines the process of creating accurate and efficient connections between wall elements.

3. Automatic Design of Ribbed Precast Concrete Panels without Openings: The prototype system automates the design of ribbed precast concrete panels that do not require openings. This functionality ensures the efficient generation of panel designs, reducing manual effort and potential errors.
4. Automatic Design of Structure Layout Surrounding Openings: The system also automates the design of the structure layout surrounding wall openings. By leveraging the 3D model and predefined parameters, the system accurately generates the necessary structural components, enhancing the overall efficiency of the design process.

These functions collectively contribute to the automation and streamlining of the design and drafting process for ribbed precast concrete panels, improving productivity and accuracy in construction projects.

In the development of this Revit add-on, Object-Oriented Programming (OOP) is used as the programming paradigm and methodology. OOP enables users to break down complex systems into smaller, more manageable objects and implement flexible, scalable, and maintainable code through object interactions. By using classes as templates for objects, solid foundation for achieving software modularity can be established, making it easier to reuse code and maintain a consistent structure.

Furthermore, the Unified Modelling Language (UML) is used as a visual notation to represent the design and structure of ConcreteX. The UML diagrams as shown in Figure 4-1 provide a clear understanding of the components and relationships between different classes, aiding in effective system design.

Overall, leveraging OOP principles and utilizing UML notations allows the development of a robust Revit add-on with improved modularity, code reusability, and a well-organized software structure.

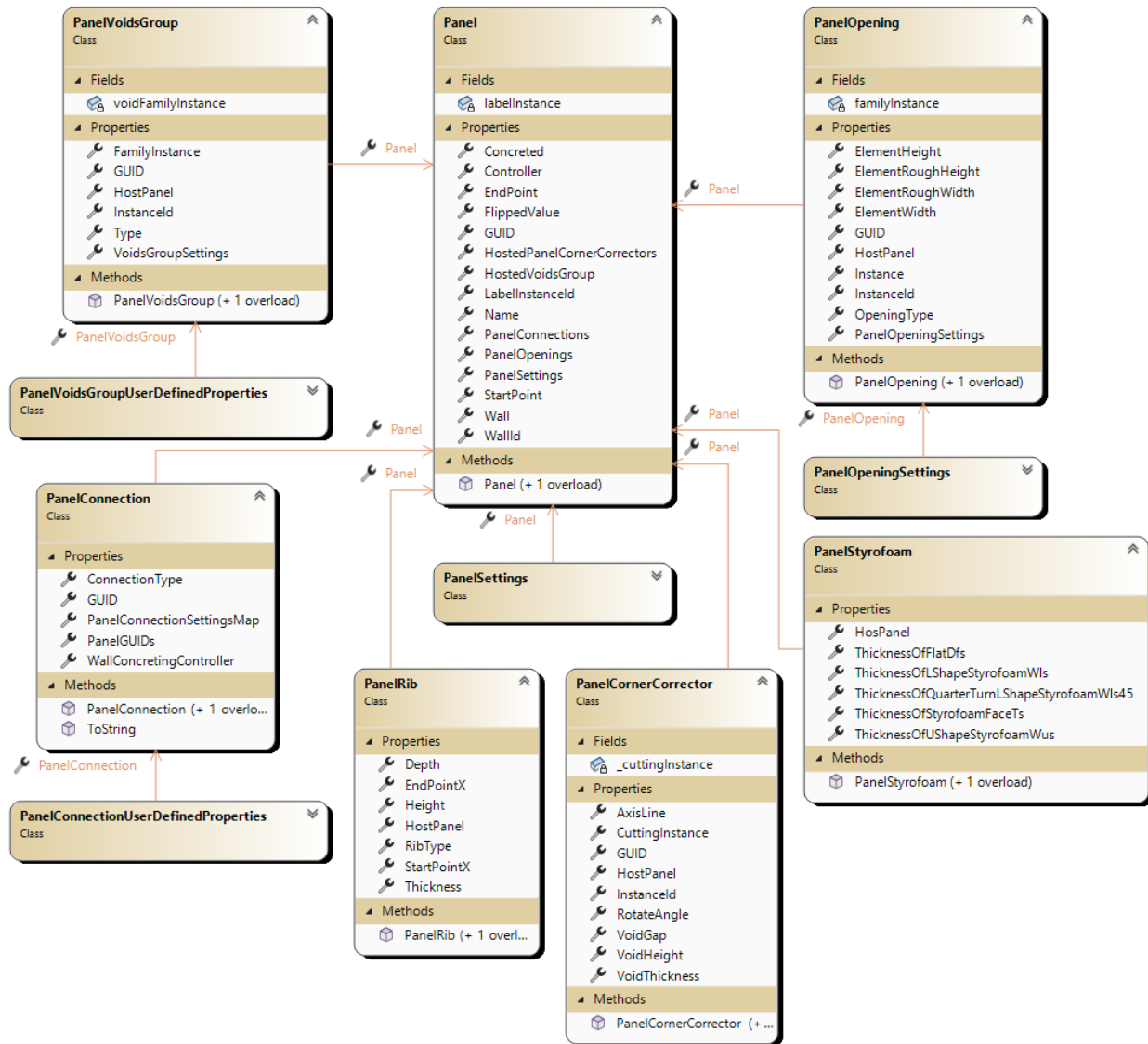


Figure 4-1. Classes in system design of automation design and drafting using UML.

## 4.2 Inputs for prototype system

### 4.2.1 BIM model preparation

To prepare for the operation of the prototype system, it is necessary to create a 3D model of the basement in Revit that contains detailed information about the walls and openings, as displayed in Figure 4-2.

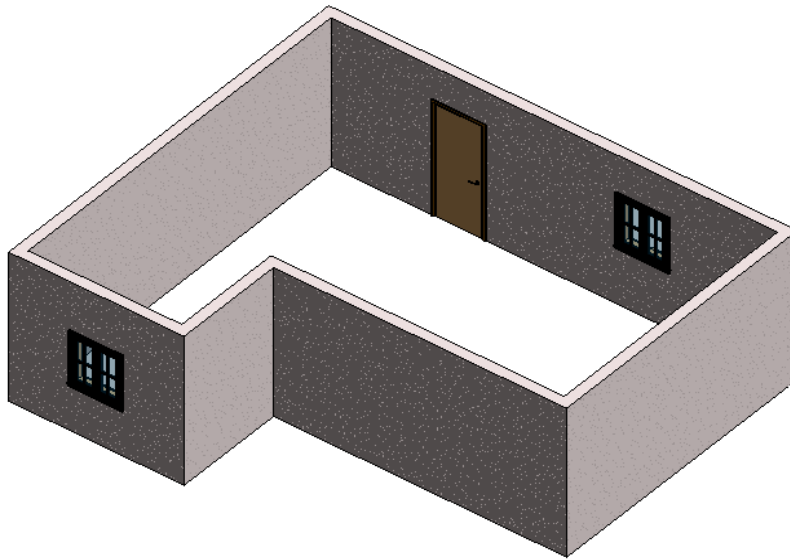


Figure 4-2. 3D Revit model prepared for prototype system.

The process involves the user's active participation in moulding the basement walls and placing rough openings for windows and doors in accordance with the provided 2D design drawings and dimension information. Additionally, while the user is drafting the wall, they need to set the location line of the wall to the exterior of the finished face, and make sure the location line is always at the exterior side of the building. The orientation of each wall can then be extracted correctly based on the wall facing the direction drafted by the user.

When drafting the walls, it is essential for the user to set the location line of each wall to the exterior of the finished face. Maintaining the location line consistently on the exterior side of the

building ensures accurate extraction of the wall's orientation, based on the direction it faces as initially drafted by the user. This meticulous approach guarantees the proper representation of the wall orientation within the model, facilitating a seamless operation of the prototype system.

Consequently, the model extraction process captures crucial information for the prototype system's operation. This includes extracting the unique identification (ID) of each wall, as well as the precise dimensions of both the walls and openings. Moreover, the locations of the openings on the walls are also extracted. These extracted details play a vital role in the subsequent utilization of the model within the prototype system, ensuring accurate and efficient functionality.

Information concerning the components of the 3i RPCPS should also be included in the model. Revit stores component information in a particular file, the .RVT file, and saves it as a Revit family model (parametric models). These family models, such as the Void that creates ribs by cutting voids on the concrete panel, all types of steel connectors, Styrofoam and wood nailer, and other necessary models, should be loaded into the prototype system. This research obtained all these Revit family models with detailed dimensions and properties from a precast construction company, 3i Precast Inc.

#### **4.2.2 Information extraction from a BIM model**

Building Information Modelling relies on parametrically defined objects to represent a design, encompassing various types of information such as geometric data (point, line, plane, and solid components), spatial data (component orientations and locations), and manufacturer's data. This structured storage of information enables efficient extraction of relevant details. In order to automate the generation of wall connections and structure layouts for ribbed precast concrete panels, specific information needs to be extracted from the BIM model.

The essential information extracted from the BIM model includes:

1. Wall properties: The wall element ID and its dimension information must be extracted, including wall thickness, height, and length. Additionally, it involves capturing the coordinates of the start-point ( $xyz_{sp}$ ) and end-point ( $xyz_{ep}$ ) as well as the orientation of each wall.
2. Opening properties: This involves extracting the opening element ID, as well as the corresponding wall element ID to which the opening belongs. Further details such as the sill height, opening width, and opening height need to be gathered. Additionally, it is necessary to obtain the location coordinates ( $xyz_{op}$ ) of each opening.

Table 4-1. Input parameter extracted from BIM model.

Notation	Description
$L_O$	Length of the ribbed precast concrete wall panel, which is the length of exterior wall
$H_O$	Height of the ribbed precast concrete wall panel
$T_O$	Thickness of the ribbed precast concrete wall panel
$W_{WLE}$	Distance between the origin and the left edge of the window in the $x$ -direction
$W_{WRE}$	Distance between the origin and the right edge of the window in the $x$ -direction
$H_{WBE}$	Height of the window opening's bottom edge
$H_{WTE}$	Height of the window opening's top edge
$W_{DLE}$	Distance between the origin and the left edge of the door in the $x$ -direction
$W_{DRE}$	Distance between the origin and the right edge of the door in the $x$ -direction
$H_{DTE}$	Height of the door opening's top edge

By extracting these specific properties from the BIM model, the prototype system can efficiently use the acquired information to automate wall connection generation and ribbed precast concrete panel layout tasks. Table 4-1 presents a comprehensive list of all parameters that must be extracted

from the 3D BIM input model for the mathematical algorithm introduced in Chapter 3 to function effectively.

### 4.2.3 User-defined inputs

The parameters from Chapter 3 that require user input are assigned as input parameters in the user interface. Upon receiving input values from the user, these parameters can be used in the mathematical algorithm implemented in the prototype system, thereby enabling the determination of component positions within the 3i RPCPS. The relevant parameters requiring user input are listed in Table 4-2.

Table 4-2. Input parameters as defined by user.

Notation	Description
$T_S$	Thickness of Styrofoam which covered on the Rib structure
$T_{CS}$	Thickness of concrete Shell
$T_{CER}$	Thickness of Edge Rib
$T_{CTR}$	Thickness of Top Rib
$T_{CBR}$	Thickness of Bottom Rib
$T_{CVR}$	Thickness of Vertical Rib
$T_{OHSR}$	Thickness of Header and Sill Rib around opening
$T_{OLRR}$	Thickness of Side Rib around opening
$T_{OCR}$	Thickness of Cripple Rib above and below opening
$W_{LS}$	Width of side of L-shape Styrofoam
$D_{FS}$	Depth of Flat-shape Styrofoam
$W_{LS45}$	Width of side of L-shape-45-degree Corner Styrofoam
$W_{US}$	Width of side of U-shape Styrofoam
$\rho_C$	Concrete density
$C_{CE}$	Concrete cover for the exterior face of wall panel
$C_{CO}$	Concrete cover for the other face of wall panel
$C_{CI}$	Concrete cover for the interior face of wall panel

### **4.3 Functionality implementation and time study**

ConcreteX is a versatile system that encompasses several essential functions, providing a comprehensive solution for ribbed precast concrete panel design and drafting. These functions include the automatic generation of panel names based on wall facing direction, the creation of diverse wall connections, and the generation of structural layouts for panels with and without openings. This section delves into the process of transforming mathematical algorithms into practical functionalities using the Revit API. It also explores the efficient storage and retrieval of information between each function, demonstrating their seamless integration and showcasing the desired output of each operation. Furthermore, a comprehensive time study carried out encompassing each functional aspect is described. It should be noted that this study involves a comparative analysis of the average time consumption calculated from collected data set between the manual and automated approaches. The objective of this analysis is to assess the effectiveness and efficiency of the prototype system in automating the design and drafting processes.

#### **4.3.1 Automatic panel label generation**

The naming system provided by 3i Precast Inc. is used for automatically naming panels in this prototype. This naming system requires walls to be named according to their facing direction, which includes front, left, back, and right. By defining a naming convention, it is easier to keep track of each wall and its corresponding information throughout the design and production process. This can help to avoid confusion and mistakes when dealing with several walls and openings in a building.

Since Revit sets the location line of the walls to the exterior of the finished face during the moulding process, the Revit API to implement this functionality can be used. By casting the wall

type from an Element to a wall instance and utilizing the *Wall.Orientation* property, the orientation of each wall can be accurately determined. To facilitate this, a dictionary within the 'Master.cs' class is created, allowing users to map walls to their respective facing directions. In this dictionary, the wall orientation is the key, and the corresponding letter representing the facing direction is the value. Refer to Table 4-3 below for the details of the Wall Name Mapper dictionary, where "F" indicates a wall facing the front, "B" signifies back, "R" denotes right, and "L" represents left.

Table 4-3. Wall Name Mapper dictionary.

Key (Orientation property of wall)	Value (Letter representing the facing direction)
Orientation (0.000000000, -1.000000000, 0.000000000)	"F"
Orientation (0.000000000, 1.000000000, 0.000000000)	"B"
Orientation (1.000000000, 0.000000000, 0.000000000)	"R"
Orientation (-1.000000000, 0.000000000, 0.000000000)	"L"

Using this dictionary, retrieving the wall label text becomes straightforward. By iterating through the orientation property for all existing walls in the model, automatically-generated names were assigned to each wall. These names are then used to populate the "Mark" field under the Identity Data section of the corresponding wall in the 3D model. Additionally, starting a new transaction using the *NewFamilyInstance* method in Revit API, label instances are generated and placed on the respective walls, indicating their base level and placement location. After clicking the Create/Edit button, the automatically-generated names are displayed on each wall within the model,

as illustrated in the accompanying Figure 4-3. This feature ensures that the assigned names are clearly visible and easily accessible for further reference and identification.

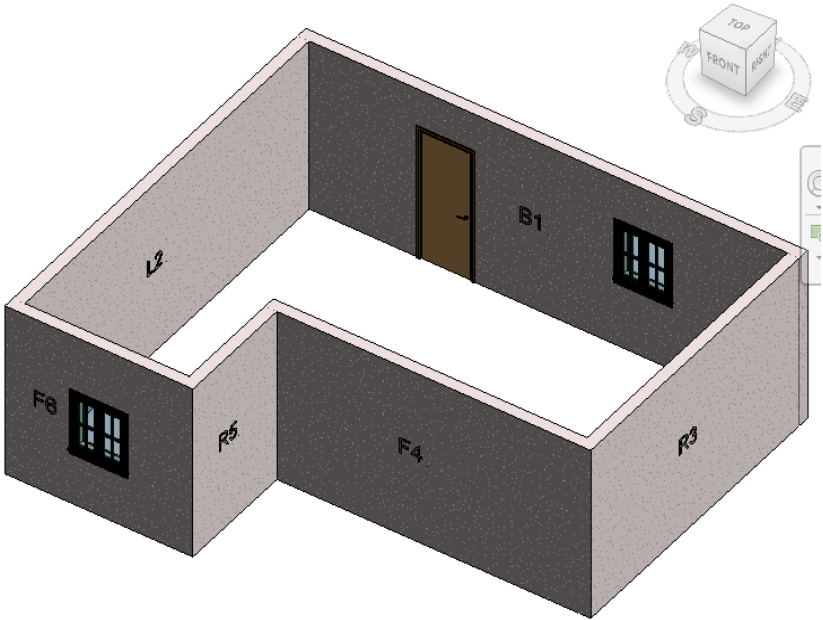


Figure 4-3. Wall panel label created for prototype system.

Table 4-4. Drafting time for manual and ConcreteX performance for generating panel name.

Panel Name	Drafting Time
Manual	7 s
ConcreteX	1 s
Savings	86%

According to Table 4-4, drafting time (t) takes seven seconds to manually add a wall label on a single wall. However, utilizing an automated drafting tool such as ConcreteX minimizes the total

drafting time to one second. The results show that ConcreteX saves up to 86% of drafting time compared to manual work in BIM.

## 4.3.2 Automatic generation of wall connection

### 4.3.2.1 Detection of connected wall pairs

With the implementation of the prototype system in Visual Studio using the Revit API, automatic generation of wall connections becomes a key feature. To facilitate the automatic generation of wall connections, a Wall Connection tab is integrated into the form interface. Before initiating the wall connection process, it is essential to present the available connected wall pairs in a combo box, encompassing all potential connections within the model. As the user selects a specific wall instance in the form, the connected wall panel combo box dynamically populates with all the potential wall pairs, and each wall pair comprises the given selected wall and one of its neighbouring walls.

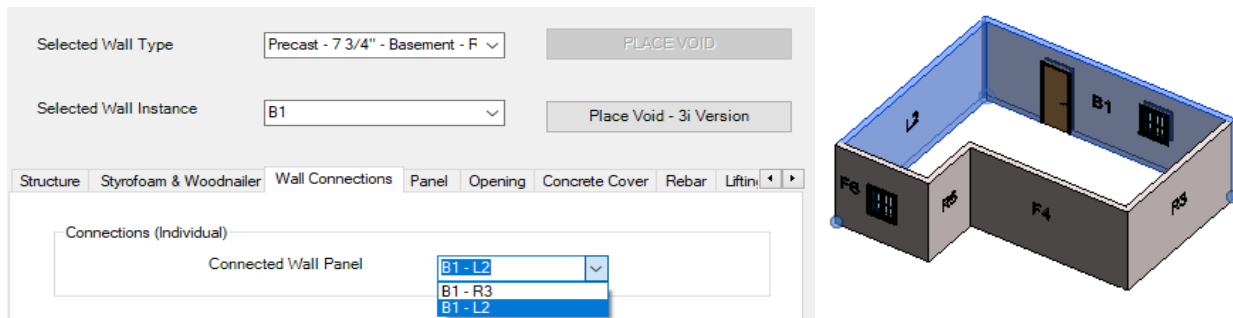


Figure 4-4. Dynamic wall pair selection with combo box update.

In the Revit model, each wall is characterized by two distinct ends, represented by index values. Index 0 signifies the start-point, while index 1 represents the end-point. The determination of these start- and end-points relies on the user's drafting direction during the model input phase. To identify the walls connected to the user-selected wall, the Revit API method *Wall*.

*Location.Get\_ElementsAtJoin(index)* is employed. This API method enables the retrieval of the wall connected at the start-point (index = 0) and the wall connected at the end-point (index = 1) of the user-selected wall.

As illustrated in Figure 4-4, once the user changes their wall instance selection, the combo box updates accordingly displaying two wall pairs: the user-selected wall along with the wall connected at its start-point, and the user-selected wall along with the wall connected at its end-point. Additionally, to further enhance the user experience, the prototype system incorporates a visual highlighting feature. Once the user chooses to modify the connected wall pair selection, the corresponding connected wall pair is visually highlighted within the model. This highlighting effect serves as a helpful visual aid, allowing users to easily identify and visualize the currently selected wall connection for modification.

By offering this interactive and dynamic update functionality, the combo box empowers users to seamlessly navigate and modify the wall connections according to their preferences. This streamlined approach enhances overall user experience and efficiency, making it effortless for users to select and generate the desired wall connections within the prototype system.

#### **4.3.2.2 Automatic selection of connection methods**

By analyzing the angle between walls within the same connection from the interior of the building, the wall connections can be categorized into three types: concave angle connection, convex angle connection, and 180-degree connection. A visualization of these three types of wall connections is illustrated in the accompanying Figure 4-5.

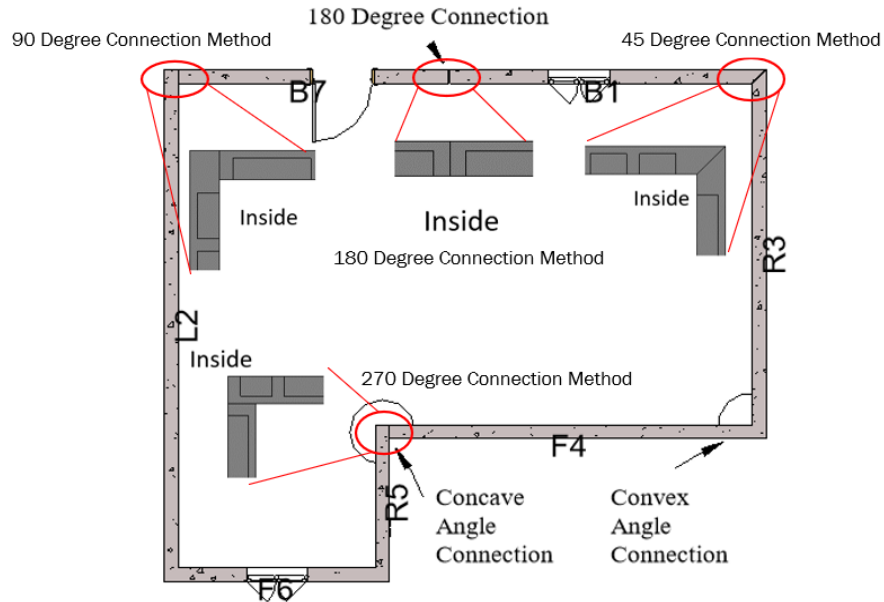


Figure 4-5. Classification of wall connections based on interior angles.

These types of connections each require a specific connection method, as informed by practical know-how and industry expertise, also depicted in Figure 4-5. For convex angle connections, the 45-degree wedge connection method and the 90-degree connection method are used. These methods ensure secure and stable connections between walls with convex angles. For concave angle connections, the 270-degree connection method is employed to achieve proper alignment and connection between walls. When walls align perfectly with each other, a 180-degree connection method is used. This method enables a seamless connection between aligned walls, ensuring a smooth transition and continuity in the building's structure.

With the implementation of the prototype system in Visual Studio using the Revit API, the automatic generation of wall connections is further enhanced to minimize human judgment errors. When the user decides to modify the selected connected wall pair, the prototype system takes over the responsibility of determining the connection type and suggesting the appropriate connection

method. This eliminates the need for the user to manually determine the connection type and select the corresponding method, streamlining the process and reducing the potential for errors.

The code within the system undergoes a thorough analysis of each wall connection in the model. By considering the orientation of each wall and the relative positions of both walls within the wall pair, the system can accurately determine the type of wall connection.

Based on the determined connection type, the prototype system automatically sets the corresponding connection method as the default setting. This ensures that the most suitable method is initially applied. However, the system also provides the user with the flexibility to modify the connection method if required by enabling the selection of alternative connection methods that are relevant to the specific connection type.

For instance, the system identifies the connected wall pair L2-B7 shown in Figure 4-6, as a convex angle connection. The suggested connection methods, such as the 45-degree wedge connection and the 90-degree connection, are enabled for the user. The 45-degree wedge connection method is the default selection, but the user has the flexibility to choose their preferred connection method.

By enabling the selection of alternative connection methods that are relevant to the specific connection type, the prototype system empowers the user to make informed decisions and customize the connection method based on their specific requirements. This flexibility ensures that the user has control over the connection process while still benefiting from the system's initial suggestions and defaults.

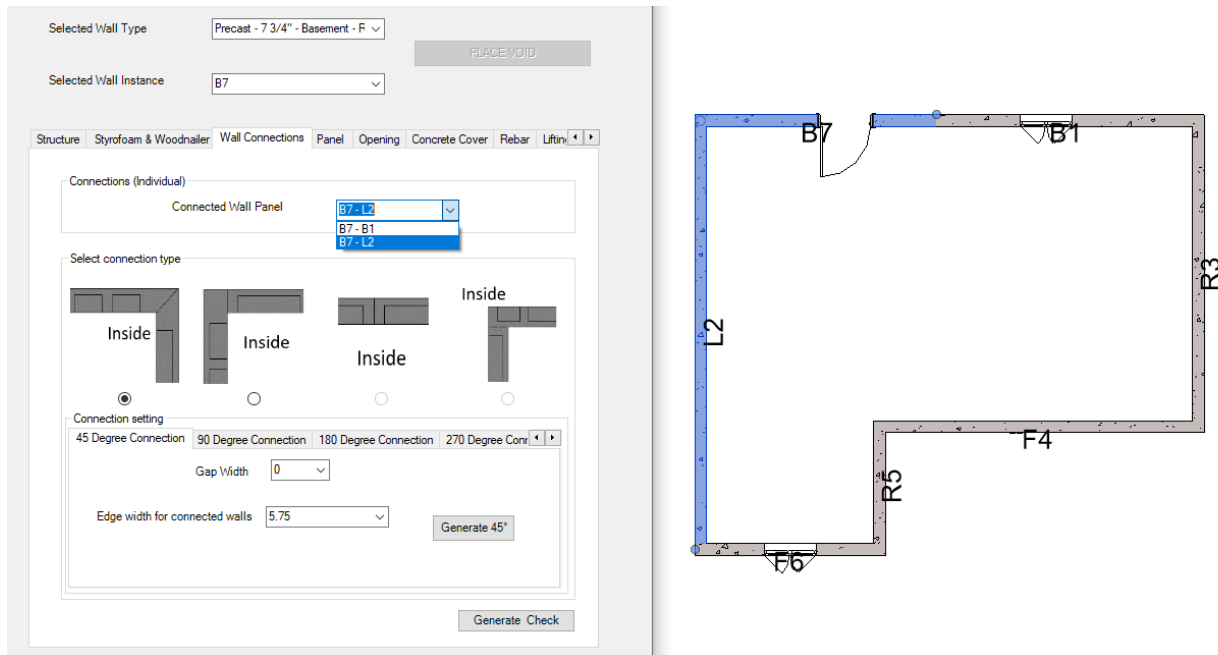


Figure 4-6. Suggested connection methods for wall connection.

With this automated approach, the prototype system ensures that the appropriate connection type and method are selected, reducing the potential for human errors, and increasing the overall efficiency of the process. By relying on the system's analysis and default settings, the user can confidently make modifications to the connected wall pairs, knowing that the suggested connection method aligns with the determined connection type.

#### 4.3.2.3 Generation of connection methods

When generating different types of connection methods, it is necessary to extend or shorten each wall in the connected wall pair to align with the exterior or interior boundary of the other wall. The Revit API provides the *CreateBound* method, which can be used to create a new linear curve and adjust the wall's location to achieve the desired extension or shortening.

The *CreateBound* method requires two *xyz* end-points to define the coordinates of the start- and end-points of the new wall location. When extending or shortening a wall, only one end-point

needs to be changed, while the other remains unchanged. It is crucial to assign the correct coordinates to the *CreateBound* method to maintain the orientation of wall, as significant logic in the code relies on the wall's orientation.

To address this issue, a tuple is created for each wall in the connected wall pair. Each tuple stores the coordinates of the end-points and their corresponding index, indicating whether it is the start- or end-point of the wall. By comparing the coordinates in the two tuples, points with identical coordinates can be identified. These points represent the overlapping locations at the wall connection, while the corresponding index indicates the position within the *CreateBound* method that needs to be assigned. The coordinates of these points can be modified to achieve the necessary location changes.

To address the issue of modifying the coordinates of these points, it is necessary to determine the correct coordinates based on the exterior and interior boundaries of the walls. The Revit API provides the *Wall.get\_BoundingBox (View)* method, which can be used to obtain the minimum and maximum coordinates of the wall's bounding box. The use of the minimum or maximum method depends on the layout orientation of the wall.

Referring to the wall orientations defined in Section 4.3.1, which include Front (F), Back (B), Left (L), and Right I, there are four possible layout orientations for connected wall pairs: Back-Left, Back-Right, Front-Left, and Front-Right.

By accessing the bounding box coordinates and considering the layout orientation, the prototype system can identify the correct coordinates by considering the gap width set by the user to modify the corresponding points at the wall connection. Implementing this process guarantees the precise

adjustment of wall coordinates within the prototype system, enabling the generation of accurate and properly aligned wall connections based on the selected connection method.

Based on the data presented in Table 4-5, the manual drafting time for generating a 45-degree connection for a convex angle wall connection type is approximately 57 s. However, utilizing an automated drafting tool such as ConcreteX can significantly reduce the drafting time to just five seconds. This substantial time reduction demonstrates the remarkable efficiency of the ConcreteX software application, offering a timesaving of approximately 91% compared to manual work on BIM.

Table 4-5. Drafting time for manual and ConcreteX performance for generating 45-degree connection method.

Wall connection method (45 degree)	Drafting Time
Manual	57 s
ConcreteX	5 s
Savings	91%

### 4.3.3 Automatic structural generation

During the process of generating the structural layout for casting, the user is required to specify their desired panel layout, which serves as the foundation into which the structural elements are to be cast. Furthermore, users input thickness values for the ribs and Styrofoam in both the selected structural layout and the Styrofoam sections, as illustrated in Figure 4-7. These input values act as crucial parameters for the embedded mathematical algorithms within the add-on.

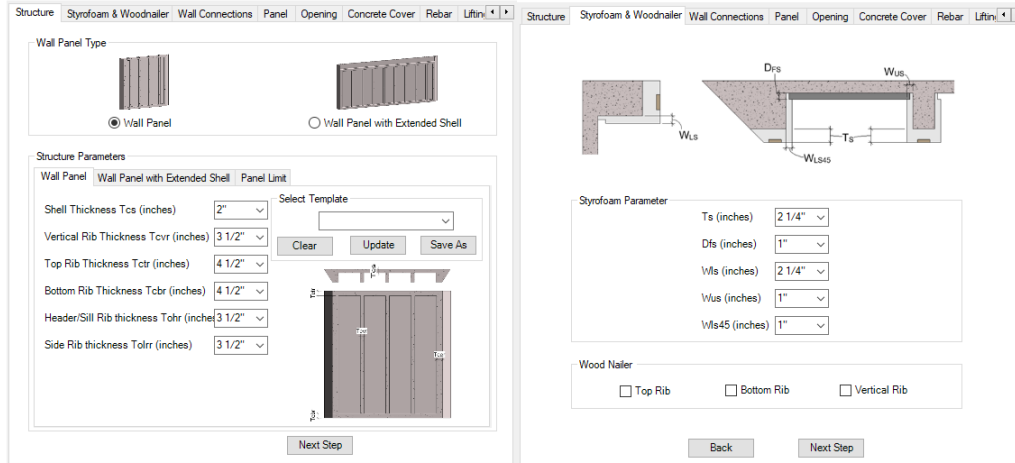


Figure 4-7. Input parameters for rib thickness and Styrofoam.

Once these specifications are provided, the information is stored as input variables that drive the built-in mathematical algorithms responsible for determining the optimal placement of the ribs. Additionally, an origin point is established for each wall, serving as a fundamental reference for the automation process of placing the Void families.

Leveraging the input variables, these algorithms precisely calculate the positioning and spacing of the ribs within the structural layout. The generated rib layout information is stored in an information file for future use, ensuring consistency and facilitating the desired structural configuration.

Based on whether openings are detected on the wall, the previously generated rib locations are used to automatically generate different Void arrangements. This is accomplished by leveraging the embedded mathematical algorithms within the add-on. These algorithms determine the Void layout, allowing for the automated generation of the rib layout.

By automating this procedure, the system ensures a consistent and efficient generation of the panel's structural layout, effectively streamlining the overall design process.

### 4.3.3.1 Void placement location determination

To generate the rib structure for precast concrete panels, it is necessary to determine the location of each rib within the panel. In the prototype system, the easiest approach to create the concrete panel is by cutting Void family instances from the complete panel, instead of individually building each rib element. Therefore, the Void family provided by 3i Inc., as shown in Figure 4-8, is loaded and used for structural generation. The parameters set within this Void family determine the appearance of the Void and, subsequently, the shape of the rib after cutting it from the wall.

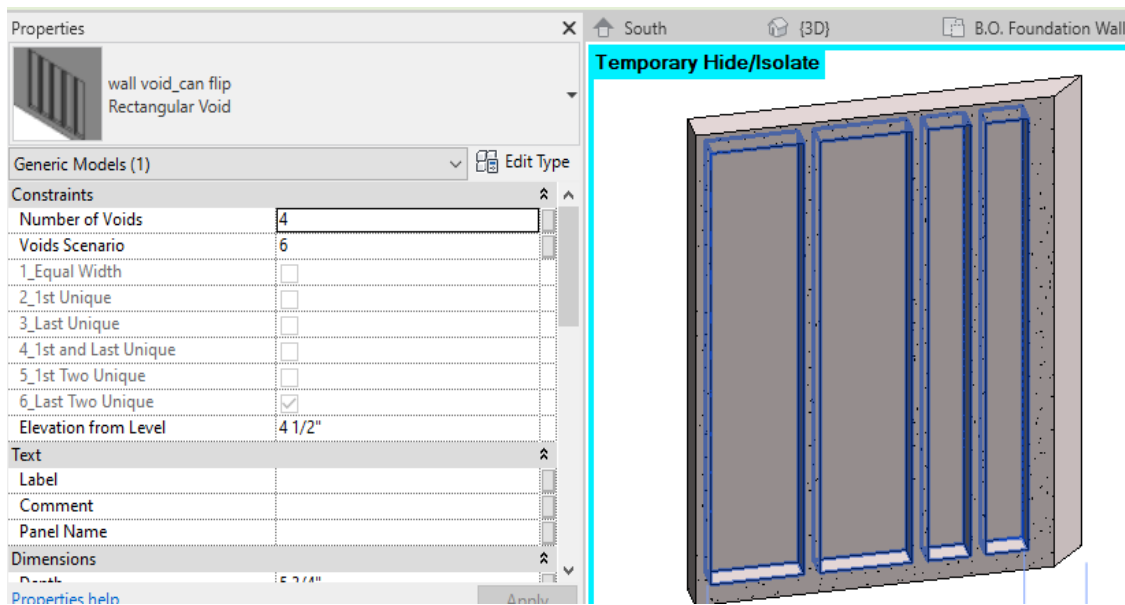


Figure 4-8. Void family for structural generation.

To accurately position the Void family instance, it is essential to establish the origin point of each wall. In the Void family, the origin point defined in the Void family editor serves as the insertion point when the family is placed in the Revit document. Notably, the origin of the Void family is consistently defined as the lower-left corner of the family, and the family itself can only be inserted from left to right. To simplify the calculation of the Void placement, the closest vertex on the wall to the origin point of the Void family is selected as the origin point of the wall, for referencing the

insertion point to place the Void family. This closest point is determined to be the lower-left corner of each wall's interior side when viewed from inside of the building. By employing the *Wall.get\_BoundingBox (View)* method, the minimum and maximum coordinates of the wall's bounding box can be obtained. Depending on the orientation of the wall, the *x*-, *y*-, or *z*-value can be extracted from *BoundingBox.Min* or *BoundingBox.Max* to determine the coordinates of the wall's origin point.

Once the origin point is determined to serve as the reference for the Void family, the structural integrity of the concrete elements is maintained by carefully determining the placement location of the Void within a specific distance from the panel's origin point. This distance is determined by combining the connection length and edge width. In essence, the sum of the connection length and edge width represents the distance at which the Void should be placed from the right of the origin point as depicted in Figure 4-9.

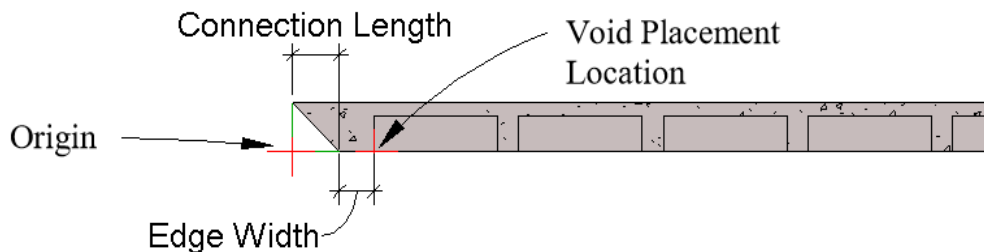


Figure 4-9. Void placement distance for structural integrity.

The connection length refers to the length that cannot be used for Void placement due to the varying connection methods employed as shown in Figure 4-10. For instance, in the case of the 45-degree edge connection method, where the edge is inclined at a 45-degree angle, the connection length is equal to the width of the wall. For the 90-degree connection method, the main wall, as defined by the user, extends to the outer boundary of the connected wall. Consequently, the

connection length is equal to the width of the connected wall at that specific corner. However, the other wall involved in the connection does not possess a connection length. For the 180-degree connection method where the walls are perfectly aligned, there is no overlap, resulting in the absence of a connection length. Moreover, the 270-degree connection method does not affect the connection length, regardless of the designated main wall, as the Void is generated on the interior side. Therefore, this connection method does not contribute to the connection length at the end of the wall.

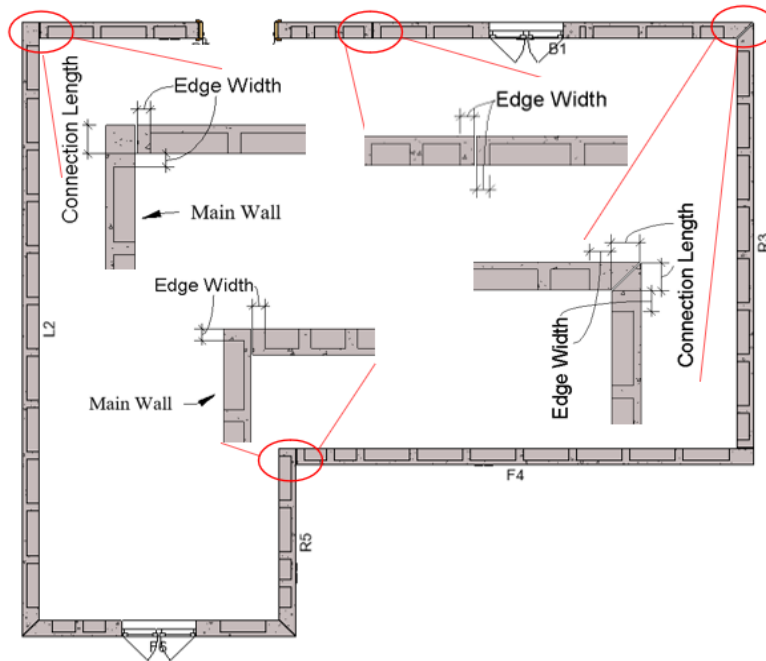


Figure 4-10. Variation in connection lengths across different connection methods.

The edge width represents the width of the Edge Rib, which is determined by user settings. Additionally, the gap width refers to the minimum distance left during manufacturing to accommodate sealant and prevent water and wind leakage through the wall connection. By adjusting the gap width, the start or end location of the wall is modified, which affects the overall length of the wall and the location of the origin point on the wall.

The placement location of the Void is determined by extracting the required parameters from the user settings form. This includes the user’s selection of the connection method and specification of values for the gap width and edge width, as outlined in Section 4.3.2.2. In the provided Figure 4-11, the 90-degree and 270-degree connection method is chosen for the F4-R3 and F4-R5 wall pairs accordingly. After the user’s selection, the system calculates and extracts the connection length and edge width information. These values are then stored in the respective ends of the walls involved in the connection. Specifically, the connection length and edge width are stored in end2 of the R5 wall, end1 of the F4 wall, end2 of the F4 wall, and end1 of the R3 wall.

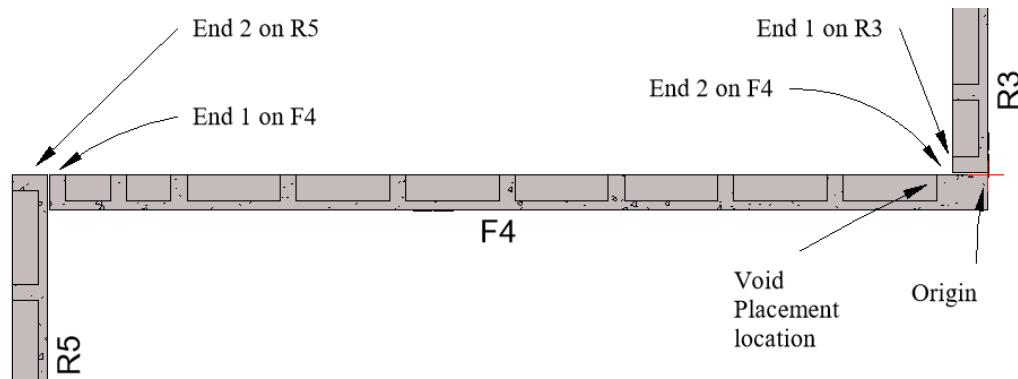


Figure 4-11. Storage of connection length and edge width information in wall ends.

In the case of the F4 wall, which has two ends, determining which end to use for the calculation of the specific distance from the wall’s origin point becomes essential. Since the origin point is defined as the left end of the interior side of the wall when viewed from inside the building, as depicted in the Figure 4-11, only the connection length and edge width from this left end (end2 on the F4 wall) can be employed to accurately calculate the placement location of the voids, with the origin point serving as the reference.

To accurately determine the specific end of all walls that corresponds to the left side, which is essential for calculating the placement location of the voids, a systematic approach is implemented

in the prototype system using a dictionary and code iteration. The dictionary is created with the wall ID as the key and a list of information as the value, including the connection length, edge width, and location for both ends of the wall.

During the execution of the code, an iteration is performed through each selected wall connection method for the corresponding connected wall pair. By analyzing the layout orientation, it becomes possible to identify which wall contains the left end and which wall contains the right end. As a result, the connection length is calculated based on the chosen connection method, and the information, along with the location, is stored for each end in their respective wall. To mark the location, an enumerated type, such as an enumeration with values for “left” and “right”, indicating whether it is the left or right end of the wall, is used. The location information is then saved to the location Point Attribute, where a value of 0 represents the left end and a value of 1 represents the right end.

By selecting the appropriate connection method for each end of the wall and storing the corresponding connection length and edge width, the system obtains the necessary information to accurately determine the placement location of the Void. However, it is important to note that only the end with a location point value of 0 (representing the left end) is used to calculate the Void’s placement location. The system ensures that the voids are positioned at the desired locations within the concrete structure.

#### **4.3.3.2 Automated structural generation for solid panels**

To achieve the desired arrangement of voids within concrete structural panels, a parameter-driven approach is employed, directly influencing the resulting layout of the rib structures. Once the

placement location of a Void is determined, the corresponding parameters for the Void family instance must be established.

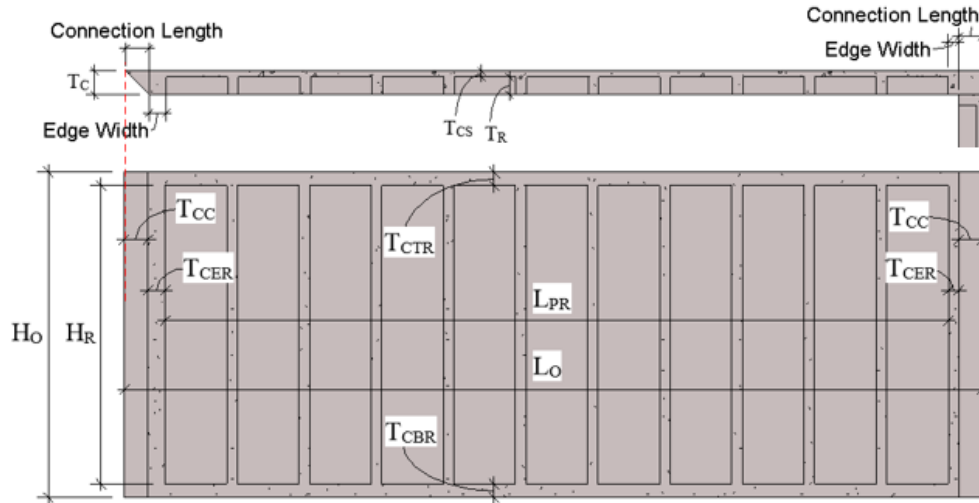


Figure 4-12. Parameters used in Void placement.

The calculation of these parameters involves determining the necessary height, length, and depth for the Void to fit precisely within the wall panel, as illustrated in Figure 4-12. For the length parameter, the Length parameter for Void Fit ( $L_{PR}$ ) is introduced.  $L_{PR}$  can be obtained by subtracting the connection length ( $T_{CC}$ ) and edge width ( $T_{CER}$ ) stored at each end of the wall from the total wall length ( $L_O$ ). The wall length is retrieved from the model using the *Wall.Location.Curve.Length* function in the Revit API. Additionally, the required information for each end of the wall, including connection length and edge width, is obtained from a dictionary based on the wall's unique identifier (wall Id).

To determine the height parameter, the Height Parameter for Void Fit ( $H_R$ ) introduced in Section 3.2 is used.  $H_R$  is obtained by subtracting the thickness of the Top Rib ( $T_{CTR}$ ) and Bottom Rib ( $T_{CBR}$ ) from the wall height ( $H_O$ ). The wall height is retrieved from the wall properties using the

*LookupParameter* function in the Revit API. The rib thickness information is retrieved from user settings within the Windows Form.

Similarly, the depth parameter is determined using the Thickness Parameter for Void Fit ( $T_R$ ) introduced in Chapter 3.2.  $T_R$  is obtained by subtracting the Shell thickness ( $T_{CS}$ ) from the total wall thickness ( $T_C$ ). The wall thickness is retrieved from the structural width of the wall family type using the *Wall.Location.Curve.Length* function, with the *Doc.GetElement(wall.GetTypeId())* as *WallType* in the Revit API. The Shell thickness information is retrieved from user settings within the Windows Form.

The process for determining the arrangement of voids is visually depicted in Figure 4-13, showcasing two scenarios based on the length for placing Vertical Ribs ( $L_{PR}$ ).

In Scenario 1, when  $L_{PR}$  is insufficient to accommodate the last rib, further adjustments are made. The width of the last rib ( $W_{LR}$ ) is determined and incorporated into the width of the last Void on the panel. Subsequently, the last Void is divided into two equal-width voids, each with a width value of  $W_{BRA}$ . These voids are then placed at the end of the panel to ensure optimal utilization of available space.

In Scenario 2, when all ribs can fit within the panel, the design is determined based on the width of the last Void on the panel ( $W_{BLE}$ ). If  $W_{BLE}$  is equal to or greater than 4 inches, indicating compatibility with the factory's current production capabilities, the design remains unchanged. In this case, only one unique-width Void with a value of  $W_{BLE}$  is placed at the end of the panel.

However, if  $W_{BLE}$  is less than 4 inches, it is incorporated into the width of the last Void. Subsequently, the last Void is divided into two equal-width voids, each with a value of  $W_{BRA}$ ,

ensuring proper spacing and structural integrity. These voids are then placed at the end of the panel to optimize the Void arrangement.

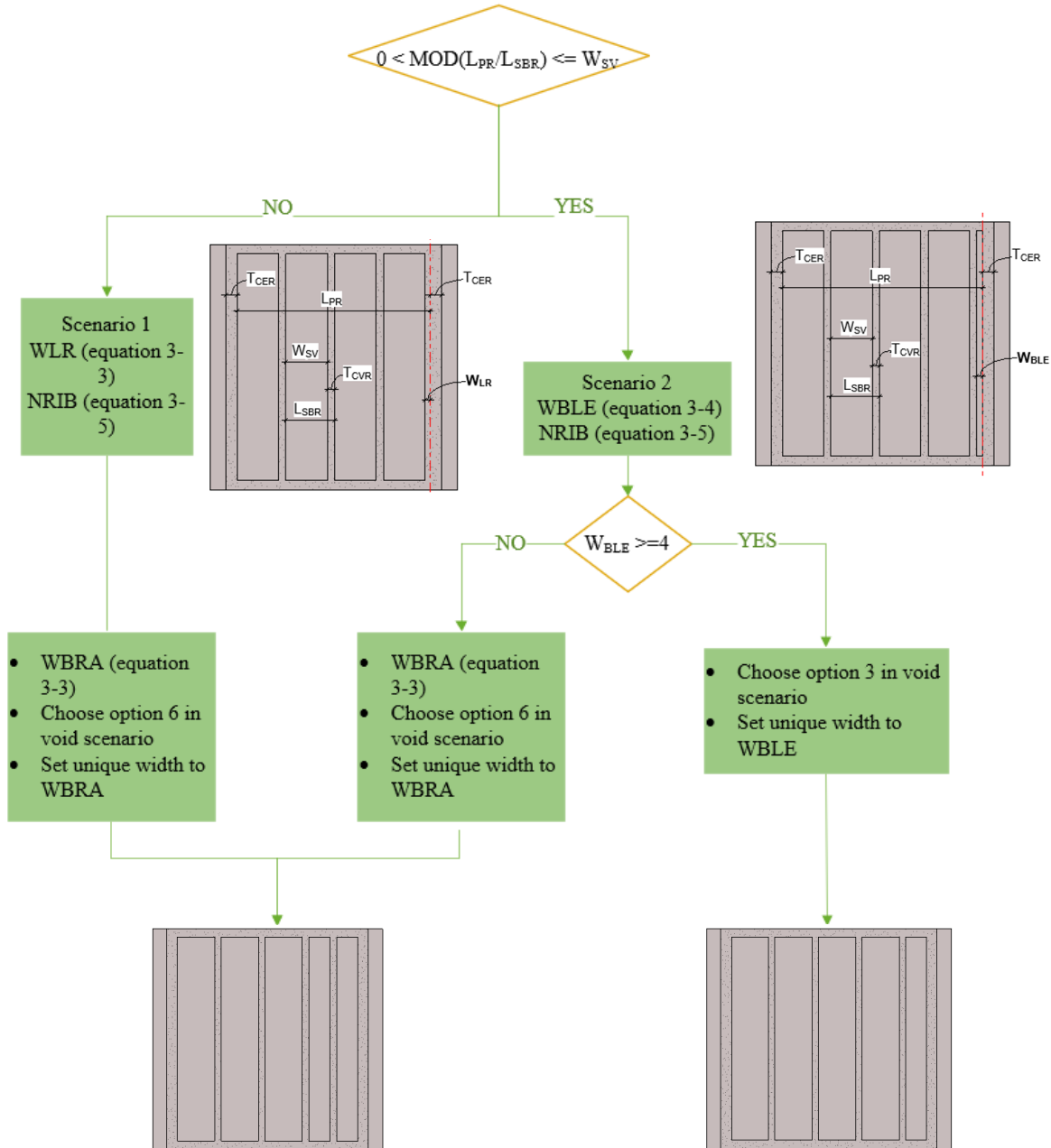


Figure 4-13. Flow chart of Void arrangement determination.

The final rib location is designed based on different scenarios for rib placement, ensuring an appropriate structural layout. Parameters such as the Void scenario determining the Void layout, the number of voids, and the unique width generated in the previous step, are then assigned to the Void family's parameters. This assignment is accomplished using the *LookupParameter.Set* function, which automates the process of creating the panel's structure layout without any openings.

According to Table 4-6, drafting time (t) to manually generate the structural layout for a single concrete panel without openings is 150 s. However, utilizing an automated drafting tool such as ConcreteX can minimize the drafting time to 12 s. The results show the automated software application, ConcreteX, can save up to 92% of drafting time compared to manual work on BIM.

Table 4-6. Drafting time for manual and ConcreteX performance for generating structural layout of solid wall.

Ribbed panel structure (solid wall)	Drafting Time
Manual	150 s
ConcreteX	10 s
Savings	92%

#### 4.3.3.3 Automated structural generation for walls with openings

To identify openings within a wall, two filters are employed to search for elements categorized as *BuiltInCategory.OST\_Windows* and *BuiltInCategory.OST\_Doors*. For each identified element, the associated wall hosting that element in the project is determined using *Element.Host.ID*. The wall

is then inserted as a key in the “wallsAndTheirOpeningsLocations” dictionary, with the locations of the openings on that wall added as corresponding values.

Through an analysis of the number of elements within the location list, the system can effectively discern the presence or absence of openings within a given wall. This automated identification and categorization of walls with openings serves as crucial information for the subsequent stages of the automatic structural generation algorithm. By accurately recognizing walls with openings, the system can appropriately adapt the structural generation process to accommodate these openings, ensuring a comprehensive and reliable automated workflow.

The structural layout around the openings adheres to a well-defined generation principle, as illustrated in Figure 4-14. This principle serves as a guideline for determining the rib structure that surrounds the openings. By leveraging the bounding box and extracting essential information such as the distances from the origin to the edges of the openings on each wall, including the left and right edges ( $W_{WLE}$ ,  $W_{WRE}$ ) and the top and bottom edges ( $H_{WBE}$ ,  $H_{WTE}$ ), the system gains valuable insights into the spatial characteristics of the openings.

To ensure a cohesive and stable structural configuration, the system uses the stored locations of the ribs as reference lines for assessing the continuity of the Vertical Ribs in relation to the extracted opening positions. This evaluation enables the system to make informed decisions regarding the placement and design of different rib types, including Cripple Ribs, Side Ribs, Header Ribs, and Sill Ribs. Through this process, the system ensures the creation of a coherent and stable structural configuration, even in the presence of openings. By combining sophisticated algorithms with accurate spatial data, the automatic structural generation algorithm can effectively

optimize the placement of ribs, guaranteeing a robust and efficient panel layout that meets the design requirements.

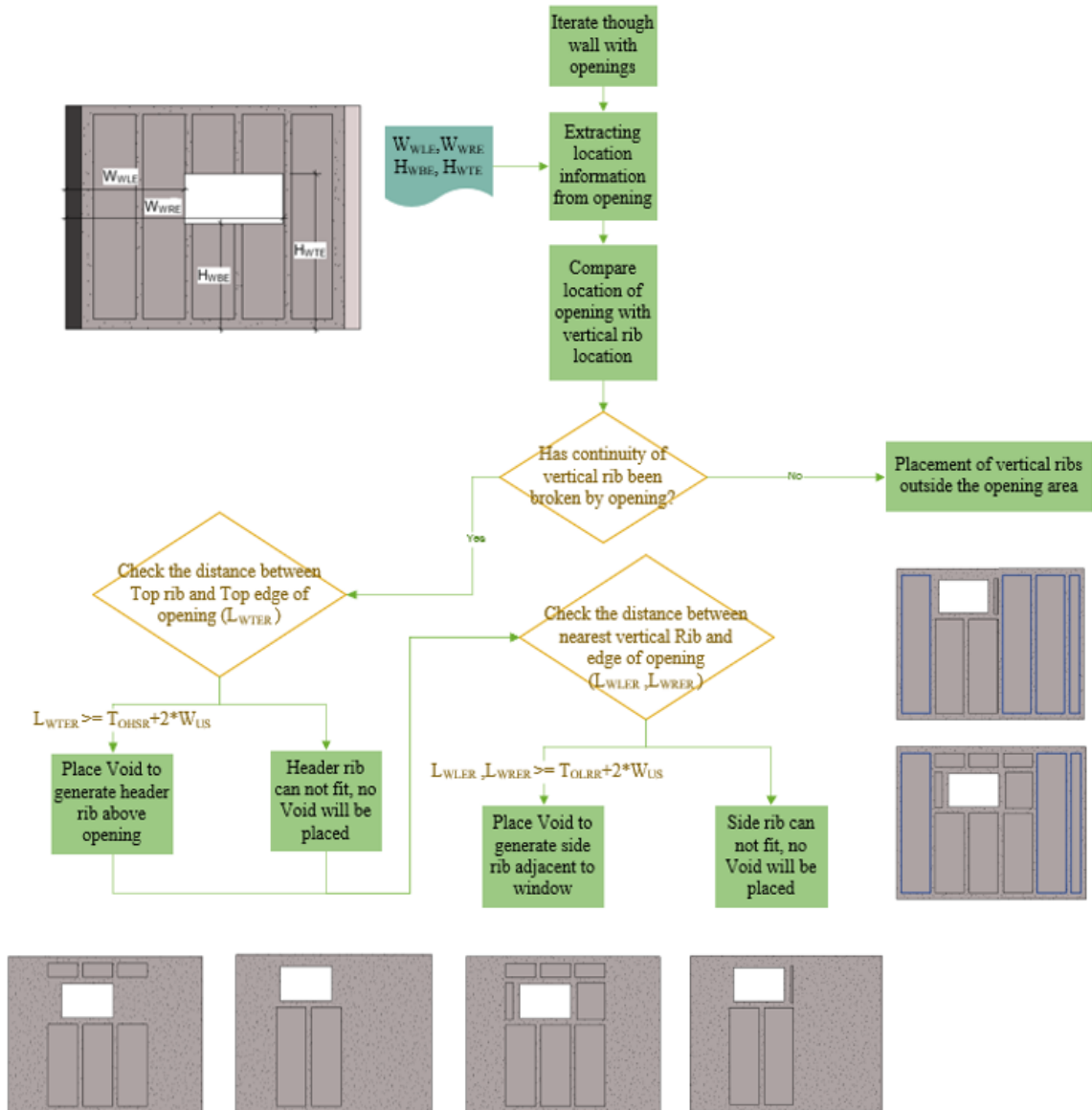


Figure 4-14. Automated generation principle for structural layout around openings.

When openings appear, the continuity of the Vertical Ribs is disrupted, necessitating the inclusion of different types of ribs. One important consideration is the generation of Cripple Ribs. To determine if a Cripple Rib can be created above the opening, the distance between the top edge of

the opening and the Top Rib ( $L_{WTER}$ ) is calculated. This distance is then compared to the thickness of the Header Rib and its Styrofoam formwork. If there is sufficient space to accommodate the Header Rib, a Void is generated above the opening to incorporate the Cripple Ribs, ensuring the overall structural integrity. However, if there is not sufficient space for the Header Rib, no Cripple Ribs will be generated above the openings. This allows for an appropriate structural configuration to be maintained.

Another important consideration is the generation of Side Ribs. The determination of whether a Side Rib is present follows the same logic as the Cripple Rib, which involves assessing if the distance between the nearest Vertical Rib and the edge of the opening ( $L_{WLER}$ ,  $L_{WRER}$ ) is wide enough to accommodate the thickness of the Side Rib along with its Styrofoam formwork. This approach ensures that the Side Rib can be properly incorporated into the structural layout of the panel, maintaining its stability and desired configuration.

On the other hand, the placement of Vertical Ribs outside the opening area is determined based on the predefined structural configuration. This approach guarantees the structural stability and desired layout of the panel, even when openings are present. By adhering to the predefined configuration, the system ensures that the Vertical Ribs are positioned strategically to provide adequate support and maintain the overall integrity of the panel's structure. This systematic approach allows for consistent and reliable generation of the structural layout, accommodating openings without compromising the stability and desired design of the panel. Various structural layouts are presented in Appendix A.

According to the data presented in Table 4-7, the manual drafting time for generating the structural layout of a concrete panel with one opening is approximately 900 s. Additionally, for each

additional opening on a wall, it typically requires an additional 5–7 min of design and drafting time to incorporate the structural layout around the openings. However, by utilizing ConcreteX, the drafting time can be reduced to 12 s for a concrete panel with one opening. Furthermore, the time required for incorporating each additional opening adds only two seconds to the process. This substantial time reduction showcases the exceptional efficiency of the ConcreteX software application, reducing time by approximately 98.6% when compared to manual work on BIM.

Table 4-7. Drafting time for manual and ConcreteX performance for generating structural layout of wall with opening.

Ribbed panel structure (one opening)	Drafting Time
Manual	900 s
ConcreteX	12 s
Savings	98.6%

## **Chapter 5. Case Study**

ConcreteX, as a Revit add-on for automating the design and drafting of ribbed precast concrete panels, is designed to save design and drafting time to eliminate the bottleneck and level out each stage in the overall project delivery process. This chapter focuses on evaluating the effectiveness and efficiency of the developed prototype system through two comprehensive studies.

The first study concentrates on the design and drafting process itself, specifically examining the extent to which ConcreteX saves time compared to manual drafting. This analysis provides valuable insights into the time-saving benefits and efficiency gains achieved by utilizing ConcreteX in design and drafting tasks.

The second study involves developing a simulation model that encompasses the broader context of the project delivery process. This model aims to mimic the various stages involved in project delivery, utilizing the data gathered from the time study conducted in Chapter 4. By incorporating the simulation model, the benefits of implementing ConcreteX can be further analyzed, including improvements in production rate and overall reduction in lead time.

The evaluation of ConcreteX is conducted using construction projects undertaken by 3i Inc to employ a 3D Building Information Model (BIM) of a single-family house basement. Detailed information about the basement can be found in Figure 5-1.

This BIM model serves as a representative example of panelized construction, where individual panels or components are manufactured in a factory and later transported to the construction site for assembly. It is worth noting that the time studies conducted focus on the casting of wall components.

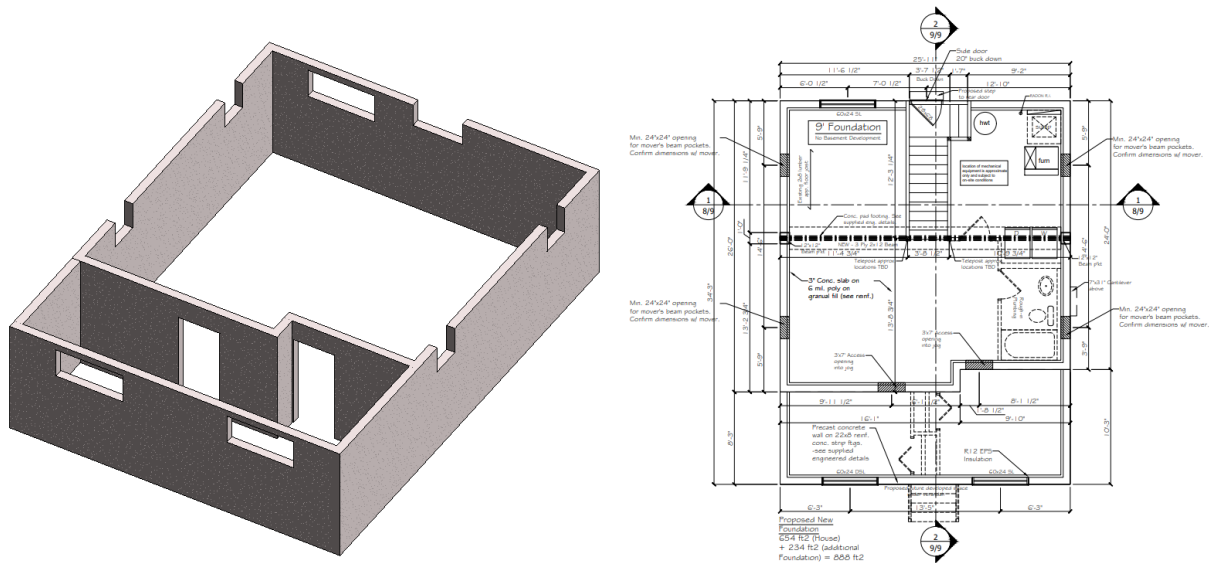


Figure 5-1. 3D Revit model and floor plan for the case study basement

## 5.1 Study 1—Evaluating time savings in design and drafting with ConcreteX

This study assesses the total time required to efficiently execute all functions sequentially when generating the desired model. By comparing these results with manual design and drafting processes, valuable insights can be gained regarding the substantial time savings facilitated by ConcreteX.

To generate the desired model using ConcreteX, the user follows a simple process. First, by selecting all the wall panels in the model, the user can click on the “Create/Edit” button under the ConcreteX tab. This allows the user to specify the desired values for rib structure and Styrofoam thickness. These user-defined parameters determine the wall structure. Additionally, the user can select the preferred connection method for different wall connection types.

Once the user has set the desired parameters and connection methods, they can proceed by clicking the “Generate” button to initiate the generation process. At this point, the ConcreteX system generates the desired model as shown in Figure 5-2 based on the specified parameters and

connection methods. Furthermore, as an important consideration, the system also checks whether any panel exceeds the weight limitations of the crane used for lifting and installation. This step ensures that the generated panels are within the acceptable weight range, prioritizing safety and practicality.

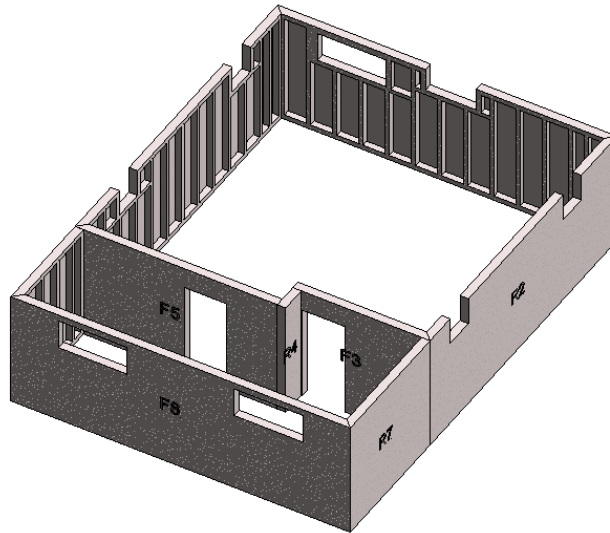


Figure 5-2. Output from ConcreteX: model with manufacturing details.

Overall, the ConcreteX user interface provides an intuitive and straightforward workflow for generating the desired wall structure, with the additional benefit of weight verification to ensure safe and efficient installation.

As shown Table 5-1, following the aforementioned process to automate the generation of the desired model using ConcreteX, the user time required is just 2.58 min (155 s). In comparison, the manual drafting process to achieve the same desired model is approximately 3.17 h (11,400 s). This time savings amounts to approximately 98.6%.

Such a substantial reduction in time signifies a remarkable efficiency improvement. The time saved with ConcreteX effectively translates into saved labour, making it equivalent to having a drafter’s work completed without any associated cost.

Table 5-1. Drafting time for manual and ConcreteX performance for generating desired model with fabrication detail.

Model with fabrication detail	Drafting Time
Manual	11,400 s
ConcreteX	155 s
Savings	98.6%

## 5.2 Study 2—Analyzing the impact of ConcreteX on project delivery

### 5.2.1 Simulation model

In order to analyze and optimize the delivery process, a comprehensive simulation model is employed. This simulation model aims to replicate the entire project delivery process, which consists of three main activities: design and drafting, prefabrication in the factory, and on-site installation. The simulation model incorporates a composite that encompasses the design and drafting process of the basement, as highlighted in the case study. The activities in the model are resource-dependent, meaning that the resources and number of servers are assigned to each activity. The simulation model is developed using the simulation environment of Symphony.NET, a widely used platform for building simulation models (AbouRizk and Mohamed, 2000). To provide a visual overview of the simulation model's structure, Figure 5-3 presents the main layout of the

project delivery process simulation model. This diagram illustrates the various components and their interconnections within the model.

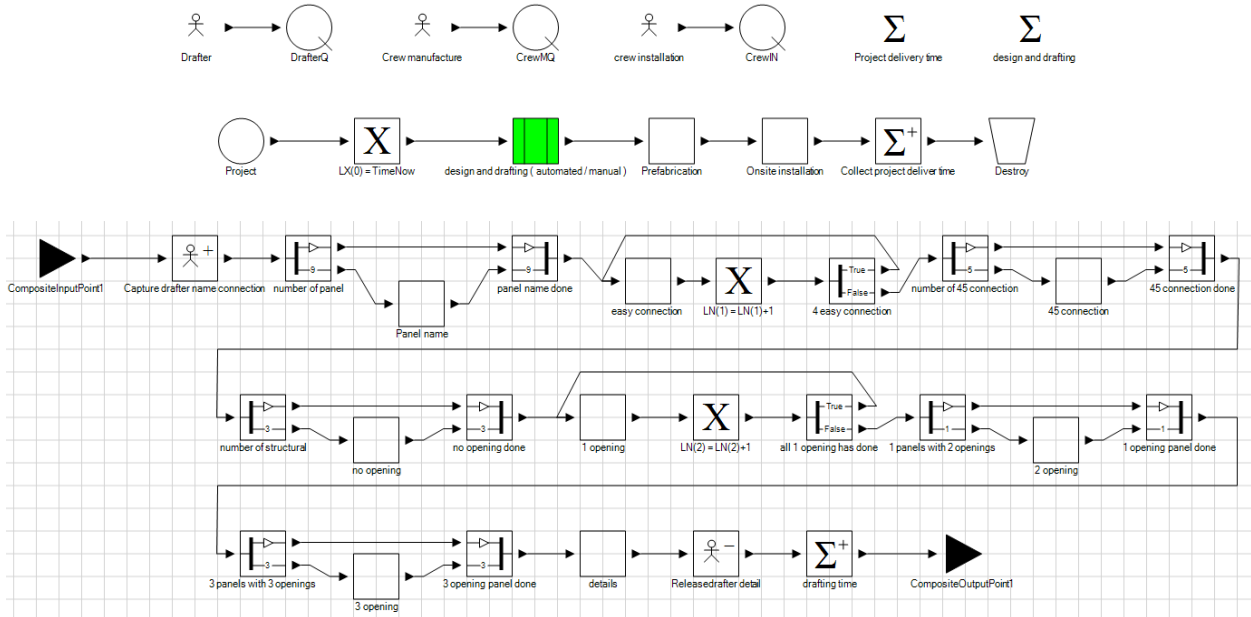


Figure 5-3. Main layout of current project delivery process simulation model.

In order to accurately represent the task durations in minutes, each task was fitted to a distribution based on recorded times from both manual and automated sources, as shown in Table 5-2. The values obtained from the previous time study for manual and automated drafting are used as distinct inputs for the current design and drafting process. Consequently, two simulation models are created with identical layouts and different task duration inputs: one model uses manually recorded time inputs (referred to as Model M), while the other uses automated time inputs (referred to as Model A). By comparing the time differences between the two approaches, the impact of using manual or automated time inputs on the overall simulation can be assessed.

Table 5-2. Duration distribution for each activity.

Event	Duration distribution	
	Manual (minutes per event)	Automated (minutes per event)
Wall connection method (45 degree)	Triangular (0.5, 1.0, 0.9)	Triangular (0.070, 0.100, 0.083)
Ribbed panel structure (solid wall)	Triangular (3.0, 10.0, 5.0)	Triangular (0.133, 0.200, 0.167)
Ribbed panel structure (one opening)	Triangular (12.0, 20.0, 16.0)	Triangular (0.150, 0.216, 0.183)
Ribbed panel structure (two openings)	Triangular (16.0, 32.0, 23.0)	Triangular (0.167, 0.230, 0.200)
Ribbed panel structure (three openings)	Triangular (23.0, 45.0, 30.0)	Triangular (0.180, 0.240, 0.215)
Prefabrication	Triangular (1680.0, 2400.0, 1920.0)	
Onsite Installation	Triangular (427.0, 480.0, 450.0)	

### 5.2.2 Validation

To ensure reliable results, 1,000 runs of the simulation were conducted due to the stochastic nature of the model. By running both Models A and M, the drafting time for each approach was obtained. The time taken to complete the design and drafting of the basement project for each approach, as obtained from the simulation report, is shown in Table 5-3.

Table 5-3. Design and drafting time collected from both simulation Models A and M.

Design and drafting time(s)	Mean Value	Standard Deviation	Minimum Value	Maximum Value
Model M	177.433	9.264	149.414	207.318
Model A	2.521	0.042	2.382	2.640

The simulation model can be validated by comparing the cycle time of the design and drafting process between the simulation results and the actual time collected from the drafter. This comparison helps to assess the accuracy of the simulation. The results of this comparison are presented in Table 5-4.

Table 5-4. Comparison of drafting time for basement project—real-world versus simulation.

Approach	Real-world collected time (s)	Model simulation time (s)	Difference
Manually	11,400	10,645.98	7.08%
Automated	155	151.26	2.47%

For the manually simulated Model M, the mean time taken to complete the design and drafting process is 177.433 min (or 10,645.98 s), compared to the actual human drafting time for this project, which is 11,400 s. The difference between the simulation and actual time is 7.08%. In the case of the automated simulated Model A, the mean time for design and drafting is 2.521 min (or 151.26 s), while the actual automated drafting time by ConcreteX for this project is 155 s. The difference between the simulation and actual time is 2.47%.

The cycle time differences between the simulation and real-world data are calculated to be 7.08% and 2.47%, respectively, with an average difference of 4.78%. These differences are considered acceptable. Therefore, the constructed simulation model accurately represents the current design and drafting process and can be considered reliable for further analysis.

### **5.2.3 Simulation results and discussion**

In order to comprehensively assess the benefits of ConcreteX within the broader context of the project delivery process, the validated simulation models A and M from the previous section were used. These models were employed in different cases to analyze the benefits of implementing ConcreteX.

To reflect the real-world scenario, the time intervals between project orders were simulated using an Exponential distribution with a mean of 960 min. This distribution closely represents the average time it takes for the company to receive an order from a customer, considering their average workload of 10–15 projects per month, equating to a new project order approximately every two working days. The simulation process continued until all 15 projects were completed, providing a comprehensive overview of the project delivery process and its dynamics. All simulation model reports for the cases discussed below can be found in Appendix D.

The results and analysis provide valuable insights into the significant benefits brought about by the implementation of ConcreteX, offering a deeper understanding of its transformative potential in streamlining the overall project delivery process.

#### **5.2.3.1 Case 1: Impact of bottleneck in project delivery process**

The design and drafting process has emerged as a potential bottleneck in the overall project delivery process, primarily due to its substantial time consumption compared to the manufacturing

phase in panelized construction. Recognizing the existence of this bottleneck, it becomes imperative to assess its severity and determine the urgency for resolution. To gain a comprehensive understanding of its impact, simulations using Model M were conducted, involving one drafter. By analyzing the drafter’s utilization and the waiting time for projects to be drafted, the magnitude of the bottleneck’s influence on the overall project delivery process can be effectively measured.

Table 5-5. Simulation results—utilization rates and waiting file (Model M).

**Resources**

Element Name	Average Utilization	Standard Deviation	Maximum Utilization	Current Utilization	Current Capacity
crew installation (Inner Resource)	1.7%	0.0%	1.8%	1.7%	6.000
Crew manufacture (Inner Resource)	7.6%	0.2%	8.4%	7.6%	6.000
Drafter (Inner Resource)	96.3%	0.3%	96.8%	96.5%	1.000

**Waiting Files**

Element Name	Average Length	Standard Deviation	Maximum Length	Current Length	Average Wait Time
CrewIN	0.000	0.000	0.000	0.000	0.000
CrewMQ	0.000	0.000	0.000	0.000	0.000
DrafterQ	5.231	0.483	6.227	5.007	23,039.358

The data in the waiting file and the utilization rates of different resources used in the simulation model were analyzed based on the report results obtained from Model M, as shown in Table 5-5. The average utilization rate for the drafter is observed to be 96.3%, indicating a consistently high workload for this resource. In contrast, the utilization rates for the manufacturing crew and installation crew are considerably lower, at 7.6% and 1.7%, respectively, suggesting relatively low workloads and frequent periods of idle time for these crews. Additionally, the average waiting time for a project to be drafted is approximately 47 days, with an average of 5.2 projects waiting in line.

Recognizing the significance of this bottleneck necessitates immediate action to address the issue and enhance the efficiency and fluidity of the project delivery process.

### 5.2.3.2 Case 2: Mitigate bottleneck in project delivery process through increased drafter count

In the case of Model M, we analyzed the impact of increasing the number of drafters on eliminating the bottleneck in the project delivery process. In this case, the following assumption is made: (1) All drafters adhere to the same design rules, and they have equal proficiency in drafting. (2) The available drafter can initiate the drafting process promptly without any undue delay. By plotting the waiting time for projects to be drafted against the number of drafters as shown in Figure 5-4, a clear trend was observed: as the number of drafters increases, the waiting time for projects decreases.

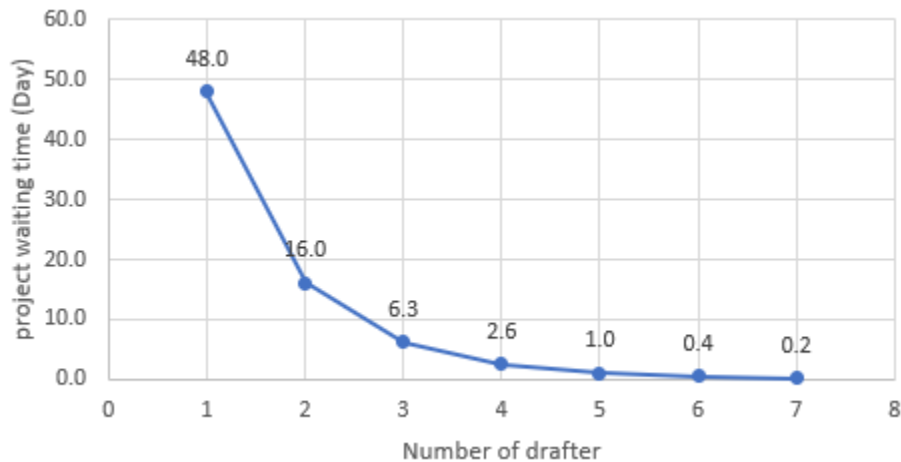


Figure 5-4. Impact of drafter count on project waiting time.

Increasing the number of drafters proves to be an effective approach in balancing the major tasks within the project delivery process. Considering that delivery time is measured in days, the graph demonstrates that when the number of drafters reaches five, the waiting time for projects is reduced to within one day. Although having more than five drafters could further decrease the waiting time, achieving a waiting time of less than one day would not have a significant impact on the total delivery time for projects.

Considering the associated costs in terms of salaries, having five drafters seems to be a viable solution for the current situation. Employing additional drafters beyond this number would result in increased salary expenses without significantly altering the overall project delivery timeline. Therefore, based on the analysis from the simulation model, it is recommended to maintain a team of five drafters to efficiently manage the project delivery process and minimize waiting times, while ensuring a cost-effective approach.

**5.2.3.3 Case 3: Streamlining project delivery with ConcreteX**

The core concept of this thesis revolves around proposing an automated design and drafting system to enhance the efficiency of the project delivery process. To evaluate the effectiveness of this automation approach, we conducted simulations using Model A, which incorporates automation drafting time as an input. The objective is to determine whether the bottleneck can be eliminated by employing a single drafter within the current operational context, thereby validating the benefits of automation.

Table 5-6. Simulation results—utilization rates and waiting file (Model A).

<b>Resources</b>					
<b>Element Name</b>	<b>Average Utilization</b>	<b>Standard Deviation</b>	<b>Maximum Utilization</b>	<b>Current Utilization</b>	<b>Current Capacity</b>
crew installation (Inner Resource)	7.5%	1.8%	14.7%	7.1%	6.000
Crew manufacture (Inner Resource)	33.1%	7.8%	66.1%	30.9%	6.000
Drafter (Inner Resource)	1.2%	0.3%	2.5%	1.1%	1.000

<b>Waiting Files</b>					
<b>Element Name</b>	<b>Average Length</b>	<b>Standard Deviation</b>	<b>Maximum Length</b>	<b>Current Length</b>	<b>Average Wait Time</b>
CrewIN	0.000	0.000	0.000	0.000	0.000
CrewMQ	0.007	0.045	1.016	0.000	4.870
DrafterQ	0.000	0.000	0.003	0.000	0.088

By analyzing the report results obtained from Model A, the data in the waiting file could be examined and the utilization rates of different resources within the simulation model could be evaluated, as depicted in Table 5-6.

The analysis revealed that the average utilization rate for the drafter is 1.2%, highlighting the efficiency gained by implementing the ConcreteX tool. Even with only one drafter where 15 projects are received in a month, the utilization of ConcreteX enables the drafter to efficiently manage the workload without causing any project delays. A waiting time of 0.088 min means that projects can be drafted promptly with zero projects in the waiting line.

Furthermore, the utilization rates for the manufacturing crew and installation crew are 33.1% and 7.5%, respectively. The average waiting time for a project to be manufactured is 4.87 min. These rates indicate that the manufacturing crew remains consistently busy and avoids unnecessary idle time. The idle time caused by waiting for shop drawings from the design and drafting process, which was observed in Case 1, is significantly reduced. This transition from conventional cast in-situ construction to panelized construction brings the advantage of employing workers as full-time staff rather than on a per-project basis. By utilizing ConcreteX and keeping the workers engaged, the monthly pay remains stable, while the increased number of projects completed reduces the hourly pay.

In summary, the results obtained from the simulation model when employing ConcreteX clearly demonstrates the elimination of the bottleneck in the project delivery process. Moreover, ConcreteX ensures that all major tasks within the project delivery process are balanced efficiently, leading to improved productivity and reduced delays.

### 5.2.3.4 Case 4: Comparative analysis of manual and automated approaches in project delivery

In Case 4, we compare the outcomes of Case 2, where the number of drafters is increased from one to five to mitigate the bottleneck, with the outcomes of Case 3, where the bottleneck is eliminated by utilizing the automation design and drafting tool, ConcreteX. By examining these two cases, which represent two distinct approaches—manual and automated drafting—we can assess how each approach influences the overall project delivery timeline, independent of any bottleneck effects. This comparison enables the overall effectiveness of the developed automation tool to be assessed, as well as its impact on streamlining the project delivery process, proving its success.

Table 5-7. Project delivery time comparison—manual drafting versus automated drafting with ConcreteX.

Approach	Project delivery time (min)	Project delivery time (days)
Case 2: Manually	7,181.755	15
Case 3: Automated	2,468.912	6
Savings		60%

As observed in Table 5-7, the average project delivery time for 15 projects in Case 2 is 7,181.755 min, which is equivalent to approximately 14.96 days, rounded to 15 days. In Case 3, the average project delivery time is 2,468.91 min, or approximately 5.14 days, rounded to six days. Through calculation, we find that there is a time of nine days is saved in delivering a project when

transitioning from manual design and drafting (Case 2) to the automated approach (Case 3). This represents a significant improvement of 60% in project delivery time.

These results strongly indicate that the implementation of the developed automation and design tool was highly successful in streamlining the overall project delivery process. The significant time improvement achieved through automation highlights the efficiency and effectiveness of ConcreteX in expediting project completion.

#### **5.2.3.5 Case 5: Impact of ConcreteX in productivity**

In Case 5, the focus is on assessing the impact of ConcreteX on productivity. Instead of simulating the completion of 15 projects, the simulation model is configured to run for a maximum of 30 days, allowing for the evaluation of the number of projects delivered within a one-month timeframe. To compare productivity between different approaches, a scenario was considered where the bottleneck effect is eliminated in the manual drafting approach by employing five drafters. In contrast, the automated approach uses only one drafter in the simulation model.

By examining the number of projects delivered within one month using these two distinct approaches, we can measure the improvement in productivity attributed to ConcreteX, independent of any bottleneck effects. This analysis provides valuable insights into the significant enhancement in productivity achieved through the implementation of ConcreteX.

As observed in Table 5-8, the number of projects delivered in one month using Model M, which represents the manually drafting approach, is 4.32, rounded to four projects. On the other hand, Model A, representing the automated drafting approach using ConcreteX, delivers 9.34 projects in one month, rounded to nine projects. This transition from the traditional manual design and

drafting process to utilizing ConcreteX in an automated manner has resulted in a significant increase of five projects per month.

Table 5-8. Comparison of delivered projects count in one month—manual drafting versus automated drafting with ConcreteX.

Approach	Number of projects delivered per month
Model M: Manually	4
Model A: Automated	9
Enhancement	125%

Comparing the productivity between the two approaches, the automated approach using ConcreteX has witnessed a remarkable improvement. With nine projects delivered per month compared to the initial four projects, there is an impressive 125% increase in productivity.

These findings emphasize the substantial impact of implementing ConcreteX in streamlining the design and drafting process. The automation provided by ConcreteX enables faster project completion and higher productivity, leading to significant benefits in project delivery efficiency.

## **Chapter 6. Conclusion**

### **6.1 Summary**

The surging in housing demand has placed considerable strain on the industry, resulting in extended lead times and operational inefficiencies. To overcome these challenges, panelized construction utilizing precast concrete panels has emerged as a promising solution. However, conventional precast designs encounter challenges, including high costs, limited flexibility, and restrictions in remodelling. To address these issues, this research introduces the 3i RPCPS. The standardized rib layout design increases the reusability of moulds and provides high flexibility for creating formwork for panels of varying sizes, enabling mass production in high efficiency. However, the presence of ribs necessitates the use of a fabrication system involving moulds and formwork, highlighting the critical importance of precision in shop drawings. To address this challenge effectively, a key factor in achieving precision is the integration of detailed BIM models, where model changes in different views are automatically updated, ensuring consistency across various views. However, it is important to note that creating a detailed 3D model with prefabrication details can significantly increase modelling time. Moreover, there is always the possibility of human error during the modelling process, leading to future revisions. As a result, the design and drafting stage, which requires substantial time to produce a detailed manufacturing-based BIM, are considered a bottleneck in the overall project delivery process. This bottleneck can cause wastage and prolong the lead time. The automation of BIM-based designs has the potential to mitigate these challenges by reducing manual effort, enhancing overall efficiency, and ensuring synchronization among project stages. Therefore, this research developed a comprehensive framework for an automated design and drafting system specifically tailored for ribbed precast concrete panels. This framework was successfully implemented in the automation tool, ConcreteX.

ConcreteX was developed, it should be noted, using two distinct design approaches. The first approach is the knowledge-based design, which incorporates the expertise and insights gained from the manual modelling process and the knowledge of experienced designers. This approach ensures that the functionalities within ConcreteX faithfully mirror the outcomes achieved through traditional manual modelling. Important functionalities developed by this approach include the automated generation of panel names based on the wall facing direction, as well as the automated suggestion and generation of connection methods tailored to different connection types. By integrating the knowledge and expertise of designers into ConcreteX, the add-on achieves a high level of accuracy and fidelity. The second approach employs Rule-based algorithm design, which aims to create mathematical algorithms that enable automated generation of structural layouts for both solid panels and panels with openings. These algorithms achieve their goal by conducting a comprehensive analysis of the design rules for panel structures, specifically customized for concrete ribbed panel systems. These rule-based mathematical algorithms serve as the backbone of ConcreteX to generate a desired output.

A single-house basement project was selected as the basis to evaluate the efficiency of ConcreteX, and two comprehensive studies were conducted to thoroughly analyze its performance. The first study focused on the design and drafting stage, where the time required to generate a desired model with fabrication details for the basement was collected for both manual and automated approaches. The results showed that by utilizing ConcreteX, a remarkable time saving of 98.6% was achieved when compared to the manual method. To further examine the benefits of ConcreteX in a broader context, a simulation model representing the overall project delivery process was developed. Through the simulation model, it showed that a manual approach with one drafter was identified as a bottleneck and it became evident that ConcreteX effectively eliminated the bottleneck with

only one designer involved, whereas the manual approach required five designers. ConcreteX allowed a significant reduction in labour resources. Specifically, it saved four designers, which led to an 80% reduction in the design and drafting workforce.

Although both approaches addressed the bottleneck issue successfully, there were significant disparities in terms of average lead time and the number of projects delivered per month. By utilizing ConcreteX, the average lead time was significantly reduced to six days, which was nine days shorter than the 15 days required by the manual approach. This represented a remarkable 60% reduction in lead time. Additionally, the implementation of ConcreteX allowed for the delivery of nine projects per month, a substantial increase of 125% compared to the four projects achieved through the manual approach. This substantial reduction in lead time and enhancement in productivity showed the efficiency and effectiveness of ConcreteX in streamlining the project delivery process.

## **6.2 Contributions**

The developed 3i RPCPS and automated design system can contribute to both academic research and current industry practices in panelized construction. The key contributions of this research can be summarized as follows:

- A mathematical algorithm is developed to transfer the complex structures of the innovative precast concrete panel system. This algorithm facilitates structural optimization and modelling by gathering comprehensive design information and criteria. The standardized design approach guarantees consistency and repeatability in the design process, regardless of whether it is executed manually or through automation.

- A parallel algorithm is developed for optimizing the utilization of the 3i forming system, enhancing construction efficiency and project outcomes.
- An innovative mathematical algorithm was developed to accommodate openings (such as windows and doors) within ribbed precast concrete panels while ensuring consistent rib spacing above and below the openings. This approach facilitates on-site drywall installation and minimizes the need for manual measurements.
- A simulation model of the project delivery process which includes a detailed process of the design and drafting stage was developed. This simulation model serves as a platform for conducting a case study to validate and quantify the differences between automated and manual approaches.
- The developed framework automates the design and drafting process for permit drawings and shop drawings of 3i RPCPS. It aims to enhance the efficiency of manufacturing-centric BIM model designs, reduce potential design errors and rework, and streamline the overall project delivery process, thereby minimizing waste, improving productivity, and reducing lead time.
- For the proof of concept, an Autodesk Revit add-on named ConcreteX was developed to automate the manufacturing-centric BIM model design. It incorporates both rule-based design and knowledge-based design to achieve a high level of model accuracy and fidelity, and it was deployed for industrial scale testing.

### **6.3 Limitations and future work**

- The current rule-based mathematical algorithms cover most scenarios for the structural layout around openings. Nevertheless, scenarios that are unaccounted for still exist,

requiring manual corrections. In future work, the algorithms could be improved by incorporating these missing scenarios to further improve accuracy and completeness.

- The current version of ConcreteX requires a 3D Revit model as input. However, most architectural designs are still generated in 2D CAD environments. In future work, it would be beneficial to directly use the 2D designs as inputs.
- The current version of ConcreteX can generate a quantity takeoff list for Styrofoam. In the future, a cutting optimization system can be incorporated to guide the transformation of raw materials into the desired dimensions specified in the takeoff list to minimize the waste.

## References

- Abanda, F.H., Tah, J.H.M. and Cheung, F.K.T., 2017. BIM in off-site manufacturing for buildings. *Journal of Building Engineering*, 14, pp.89-102.
- Abushwereb, M., Liu, H. and Al-Hussein, M., 2019. A knowledge-based approach towards automated manufacturing-centric BIM: wood frame design and modelling for light-frame buildings. *Proceedings, Modular and Offsite Construction (MOC) Summit*, pp.100-107.
- Von Der Ahe, W.R., Piekarz, R. and Newkirk, C.R., 1999. Precast soundwall panels make ideal housing components. *PCI Journal*, 44, pp.22-33.
- Alwisy, A., Al-Hussein, M. and Al-Jibouri, S.H., 2012. BIM approach for automated drafting and design for modular construction manufacturing. *Proceedings, International Workshop on Computing in Civil Engineering*, pp.221-228.
- Alwisy, A., Bu Hamdan, S., Barkokébas, B., Bouferguene, A. and Al-Hussein, M., 2019. A BIM-based automation of design and drafting for manufacturing of wood panels for modular residential buildings. *International Journal of Construction Management*, 19(3), pp.187-205.
- Garza-Reyes, J.A., Oraifige, I., Soriano-Meier, H., Forrester, P.L. and Harmanto, D., 2012. The development of a lean park homes production process using process flow and simulation methods. *Journal of Manufacturing Technology Management*, 23(2), pp.178-197.
- Azhar, S., 2011. Building Information Modeling (BIM): Trends, benefits, risks, and challenges for the AEC industry. *Leadership and Management in Engineering*, 11(3), pp.241-252.

- Cavieres, A., Gentry, R. and Al-Haddad, T., 2011. Knowledge-based parametric tools for concrete masonry walls: Conceptual design and preliminary structural analysis. *Automation in Construction*, 20(6), pp.716-728.
- NAHB Research Center, Inc., 2002. Design, fabrication, and installation of engineered panelized walls: Two case studies. U.S. Department of Housing and Urban Development.
- Ding, L., Zhou, Y. and Akinci, B., 2014. Building Information Modeling (BIM) application framework: The process of expanding from 3D to computable nD. *Automation in Construction*, 46, pp.82-93.
- Eastman, C.M. and Sacks, R., 2008. Relative productivity in the AEC industries in the United States for on-site and off-site activities. *Journal of Construction Engineering and Management*, 134(7), pp.517-526.
- Salmon, D.C., Tadros, M.K. and Culp, T., 1994. A new structurally and thermally efficient precast sandwich panel system. *PCI Journal*, 39(4), pp.90-101.
- Ezcan, V., Isikdag, U. and Goulding, J.S., 2013. BIM and off-site manufacturing: recent research and opportunities. *Proceedings, 19<sup>th</sup> CIB World Building Congress, Brisbane, Australia*.
- Holmes, W.W., Kusolthamarat, D. and Tadros, M.K., 2005. NU precast concrete house provides spacious and energy efficient solution for residential construction. *PCI Journal*, 50(3), pp.16-25.
- Hurd, M.K., 1994. Precast concrete homes for safety, strength and durability. *PCI Journal*, 39(2), pp.56-73.
- Johnson, P.G. ed., 2003. *Performance of exterior building walls*. Vol. 1422. ASTM International.

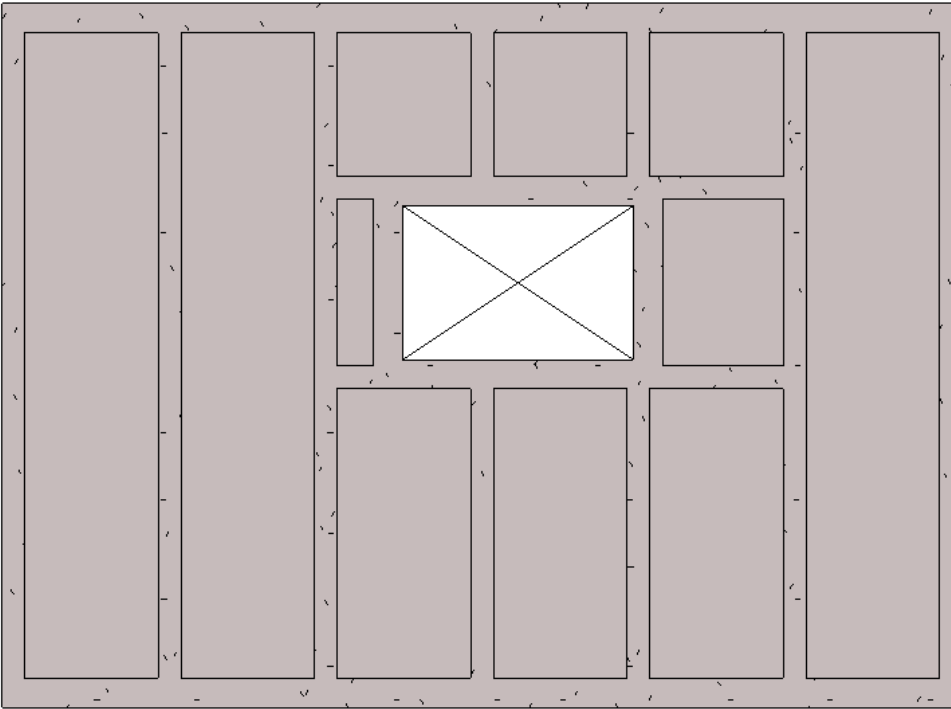
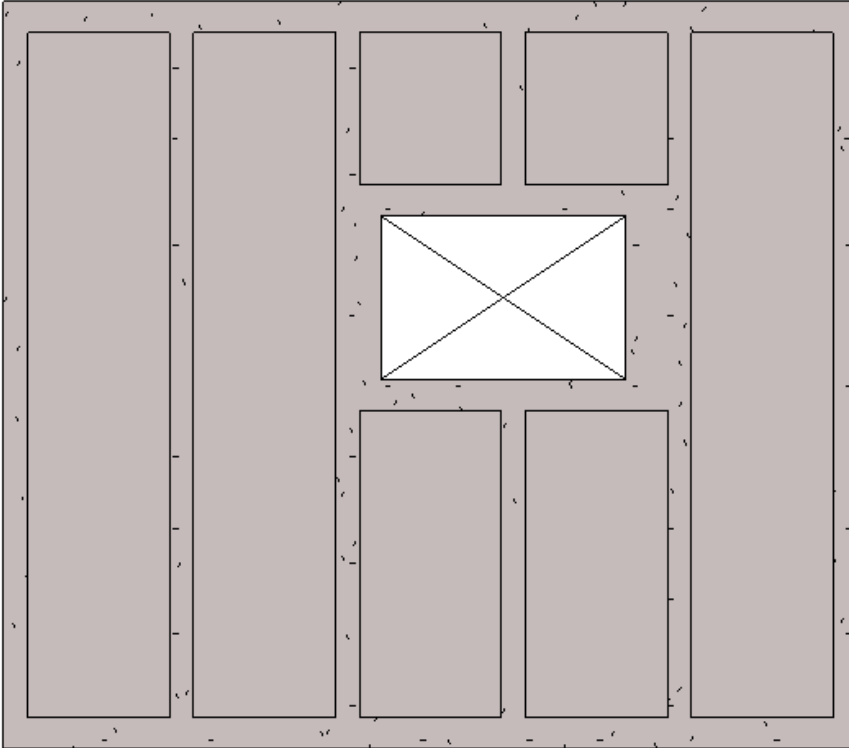
- Leite, F., Akcamete, A., Akinici, B., Atasoy, G. and Kiziltas, S., 2011. Analysis of modeling effort and impact of different levels of detail in building information models. *Automation in Construction*, 20(5), pp.601-609.
- Liu, H., 2016. BIM-based automated planning for panelized construction in the light-frame building industry. PhD thesis, University of Alberta, Edmonton, Canada.
- Liu, H., Holmwood, B., Sydora, C., Singh, G. and Al-Hussein, M., 2017. Optimizing multi-wall panel configuration for panelized construction using BIM. *Proceedings, International Structural Engineering and Construction Conference, Valencia, Spain*, pp.24-29.
- Liu, H., Singh, G., Lu, M., Bouferguene, A. and Al-Hussein, M., 2018. BIM-based automated design and planning for boarding of light-frame residential buildings. *Automation in Construction*, 89, pp.235-249.
- Lopez, D. and Froese, T.M., 2016. Analysis of costs and benefits of panelized and modular prefabricated homes. *Procedia Engineering*, 145, pp.1291-1297.
- Manrique Mogollon, J.D., 2009. Automation of design and drafting for wood frame structures and construction material waste minimization. PhD thesis, University of Alberta, Edmonton, Canada.
- Martínez-Aires, M.D., López-Alonso, M. and Martínez-Rojas, M., 2018. Building Information Modeling and safety management: A systematic review. *Safety Science*, 101, pp.11-18.
- McFarland, J.E., 2007. Building Information Modeling for MEP. MSc thesis, Kansas State University, Manhattan, United States.

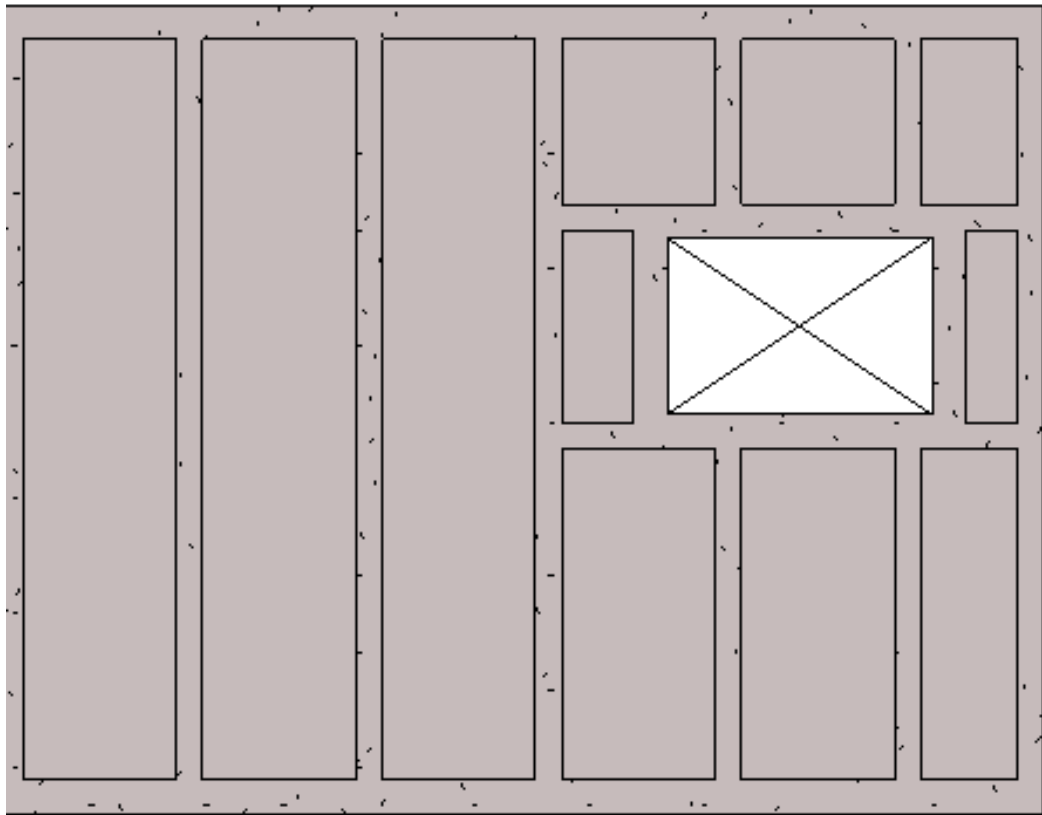
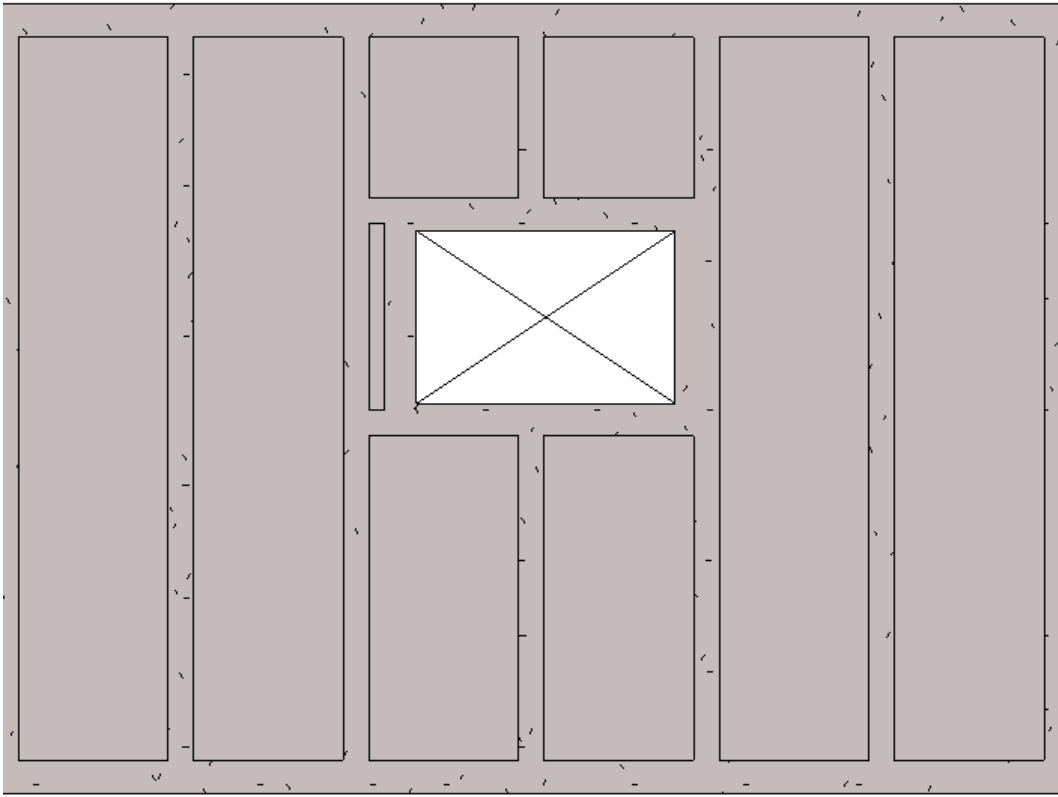
- Mostafa, S., Kim, K.P., Tam, V.W. and Rahnamayiezekavat, P., 2020. Exploring the status, benefits, barriers and opportunities of using BIM for advancing prefabrication practice. *International Journal of Construction Management*, 20(2), pp.146-156.
- Nahmens, I. and Mullens, M.A., 2011. Lean homebuilding: Lessons learned from a precast concrete panelizer. *Journal of Architectural Engineering*, 17(4), pp.155-161.
- Navaratnam, S., Satheeskumar, A., Zhang, G., Nguyen, K., Venkatesan, S. and Poologanathan, K., 2022. The challenges confronting the growth of sustainable prefabricated building construction in Australia: Construction industry views. *Journal of Building Engineering*, 48, p.103935.
- Nawari, N.O., 2012. BIM standard in off-site construction. *Journal of Architectural Engineering*, 18(2), pp.107-113.
- Ramaji, I.J. and Memari, A.M., 2016. Product architecture model for multistory modular buildings. *Journal of Construction Engineering and Management*, 142(10), p.04016047.
- Thompson, L.L., 2002. Advanced panelized construction. U.S. Department of Housing and Urban Development.
- Tian, Y., 2019. A framework for BIM-based automated cabinet manufacturing drafting and planning. MSc thesis, University of Alberta, Edmonton, Canada.
- Vernikos, V., 2012. Optimising Building Information Modelling and off-site construction for civil engineering. *Proceedings, Institution of Civil Engineers-Civil Engineering*, 165(4), p.147.

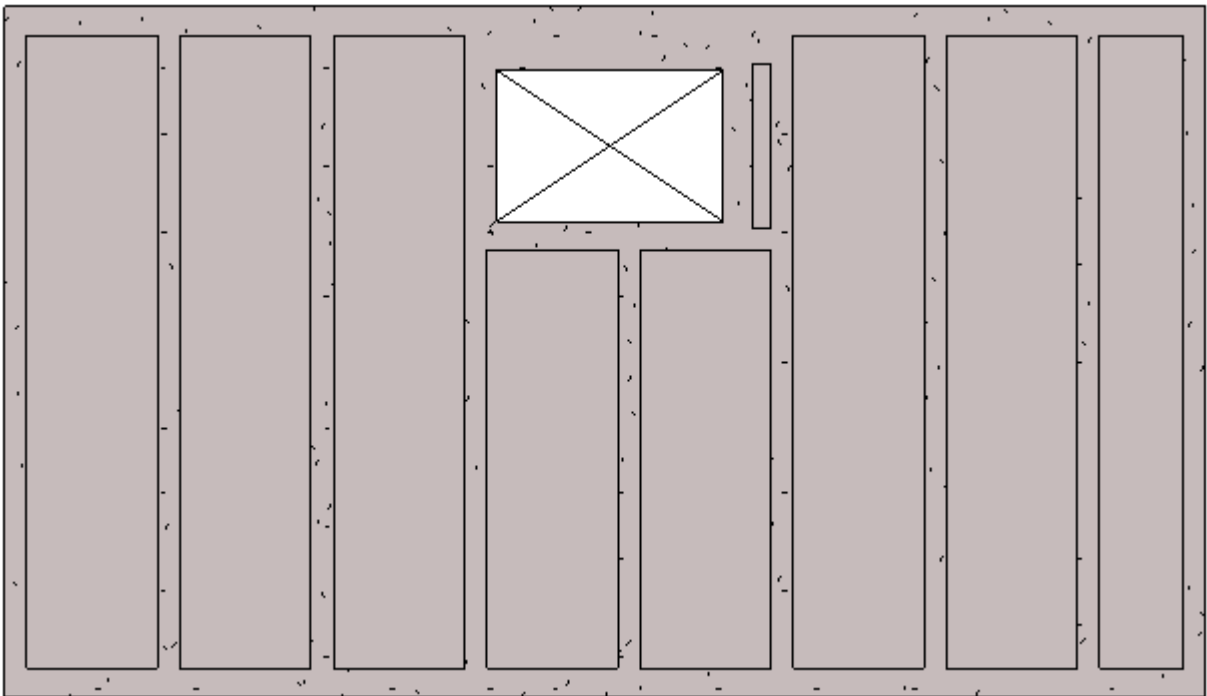
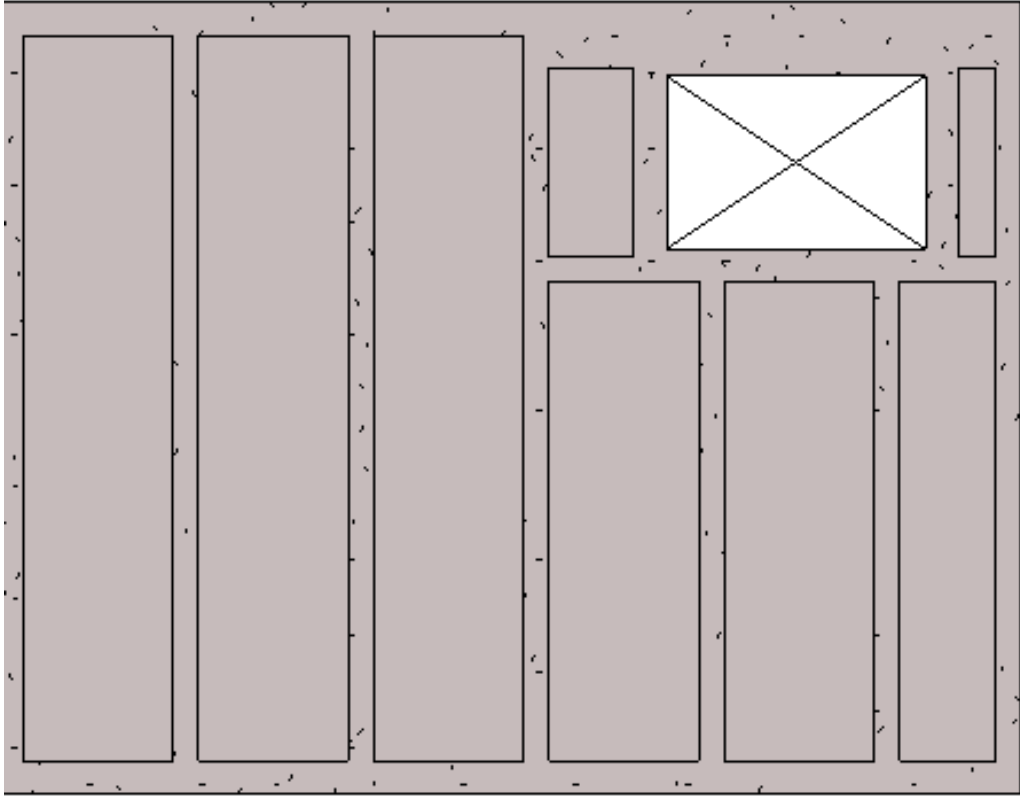
Zhang, C., Zayed, T., Hijazi, W. and Alkass, S., 2016. Quantitative assessment of building constructability using BIM and 4D simulation. *Open Journal of Civil Engineering*, 6(3), pp.442-461.

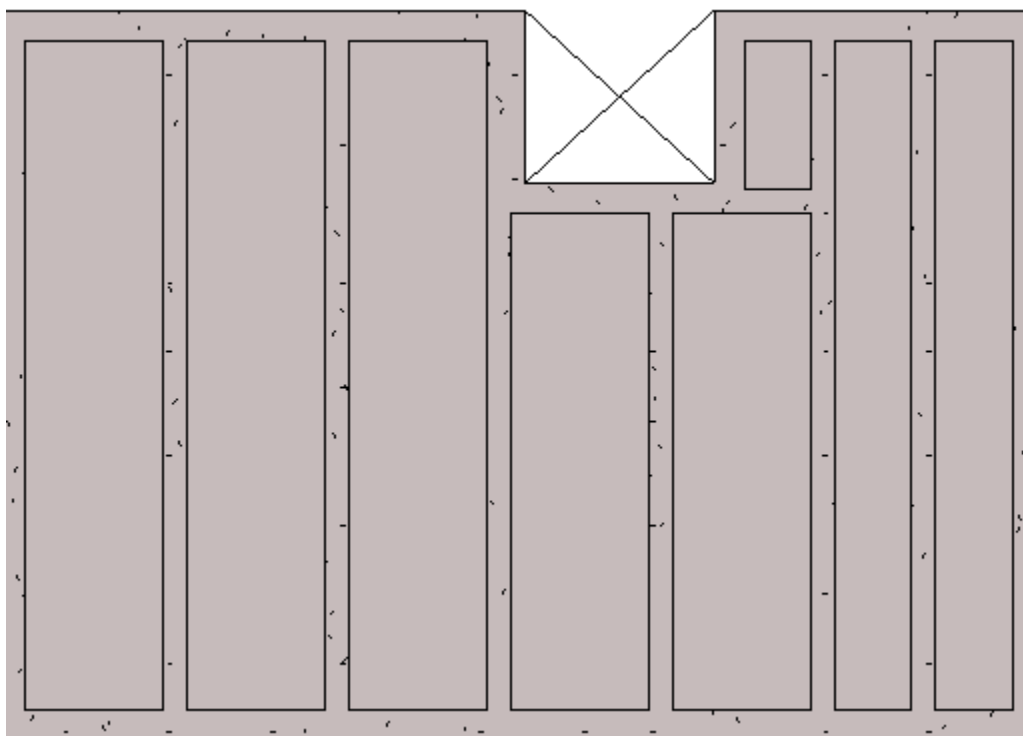
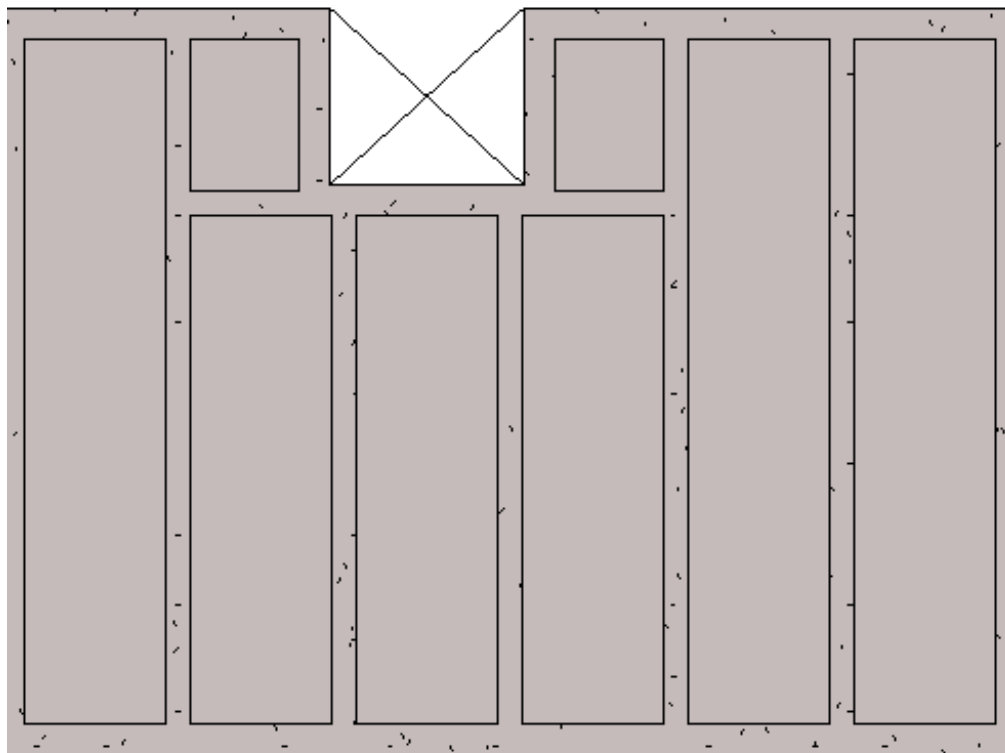
Zhang, N., Wang, J., Al-Hussein, M. and Yin, X., 2022. BIM-based automated design of drainage systems for panelized residential buildings. *International Journal of Construction Management*, pp.1-16.

**Appendix A: Structural Layouts for Ribbed Panel**









# Appendix B: Simulation Reports

## Statistics Report

Date: 2023-07-13

Project: Model

Scenario: 15 projects Manully

Run: All Runs (of 1000)

Note: When summarized across all runs, the mean value reported for a statistic is the mean of the means of each run; the minimum value reported is the minimum of the means of each run; the maximum value reported is the maximum of the means of each run; and so forth.

### Non-Intrinsic Statistics

Element Name	Mean Value	Standard Deviation	Observation Count	Minimum Value	Maximum Value
15 projects Manully (Termination Time)	66,061.832	1,161.211	1,000.000	62,149.276	69,559.719
design and drafting	27,279.418	2,197.645	1,000.000	18,160.474	32,337.456
1 opening (Duration)	16.002	0.301	1,000.000	15.039	16.972
2 opening (Duration)	23.659	0.858	1,000.000	20.685	26.159
3 opening (Duration)	32.678	0.692	1,000.000	30.167	34.787
45 connection (Duration)	0.800	0.013	1,000.000	0.767	0.839
easy connection (Duration)	0.083	0.000	1,000.000	0.083	0.083
no opening (Duration)	5.999	0.218	1,000.000	5.268	6.638
Panel name (Duration)	0.117	0.000	1,000.000	0.117	0.117
Project delivery time	29,732.458	2,197.506	1,000.000	20,605.193	34,853.294

### Resources

Element Name	Average Utilization	Standard Deviation	Maximum Utilization	Current Utilization	Current Capacity
crew installation (Inner Resource)	1.7%	0.0%	1.8%	1.7%	6.000
Crew manufacture (Inner Resource)	7.6%	0.2%	8.4%	7.6%	6.000
1 opening (InnerResource)	0.7%	0.0%	0.8%	0.7%	1.000
2 opening (InnerResource)	0.5%	0.0%	0.6%	0.6%	1.000
3 opening (InnerResource)	2.2%	0.1%	2.4%	2.2%	1.000
45 connection (InnerResource)	0.1%	0.0%	0.1%	0.1%	1.000
easy connection (InnerResource)	0.0%	0.0%	0.0%	0.0%	1.000
no opening (InnerResource)	0.4%	0.0%	0.5%	0.4%	1.000
Panel name (InnerResource)	0.0%	0.0%	0.0%	0.0%	1.000
Drafter (Inner Resource)	96.3%	0.3%	96.8%	96.5%	1.000

### Waiting Files

Element Name	Average Length	Standard Deviation	Maximum Length	Current Length	Average Wait Time
CrewIN	0.000	0.000	0.000	0.000	0.000
CrewMQ	0.000	0.000	0.000	0.000	0.000
1 opening (InnerFile)	0.000	0.000	0.000	0.000	0.000
1 opening panel done (InnerFile)	0.005	0.000	0.006	0.006	23.659
2 opening (InnerFile)	0.000	0.000	0.000	0.000	0.000
3 opening (InnerFile)	0.022	0.001	0.024	0.023	32.700
3 opening panel done (InnerFile)	0.022	0.001	0.024	0.022	98.034
45 connection (InnerFile)	0.002	0.000	0.002	0.002	1.600
45 connection done (InnerFile)	0.001	0.000	0.001	0.001	3.999
easy connection (InnerFile)	0.000	0.000	0.000	0.000	0.000
no opening (InnerFile)	0.004	0.000	0.005	0.005	5.992
no opening done (InnerFile)	0.004	0.000	0.005	0.004	17.997
Panel name (InnerFile)	0.001	0.000	0.001	0.001	0.468
panel name done (InnerFile)	0.000	0.000	0.000	0.000	1.053
DrafterQ	5.231	0.483	6.227	5.007	23,039.358

\*\*\* FURTHER STATISTICS CAN BE OBTAINED FROM INDIVIDUAL ELEMENTS \*\*\*

## Statistics Report

Date: 2023-07-13

Project: Model

Scenario: 15 projects Manully

Run: All Runs (of 1000)

**Note:** When summarized across all runs, the mean value reported for a statistic is the mean of the means of each run; the minimum value reported is the minimum of the means of each run; the maximum value reported is the maximum of the means of each run; and so forth.

### Non-Intrinsic Statistics

Element Name	Mean Value	Standard Deviation	Observation Count	Minimum Value	Maximum Value
15 projects Manully (Termination Time)	36,370.946	1,011.696	1,000.000	33,912.506	45,965.022
design and drafting	11,943.039	1,796.712	1,000.000	5,553.109	16,095.955
1 opening (Duration)	16.006	0.307	1,000.000	15.157	17.062
2 opening (Duration)	23.624	0.852	1,000.000	20.990	26.417
3 opening (Duration)	32.627	0.668	1,000.000	30.890	34.622
45 connection (Duration)	0.799	0.013	1,000.000	0.762	0.845
easy connection (Duration)	0.083	0.000	1,000.000	0.083	0.083
no opening (Duration)	5.998	0.219	1,000.000	5.437	6.628
Panel name (Duration)	0.117	0.000	1,000.000	0.117	0.117
Project delivery time	14,395.771	1,800.440	1,000.000	8,023.775	18,517.736

### Resources

Element Name	Average Utilization	Standard Deviation	Maximum Utilization	Current Utilization	Current Capacity
crew installation (Inner Resource)	3.1%	0.1%	3.3%	3.1%	6.000
Crew manufacture (Inner Resource)	13.8%	0.4%	15.2%	13.7%	6.000
1 opening (InnerResource)	1.3%	0.0%	1.5%	1.3%	1.000
2 opening (InnerResource)	1.0%	0.0%	1.1%	0.9%	1.000
3 opening (InnerResource)	4.0%	0.1%	4.4%	4.0%	1.000
45 connection (InnerResource)	0.2%	0.0%	0.2%	0.2%	1.000
easy connection (InnerResource)	0.0%	0.0%	0.0%	0.0%	1.000
no opening (InnerResource)	0.7%	0.0%	0.8%	0.7%	1.000
Panel name (InnerResource)	0.0%	0.0%	0.0%	0.0%	1.000
Drafter (Inner Resource)	87.6%	1.8%	91.4%	86.3%	2.000

### Waiting Files

Element Name	Average Length	Standard Deviation	Maximum Length	Current Length	Average Wait Time
CrewIN	0.000	0.000	0.000	0.000	0.000
CrewMQ	0.000	0.000	0.000	0.000	0.000
1 opening (InnerFile)	0.000	0.000	0.002	0.000	0.085
1 opening panel done (InnerFile)	0.010	0.000	0.011	0.009	23.642
2 opening (InnerFile)	0.000	0.000	0.001	0.000	0.017
3 opening (InnerFile)	0.042	0.004	0.059	0.041	34.147
3 opening panel done (InnerFile)	0.041	0.002	0.048	0.040	99.410
45 connection (InnerFile)	0.003	0.000	0.004	0.003	1.602
45 connection done (InnerFile)	0.002	0.000	0.002	0.002	3.999
easy connection (InnerFile)	0.000	0.000	0.000	0.000	0.000
no opening (InnerFile)	0.008	0.000	0.010	0.007	6.063
no opening done (InnerFile)	0.007	0.000	0.009	0.007	18.055
Panel name (InnerFile)	0.002	0.000	0.002	0.002	0.468
panel name done (InnerFile)	0.000	0.000	0.000	0.000	1.053
DrafterQ	3.180	0.748	4.938	2.448	7,697.797

\*\*\* FURTHER STATISTICS CAN BE OBTAINED FROM INDIVIDUAL ELEMENTS \*\*\*

## Statistics Report

Date: 2023-07-13

Project: Model

Scenario: 15 projects Manully

Run: All Runs (of 1000)

**Note:** When summarized across all runs, the mean value reported for a statistic is the mean of the means of each run; the minimum value reported is the minimum of the means of each run; the maximum value reported is the maximum of the means of each run; and so forth.

### Non-Intrinsic Statistics

Element Name	Mean Value	Standard Deviation	Observation Count	Minimum Value	Maximum Value
15 projects Manully (Termination Time)	26,237.405	1,724.027	1,000.000	23,410.338	35,887.540
design and drafting	7,264.082	1,357.221	1,000.000	4,350.725	10,804.341
1 opening (Duration)	16.001	0.290	1,000.000	15.190	16.932
2 opening (Duration)	23.593	0.829	1,000.000	21.296	26.097
3 opening (Duration)	32.697	0.674	1,000.000	29.751	35.265
45 connection (Duration)	0.800	0.013	1,000.000	0.760	0.838
easy connection (Duration)	0.083	0.000	1,000.000	0.083	0.083
no opening (Duration)	5.993	0.222	1,000.000	5.262	6.591
Panel name (Duration)	0.117	0.000	1,000.000	0.117	0.117
Project delivery time	9,717.046	1,359.055	1,000.000	6,786.169	13,188.282

### Resources

Element Name	Average Utilization	Standard Deviation	Maximum Utilization	Current Utilization	Current Capacity
crew installation (Inner Resource)	4.3%	0.3%	4.8%	4.7%	6.000
Crew manufacture (Inner Resource)	19.1%	1.2%	21.7%	21.4%	6.000
1 opening (InnerResource)	1.8%	0.1%	2.1%	2.0%	1.000
2 opening (InnerResource)	1.4%	0.1%	1.6%	1.5%	1.000
3 opening (InnerResource)	5.6%	0.4%	6.4%	6.2%	1.000
45 connection (InnerResource)	0.2%	0.0%	0.3%	0.3%	1.000
easy connection (InnerResource)	0.0%	0.0%	0.0%	0.0%	1.000
no opening (InnerResource)	1.0%	0.1%	1.2%	1.2%	1.000
Panel name (InnerResource)	0.1%	0.0%	0.1%	0.1%	1.000
Drafter (Inner Resource)	81.2%	4.9%	88.8%	86.2%	3.000

### Waiting Files

Element Name	Average Length	Standard Deviation	Maximum Length	Current Length	Average Wait Time
CrewIN	0.000	0.000	0.000	0.000	0.000
CrewMQ	0.000	0.000	0.000	0.000	0.000
1 opening (InnerFile)	0.000	0.000	0.003	0.000	0.116
1 opening panel done (InnerFile)	0.014	0.001	0.016	0.015	23.616
2 opening (InnerFile)	0.000	0.000	0.001	0.000	0.023
3 opening (InnerFile)	0.061	0.008	0.120	0.063	35.105
3 opening panel done (InnerFile)	0.058	0.005	0.079	0.062	100.481
45 connection (InnerFile)	0.005	0.000	0.006	0.005	1.605
45 connection done (InnerFile)	0.002	0.000	0.003	0.003	4.005
easy connection (InnerFile)	0.000	0.000	0.000	0.000	0.000
no opening (InnerFile)	0.010	0.001	0.016	0.011	6.060
no opening done (InnerFile)	0.010	0.001	0.013	0.012	18.058
Panel name (InnerFile)	0.002	0.000	0.003	0.003	0.469
panel name done (InnerFile)	0.001	0.000	0.001	0.001	1.054
DrafterQ	1.755	0.819	4.019	1.181	3,017.415

\*\*\* FURTHER STATISTICS CAN BE OBTAINED FROM INDIVIDUAL ELEMENTS \*\*\*

## Statistics Report

Date: 2023-07-13

Project: Model

Scenario: 15 projects Manully

Run: All Runs (of 1000)

**Note:** When summarized across all runs, the mean value reported for a statistic is the mean of the means of each run; the minimum value reported is the minimum of the means of each run; the maximum value reported is the maximum of the means of each run; and so forth.

### Non-Intrinsic Statistics

Element Name	Mean Value	Standard Deviation	Observation Count	Minimum Value	Maximum Value
15 projects Manully (Termination Time)	22,615.256	2,327.547	1,000.000	19,096.785	33,693.614
design and drafting	5,493.624	902.048	1,000.000	4,131.563	9,074.263
1 opening (Duration)	15.990	0.302	1,000.000	14.978	16.886
2 opening (Duration)	23.685	0.857	1,000.000	21.394	26.446
3 opening (Duration)	32.693	0.697	1,000.000	30.633	34.507
45 connection (Duration)	0.799	0.012	1,000.000	0.765	0.837
easy connection (Duration)	0.083	0.000	1,000.000	0.083	0.083
no opening (Duration)	5.997	0.228	1,000.000	5.291	6.647
Panel name (Duration)	0.117	0.000	1,000.000	0.117	0.117
Project delivery time	7,944.865	904.193	1,000.000	6,492.993	11,583.031

### Resources

Element Name	Average Utilization	Standard Deviation	Maximum Utilization	Current Utilization	Current Capacity
crew installation (Inner Resource)	5.1%	0.5%	6.0%	5.1%	6.000
Crew manufacture (Inner Resource)	22.3%	2.1%	26.7%	21.1%	6.000
1 opening (InnerResource)	2.1%	0.2%	2.6%	2.2%	1.000
2 opening (InnerResource)	1.6%	0.2%	2.0%	1.5%	1.000
3 opening (InnerResource)	6.6%	0.6%	7.8%	6.6%	1.000
45 connection (InnerResource)	0.3%	0.0%	0.3%	0.3%	1.000
easy connection (InnerResource)	0.0%	0.0%	0.0%	0.0%	1.000
no opening (InnerResource)	1.2%	0.1%	1.5%	1.2%	1.000
Panel name (InnerResource)	0.1%	0.0%	0.1%	0.1%	1.000
Drafter (Inner Resource)	71.0%	6.6%	81.7%	70.7%	4.000

### Waiting Files

Element Name	Average Length	Standard Deviation	Maximum Length	Current Length	Average Wait Time
CrewIN	0.000	0.000	0.000	0.000	0.000
CrewMQ	0.000	0.000	0.000	0.000	0.000
1 opening (InnerFile)	0.000	0.000	0.004	0.000	0.161
1 opening panel done (InnerFile)	0.016	0.002	0.020	0.015	23.717
2 opening (InnerFile)	0.000	0.000	0.001	0.000	0.032
3 opening (InnerFile)	0.072	0.011	0.139	0.065	35.727
3 opening panel done (InnerFile)	0.068	0.007	0.096	0.066	101.109
45 connection (InnerFile)	0.005	0.001	0.007	0.005	1.604
45 connection done (InnerFile)	0.003	0.000	0.003	0.003	4.002
easy connection (InnerFile)	0.000	0.000	0.000	0.000	0.000
no opening (InnerFile)	0.012	0.001	0.018	0.012	6.103
no opening done (InnerFile)	0.012	0.001	0.016	0.012	18.098
Panel name (InnerFile)	0.003	0.000	0.003	0.003	0.469
panel name done (InnerFile)	0.001	0.000	0.001	0.001	1.054
DrafterQ	0.870	0.652	3.379	0.753	1,251.554

\*\*\* FURTHER STATISTICS CAN BE OBTAINED FROM INDIVIDUAL ELEMENTS \*\*\*

## Statistics Report

Date: 2023-07-13

Project: Model

Scenario: 15 projects Manully

Run: All Runs (of 1000)

**Note:** When summarized across all runs, the mean value reported for a statistic is the mean of the means of each run; the minimum value reported is the minimum of the means of each run; the maximum value reported is the maximum of the means of each run; and so forth.

### Non-Intrinsic Statistics

Element Name	Mean Value	Standard Deviation	Observation Count	Minimum Value	Maximum Value
15 projects Manully (Termination Time)	21,102.993	3,016.864	1,000.000	15,644.461	35,014.102
design and drafting	4,728.394	505.645	1,000.000	4,092.671	7,273.443
1 opening (Duration)	15.996	0.290	1,000.000	14.872	16.843
2 opening (Duration)	23.698	0.893	1,000.000	21.022	26.384
3 opening (Duration)	32.665	0.669	1,000.000	30.270	34.628
45 connection (Duration)	0.800	0.013	1,000.000	0.751	0.839
easy connection (Duration)	0.083	0.000	1,000.000	0.083	0.083
no opening (Duration)	5.992	0.216	1,000.000	5.211	6.652
Panel name (Duration)	0.117	0.000	1,000.000	0.117	0.117
Project delivery time	7,181.755	506.632	1,000.000	6,502.189	9,668.012

### Resources

Element Name	Average Utilization	Standard Deviation	Maximum Utilization	Current Utilization	Current Capacity
crew installation (Inner Resource)	5.5%	0.7%	7.2%	5.4%	6.000
Crew manufacture (Inner Resource)	24.2%	3.2%	33.0%	24.2%	6.000
1 opening (InnerResource)	2.3%	0.3%	3.1%	2.3%	1.000
2 opening (InnerResource)	1.7%	0.2%	2.3%	1.7%	1.000
3 opening (InnerResource)	7.1%	0.9%	9.3%	7.0%	1.000
45 connection (InnerResource)	0.3%	0.0%	0.4%	0.3%	1.000
easy connection (InnerResource)	0.0%	0.0%	0.0%	0.0%	1.000
no opening (InnerResource)	1.3%	0.2%	1.8%	1.3%	1.000
Panel name (InnerResource)	0.1%	0.0%	0.1%	0.1%	1.000
Drafter (Inner Resource)	61.4%	8.1%	81.6%	61.6%	5.000

### Waiting Files

Element Name	Average Length	Standard Deviation	Maximum Length	Current Length	Average Wait Time
CrewIN	0.000	0.000	0.000	0.000	0.000
CrewMQ	0.000	0.000	0.000	0.000	0.000
1 opening (InnerFile)	0.000	0.001	0.007	0.000	0.162
1 opening panel done (InnerFile)	0.017	0.002	0.023	0.017	23.731
2 opening (InnerFile)	0.000	0.000	0.001	0.000	0.033
3 opening (InnerFile)	0.079	0.016	0.181	0.079	36.205
3 opening panel done (InnerFile)	0.074	0.011	0.122	0.073	101.537
45 connection (InnerFile)	0.006	0.001	0.008	0.006	1.605
45 connection done (InnerFile)	0.003	0.000	0.004	0.003	4.004
easy connection (InnerFile)	0.000	0.000	0.000	0.000	0.000
no opening (InnerFile)	0.013	0.002	0.022	0.013	6.118
no opening done (InnerFile)	0.013	0.002	0.019	0.013	18.097
Panel name (InnerFile)	0.003	0.000	0.004	0.003	0.468
panel name done (InnerFile)	0.001	0.000	0.001	0.001	1.053
DrafterQ	0.383	0.418	2.779	0.537	487.664

\*\*\* FURTHER STATISTICS CAN BE OBTAINED FROM INDIVIDUAL ELEMENTS \*\*\*

## Statistics Report

**Date:** 2023-07-13

**Project:** Model

**Scenario:** 15 projects Manully

**Run:** All Runs (of 1000)

**Note:** When summarized across all runs, the mean value reported for a statistic is the mean of the means of each run; the minimum value reported is the minimum of the means of each run; the maximum value reported is the maximum of the means of each run; and so forth.

### Non-Intrinsic Statistics

Element Name	Mean Value	Standard Deviation	Observation Count	Minimum Value	Maximum Value
15 projects Manully (Termination Time)	20,627.818	3,320.453	1,000.000	15,191.759	36,701.389
design and drafting	4,452.923	308.930	1,000.000	4,011.047	6,105.605
1 opening (Duration)	16.011	0.298	1,000.000	15.092	16.997
2 opening (Duration)	23.737	0.817	1,000.000	21.115	26.264
3 opening (Duration)	32.638	0.686	1,000.000	30.699	34.663
45 connection (Duration)	0.800	0.012	1,000.000	0.757	0.837
easy connection (Duration)	0.083	0.000	1,000.000	0.083	0.083
no opening (Duration)	6.002	0.226	1,000.000	5.315	6.741
Panel name (Duration)	0.117	0.000	1,000.000	0.117	0.117
Project delivery time	6,905.474	309.982	1,000.000	6,426.944	8,571.615

### Resources

Element Name	Average Utilization	Standard Deviation	Maximum Utilization	Current Utilization	Current Capacity
crew installation (Inner Resource)	5.6%	0.8%	7.5%	5.8%	6.000
Crew manufacture (Inner Resource)	24.8%	3.7%	34.4%	25.9%	6.000
1 opening (InnerResource)	2.4%	0.4%	3.3%	2.5%	1.000
2 opening (InnerResource)	1.8%	0.3%	2.5%	1.9%	1.000
3 opening (InnerResource)	7.3%	1.1%	9.9%	7.7%	1.000
45 connection (InnerResource)	0.3%	0.0%	0.4%	0.3%	1.000
easy connection (InnerResource)	0.0%	0.0%	0.0%	0.0%	1.000
no opening (InnerResource)	1.3%	0.2%	1.8%	1.4%	1.000
Panel name (InnerResource)	0.1%	0.0%	0.1%	0.1%	1.000
Drafter (Inner Resource)	52.7%	7.9%	70.8%	55.7%	6.000

### Waiting Files

Element Name	Average Length	Standard Deviation	Maximum Length	Current Length	Average Wait Time
CrewIN	0.000	0.000	0.000	0.000	0.000
CrewMQ	0.000	0.000	0.000	0.000	0.000
1 opening (InnerFile)	0.000	0.001	0.006	0.000	0.190
1 opening panel done (InnerFile)	0.018	0.003	0.025	0.019	23.771
2 opening (InnerFile)	0.000	0.000	0.001	0.000	0.034
3 opening (InnerFile)	0.082	0.018	0.152	0.077	36.607
3 opening panel done (InnerFile)	0.076	0.013	0.112	0.077	101.864
45 connection (InnerFile)	0.006	0.001	0.009	0.006	1.606
45 connection done (InnerFile)	0.003	0.000	0.004	0.003	4.007
easy connection (InnerFile)	0.000	0.000	0.000	0.000	0.000
no opening (InnerFile)	0.014	0.002	0.022	0.014	6.123
no opening done (InnerFile)	0.014	0.002	0.019	0.014	18.131
Panel name (InnerFile)	0.003	0.000	0.004	0.003	0.468
panel name done (InnerFile)	0.001	0.000	0.001	0.001	1.053
DrafterQ	0.174	0.259	1.573	0.095	208.095

\*\*\* FURTHER STATISTICS CAN BE OBTAINED FROM INDIVIDUAL ELEMENTS \*\*\*

## Statistics Report

**Date:** 2023-07-13

**Project:** Model

**Scenario:** 15 projects Manully

**Run:** All Runs (of 1000)

**Note:** When summarized across all runs, the mean value reported for a statistic is the mean of the means of each run; the minimum value reported is the minimum of the means of each run; the maximum value reported is the maximum of the means of each run; and so forth.

### Non-Intrinsic Statistics

Element Name	Mean Value	Standard Deviation	Observation Count	Minimum Value	Maximum Value
15 projects Manully (Termination Time)	20,242.441	3,383.817	1,000.000	14,227.236	36,383.259
design and drafting	4,319.651	185.660	1,000.000	4,013.699	5,613.186
1 opening (Duration)	15.989	0.286	1,000.000	15.202	16.951
2 opening (Duration)	23.612	0.821	1,000.000	21.159	26.677
3 opening (Duration)	32.639	0.680	1,000.000	30.674	34.881
45 connection (Duration)	0.800	0.012	1,000.000	0.761	0.844
easy connection (Duration)	0.083	0.000	1,000.000	0.083	0.083
no opening (Duration)	5.994	0.225	1,000.000	5.319	6.660
Panel name (Duration)	0.117	0.000	1,000.000	0.117	0.117
Project delivery time	6,772.105	190.684	1,000.000	6,452.880	8,028.848

### Resources

Element Name	Average Utilization	Standard Deviation	Maximum Utilization	Current Utilization	Current Capacity
crew installation (Inner Resource)	5.7%	0.9%	8.0%	5.5%	6.000
Crew manufacture (Inner Resource)	25.4%	4.1%	35.7%	24.4%	6.000
1 opening (InnerResource)	2.4%	0.4%	3.4%	2.3%	1.000
2 opening (InnerResource)	1.8%	0.3%	2.6%	1.7%	1.000
3 opening (InnerResource)	7.5%	1.2%	10.6%	7.1%	1.000
45 connection (InnerResource)	0.3%	0.0%	0.4%	0.3%	1.000
easy connection (InnerResource)	0.0%	0.0%	0.0%	0.0%	1.000
no opening (InnerResource)	1.4%	0.2%	2.0%	1.3%	1.000
Panel name (InnerResource)	0.1%	0.0%	0.1%	0.1%	1.000
Drafter (Inner Resource)	46.2%	7.5%	64.3%	44.2%	7.000

### Waiting Files

Element Name	Average Length	Standard Deviation	Maximum Length	Current Length	Average Wait Time
CrewIN	0.000	0.000	0.000	0.000	0.000
CrewMQ	0.001	0.005	0.099	0.000	0.815
1 opening (InnerFile)	0.000	0.001	0.010	0.000	0.231
1 opening panel done (InnerFile)	0.018	0.003	0.026	0.017	23.660
2 opening (InnerFile)	0.000	0.000	0.002	0.000	0.048
3 opening (InnerFile)	0.085	0.020	0.207	0.073	37.049
3 opening panel done (InnerFile)	0.078	0.014	0.137	0.071	102.330
45 connection (InnerFile)	0.006	0.001	0.008	0.006	1.606
45 connection done (InnerFile)	0.003	0.000	0.004	0.003	4.006
easy connection (InnerFile)	0.000	0.000	0.000	0.000	0.000
no opening (InnerFile)	0.014	0.003	0.024	0.013	6.150
no opening done (InnerFile)	0.014	0.002	0.020	0.013	18.139
Panel name (InnerFile)	0.003	0.001	0.004	0.003	0.468
panel name done (InnerFile)	0.001	0.000	0.001	0.001	1.053
DrafterQ	0.067	0.154	1.228	0.000	74.355

\*\*\* FURTHER STATISTICS CAN BE OBTAINED FROM INDIVIDUAL ELEMENTS \*\*\*

## Statistics Report

**Date:** 2023-07-13

**Project:** Model

**Scenario:** 15 projects ConcreteX

**Run:** All Runs (of 1000)

**Note:** When summarized across all runs, the mean value reported for a statistic is the mean of the means of each run; the minimum value reported is the minimum of the means of each run; the maximum value reported is the maximum of the means of each run; and so forth.

### Non-Intrinsic Statistics

Element Name	Mean Value	Standard Deviation	Observation Count	Minimum Value	Maximum Value
15 projects ConcreteX (Termination Time)	15,868.453	3,509.947	1,000.000	7,669.763	27,985.995
design and drafting	12.466	0.551	1,000.000	10.831	14.437
1 opening (Duration)	0.183	0.002	1,000.000	0.175	0.190
2 opening (Duration)	0.199	0.003	1,000.000	0.188	0.211
3 opening (Duration)	0.212	0.002	1,000.000	0.206	0.217
45 connection (Duration)	0.084	0.001	1,000.000	0.082	0.087
easy connection (Duration)	0.083	0.000	1,000.000	0.083	0.083
no opening (Duration)	0.167	0.002	1,000.000	0.161	0.173
Panel name (Duration)	0.017	0.000	1,000.000	0.017	0.017
Project delivery time	2,468.912	47.147	1,000.000	2,354.982	2,942.661

### Resources

Element Name	Average Utilization	Standard Deviation	Maximum Utilization	Current Utilization	Current Capacity
crew installation (Inner Resource)	7.5%	1.8%	14.7%	7.1%	6.000
Crew manufacture (Inner Resource)	33.1%	7.8%	66.1%	30.9%	6.000
1 opening (InnerResource)	0.0%	0.0%	0.1%	0.0%	1.000
2 opening (InnerResource)	0.0%	0.0%	0.0%	0.0%	1.000
3 opening (InnerResource)	0.1%	0.0%	0.1%	0.1%	1.000
45 connection (InnerResource)	0.0%	0.0%	0.1%	0.0%	1.000
easy connection (InnerResource)	0.0%	0.0%	0.0%	0.0%	1.000
no opening (InnerResource)	0.0%	0.0%	0.1%	0.0%	1.000
Panel name (InnerResource)	0.0%	0.0%	0.0%	0.0%	1.000
Drafter (Inner Resource)	1.2%	0.3%	2.5%	1.1%	1.000

### Waiting Files

Element Name	Average Length	Standard Deviation	Maximum Length	Current Length	Average Wait Time
CrewIN	0.000	0.000	0.000	0.000	0.000
CrewMQ	0.007	0.045	1.016	0.000	4.870
1 opening (InnerFile)	0.000	0.000	0.000	0.000	0.000
1 opening panel done (InnerFile)	0.000	0.000	0.000	0.000	0.199
2 opening (InnerFile)	0.000	0.000	0.000	0.000	0.000
3 opening (InnerFile)	0.001	0.000	0.001	0.001	0.212
3 opening panel done (InnerFile)	0.001	0.000	0.001	0.001	0.635
45 connection (InnerFile)	0.001	0.000	0.002	0.001	0.169
45 connection done (InnerFile)	0.000	0.000	0.001	0.000	0.422
easy connection (InnerFile)	0.000	0.000	0.000	0.000	0.000
no opening (InnerFile)	0.000	0.000	0.001	0.000	0.167
no opening done (InnerFile)	0.000	0.000	0.001	0.000	0.500
Panel name (InnerFile)	0.001	0.000	0.001	0.001	0.067
panel name done (InnerFile)	0.000	0.000	0.000	0.000	0.150
DrafterQ	0.000	0.000	0.003	0.000	0.088

\*\*\* FURTHER STATISTICS CAN BE OBTAINED FROM INDIVIDUAL ELEMENTS \*\*\*

## Statistics Report

Date: 2023-07-14

Project: Model

Scenario: 15 projects ConcreteX

Run: All Runs (of 1000)

**Note:** When summarized across all runs, the mean value reported for a statistic is the mean of the means of each run; the minimum value reported is the minimum of the means of each run; the maximum value reported is the maximum of the means of each run; and so forth.

### Non-Intrinsic Statistics

Element Name	Mean Value	Standard Deviation	Observation Count	Minimum Value	Maximum Value
15 projects ConcreteX (Termination Time)	10,560.000	0.000	1,000.000	10,560.000	10,560.000
design and drafting	12.465	0.661	1,000.000	10.509	15.330
1 opening (Duration)	0.183	0.003	1,000.000	0.172	0.192
2 opening (Duration)	0.199	0.004	1,000.000	0.187	0.213
3 opening (Duration)	0.212	0.002	1,000.000	0.204	0.220
45 connection (Duration)	0.084	0.001	1,000.000	0.082	0.087
easy connection (Duration)	0.083	0.000	1,000.000	0.083	0.083
no opening (Duration)	0.167	0.002	1,000.000	0.158	0.175
Panel name (Duration)	0.017	0.000	1,000.000	0.017	0.017
Project delivery time	2,467.185	56.369	1,000.000	2,314.917	2,758.215

### Counters

Element Name	Final Count	Production Rate	Average Interarrival	First Arrival	Last Arrival
number of project	9.342	0.001	953.596	2,448.391	9,595.572

### Resources

Element Name	Average Utilization	Standard Deviation	Maximum Utilization	Current Utilization	Current Capacity
crew installation (Inner Resource)	6.8%	2.0%	17.1%	9.0%	6.000
Crew manufacture (Inner Resource)	34.2%	9.5%	80.3%	50.7%	6.000
1 opening (InnerResource)	0.0%	0.0%	0.1%	0.1%	1.000
2 opening (InnerResource)	0.0%	0.0%	0.1%	0.0%	1.000
3 opening (InnerResource)	0.1%	0.0%	0.2%	0.1%	1.000
45 connection (InnerResource)	0.0%	0.0%	0.1%	0.1%	1.000
easy connection (InnerResource)	0.0%	0.0%	0.0%	0.0%	1.000
no opening (InnerResource)	0.1%	0.0%	0.1%	0.1%	1.000
Panel name (InnerResource)	0.0%	0.0%	0.0%	0.0%	1.000
Drafter (Inner Resource)	1.4%	0.4%	3.2%	2.0%	1.000

### Waiting Files

Element Name	Average Length	Standard Deviation	Maximum Length	Current Length	Average Wait Time
CrewIN	0.000	0.000	0.000	0.000	0.000
CrewMQ	0.008	0.042	0.635	0.011	4.963
1 opening (InnerFile)	0.000	0.000	0.000	0.000	0.000
1 opening panel done (InnerFile)	0.000	0.000	0.001	0.000	0.199
2 opening (InnerFile)	0.000	0.000	0.000	0.000	0.000
3 opening (InnerFile)	0.001	0.000	0.002	0.001	0.212
3 opening panel done (InnerFile)	0.001	0.000	0.002	0.001	0.635
45 connection (InnerFile)	0.001	0.000	0.002	0.001	0.169
45 connection done (InnerFile)	0.000	0.000	0.001	0.001	0.422
easy connection (InnerFile)	0.000	0.000	0.000	0.000	0.000
no opening (InnerFile)	0.001	0.000	0.001	0.001	0.166
no opening done (InnerFile)	0.001	0.000	0.001	0.001	0.500
Panel name (InnerFile)	0.001	0.000	0.002	0.001	0.067
panel name done (InnerFile)	0.000	0.000	0.000	0.000	0.150
DrafterQ	0.000	0.000	0.003	0.000	0.075

\*\*\* FURTHER STATISTICS CAN BE OBTAINED FROM INDIVIDUAL ELEMENTS \*\*\*

## Statistics Report

**Date:** 2023-07-14  
**Project:** Model  
**Scenario:** 15 projects Manully  
**Run:** All Runs (of 1000)

**Note:** When summarized across all runs, the mean value reported for a statistic is the mean of the means of each run; the minimum value reported is the minimum of the means of each run; the maximum value reported is the maximum of the means of each run; and so forth.

### Non-Intrinsic Statistics

Element Name	Mean Value	Standard Deviation	Observation Count	Minimum Value	Maximum Value
15 projects Manully (Termination Time)	10,560.000	0.000	1,000.000	10,560.000	10,560.000
design and drafting	4,411.621	317.760	1,000.000	3,697.875	5,679.061
1 opening (Duration)	15.998	0.363	1,000.000	14.791	17.163
2 opening (Duration)	23.676	1.029	1,000.000	20.383	27.820
3 opening (Duration)	32.682	0.843	1,000.000	29.606	35.275
45 connection (Duration)	0.799	0.014	1,000.000	0.751	0.843
easy connection (Duration)	0.083	0.000	1,000.000	0.083	0.083
no opening (Duration)	5.984	0.262	1,000.000	5.070	7.090
Panel name (Duration)	0.117	0.000	1,000.000	0.117	0.117
Project delivery time	6,697.594	179.577	1,000.000	6,150.352	7,373.559

### Counters

Element Name	Final Count	Production Rate	Average Interarrival	First Arrival	Last Arrival
number of project	4.321	0.000	NaN	6,639.868	9,402.534

### Resources

Element Name	Average Utilization	Standard Deviation	Maximum Utilization	Current Utilization	Current Capacity
crew installation (Inner Resource)	3.2%	0.9%	5.5%	3.7%	6.000
Crew manufacture (Inner Resource)	18.6%	5.0%	29.6%	27.0%	6.000
1 opening (InnerResource)	3.3%	0.7%	4.7%	4.2%	1.000
2 opening (InnerResource)	2.4%	0.6%	3.7%	3.1%	1.000
3 opening (InnerResource)	10.1%	2.2%	14.4%	13.0%	1.000
45 connection (InnerResource)	0.4%	0.1%	0.6%	0.5%	1.000
easy connection (InnerResource)	0.0%	0.0%	0.0%	0.0%	1.000
no opening (InnerResource)	1.9%	0.4%	2.8%	2.5%	1.000
Panel name (InnerResource)	0.1%	0.0%	0.1%	0.1%	1.000
Drafter (Inner Resource)	71.1%	15.7%	97.9%	94.5%	5.000

### Waiting Files

Element Name	Average Length	Standard Deviation	Maximum Length	Current Length	Average Wait Time
CrewIN	0.000	0.000	0.000	0.000	0.000
CrewMQ	0.000	0.000	0.000	0.000	0.000
1 opening (InnerFile)	0.000	0.001	0.005	0.001	0.148
1 opening panel done (InnerFile)	0.024	0.006	0.037	0.031	23.698
2 opening (InnerFile)	0.000	0.000	0.001	0.000	0.023
3 opening (InnerFile)	0.112	0.032	0.300	0.154	35.895
3 opening panel done (InnerFile)	0.104	0.025	0.192	0.138	101.321
45 connection (InnerFile)	0.008	0.002	0.013	0.010	1.604
45 connection done (InnerFile)	0.004	0.001	0.006	0.005	4.001
easy connection (InnerFile)	0.000	0.000	0.000	0.000	0.000
no opening (InnerFile)	0.019	0.005	0.033	0.027	6.086
no opening done (InnerFile)	0.019	0.004	0.030	0.026	18.065
Panel name (InnerFile)	0.004	0.001	0.006	0.006	0.468
panel name done (InnerFile)	0.001	0.000	0.002	0.001	1.053
DrafterQ	0.576	0.811	6.239	2.055	369.432

\*\*\* FURTHER STATISTICS CAN BE OBTAINED FROM INDIVIDUAL ELEMENTS \*\*\*